Politecnico di Torino

Master of Science in Biomedical Engineering

Drug-releasing supramolecular hydrogels based on custom-made polyurethanes and cyclodextrins

Supervisors

Prof. Gianluca Ciardelli

Dot. Monica Boffito

Eng. Alessandro Torchio

Candidate

Alice Stefani

December 2019

Ai miei genitori,

la mia fonte di ispirazione, sapere e amore.

Table of content

1. Abstract

Supramolecular hydrogels based on host-guest complexes are gaining increasing interest as effective drug delivery systems for biomedical application. A well-known and widely exploited supramolecular interaction is the one occurring between α-cyclodextrin and linear polymers containing poly(ethylene oxide) (PEO) moieties. In this thesis work a library of newly-designed supramolecular hydrogels based on properly synthesized amphiphilic poly(ether urethane)s (PEUs) and α-cyclodextrins has been developed for advanced drug release applications. Poly(ether urethane)s containing PEO as building block have been selected as the synthetic part of the supramolecular hydrogels for their versatility, which allows the achievement of different chemical and mechanical characteristics depending on the selected building blocks. The poly(ether urethane)s used in this work were all synthesized using Poloxamers® as macrodiol. Poloxamers are commercial copolymers formed by three blocks of poly(ethylene oxide)-poly(propylene oxide)-poly(ethylene oxide) (PEO-PPO-PEO) and they are differentiated according to their molecular weight, the molecular weight of PEO and PPO blocks as well as their ratio. In detail, two PEUs were synthesized starting from Poloxamer 407 (M_n=12600 Da, 70% PEO) as macrodiol, 1,6-hexamethylene diisocyanate and N-Boc serinol or 1,4-cyclohexane dimethanol as chain extenders. The two polyurethanes were coded as NHP407 and CHP407, respectively. In order to evaluate the effect of Poloxamer composition on the resulting supramolecular complexes, another PEU (acronym NHF68) was synthesized using Pluronic F68 (M_n=8400 Da, 80% PEO) as macrodiol, 1,6-hexamethylene diisocyanate as diisocyanate and N-Boc Serinol as chain extender. A process of cleavage of Boc groups was also conducted on NHF68 and NHP407 (obtaining SHF68 and SHP407, respectively) in order to obtain a material that exposes free amino groups with additional antibacterial properties and functional moieties available for functionalization through carbodiimide chemistry. Attenuated Total Reflectance – Fourier Transformed Infra-Red (ATR-FTIR) analyses were conducted to validate the polyurethane synthesis by observing the presence of the characteristic peaks of the urethane bond. Size-Exclusion Chromatography (SEC) characterization allowed the estimation of PEU molecular weight (M_n=30000 Da). These analyses were also performed to confirm the molecular integrity of the deprotected polyurethanes. The effective deprotection of BOC-protected amino groups along SHF68

and SHP407 chains was proved by Kaiser Test (Ninhydrin Assay) which also allowed a quantification of the exposed functionalities, which turned out to be $1.6 * 10^{18}\ units\ of\ NH_2/gram$ and $0{,}07 * 10^{18}\ units\ of\ NH_2/gram$ of SHF68 and SHP407, respectively. The temperature-dependent stability of PEU micelles and their aggregates was investigated by Dynamic Light Scattering analysis, showing that CHP407 forms stable structures even at 25°C, SHP407 only at 37°C and SHF68 neither at 25°C nor at 37°C. Supramolecular hydrogels were then designed by mixing a SHP407, SHF68 or CHP407 solution with an α-cyclodextrin (α-CD) solution to finally achieve a PEU concentration ranging between 1 and 5% w/v and a α-CD concentration of 10% w/v. SHF68-based hydrogels showed slow gelation kinetics (from five hours to overnight) and poor stability in aqueous environment (rapid dissolution and de-swelling of the hydrogel), meanwhile the use of CHP407 or SHP407 as synthetic component led to the design of supramolecular hydrogels with fast gelation kinetics (around the two or three hours), good mechanical properties (around 5000- 10000 Pa of elastic modulus), shear thinning behaviour and self-healing capability (about 90% elastic modulus recovery), as assessed by rheological characterization (frequency sweep, strain sweep and strain tests). Additionally, being hydrogel composition the same, CHP407-based supramolecular hydrogels showed enhanced mechanical properties (around 10000 Pa of elastic modulus) and stability in aqueous environment (maintains wet weight with a slight de-swelling of 10% to the advantage of a significant dissolution of the hydrogel) compared to SHF68-based ones. Finally, in order to overcome the previously mentioned drawback of SHF68, a new hydrogel formulation bringing together the best properties of both CHP407 and SHF68 was developed by mixing a CHP407/SHF68 blend (80:20 %w/w, overall PEU concentration 1%w/v, 3%w/v and 5%w/v) as synthetic component and α-CD at a final concentration of 10% w/v. As a matter of fact, stability in aqueous environment (10% de-swelling with 90% dissolution of the hydrogel) and good mechanical properties (around 10000 Pa of elastic modulus) were achieved thanks to the presence of CHP407, meanwhile the abundance of free amino groups of SHF68 opens the way to potential functionalization procedures as well as to the design of hydrogels with antibacterial properties. Additionally, stability and swelling tests confirmed that the herein-designed supramolecular hydrogels showed a high outward mass exchange even if their wet weight did not vary significantly: this behaviour is favourable for obtaining a controlled release of drug molecules. Moreover, all the

supramolecular hydrogel formulations turned out to be cytocompatible, with cell viability in the range 100%. With regard to drug release, the designed supramolecular hydrogels were used for the encapsulation of Curcumin, an effective antioxidant and antitumor hydrophobic molecule. The drug was encapsulated at a final concentration of 80 μg/mL, which is expected to be sufficient for an effective and sustained treatment of important diseases (e.g., prostate cancer). All the obtained hydrogels succeed in releasing curcumin progressively and with tuneable release profiles within 3 days, avoiding any burst release. The supramolecular gels developed in this work thus require a remarkably low amount of synthetic component (i.e., min. required PEU concentration 1% w/v) to undergo gelation, which is an excellent feature to obtain bioartificial hydrogels with enhanced biological properties and lower production costs compared to pure synthetic systems. In addition, the combination of custom-made polyurethanes with α-cyclodextrins has opened the way to the development of injectable thixotropic systems with high potential as drug-loaded hydrogels for localized delivery.

2. Introduction and State of the Art

2.1 Polymer

A polymer (from Greek πολυμερής: poly – many, meros – parts) is an organic or inorganic compound, of natural or synthetic origin, composed of many chemical units called Constitutional Repeating Unit or monomer units. The structure can be simply represented in this form

A-B-B-B-B-B-B-B-B-B-B-B-B-B-B-B-B-B-B-B-B-B-B-B-B-B-A

where B corresponds to the repeating monomer unit and A is the terminal group which typically does not affect the chemical properties of the polymer. The bonds between each group are covalent and the structure results from a polymerization reaction.

It is possible to classify this kind of chemical compounds depending on the number of involved monomers. Indeed, an oligomer is defined as a macromolecule with high molecular weight but low degree of polymerization (which means that it is composed of less than 10 monomers), whereas a polymer is characterized by a higher molecular weight than oligomers and a higher degree of polymerization. Three types of polymers can be distinguished:

1. Low Polymer: 10-100 monomers
2. Middle Polymer: 100-1000 monomers
3. High Polymer: >1000 monomers.

Another valid classification is that based on the polymer structure: linear, cross-linked and branched polymers, as reported in Figure 1.

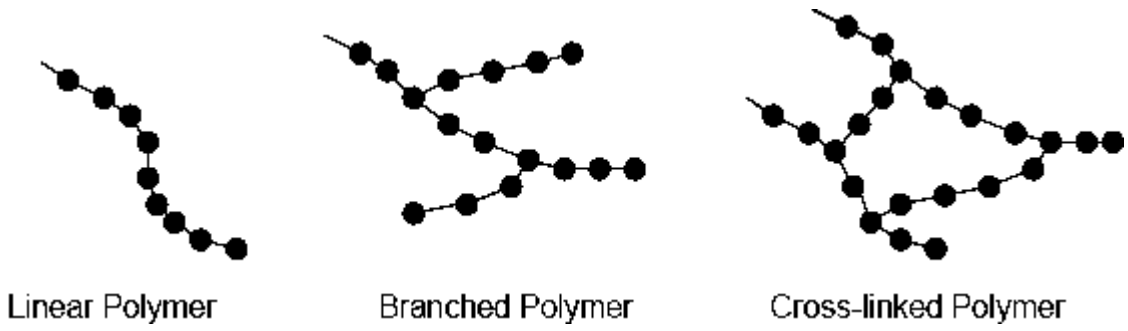

Figure 1 Polymer Structure

As mentioned above, the polymerization is a chemical reaction that allows the formation of the polymer chains. During this process, it is possible to obtain different chain compositions and also different properties of the resulting polymer. Homopolymers are composed only of monomers of the same type, while copolymers are characterized by different types of structural units. Depending on how the different monomers are positioned, different types of copolymers can be obtained: random, alternate, block and grafted (where the main and side chains are composed of different monomers). The different kinds of copolymers are schematized in Figure 2.

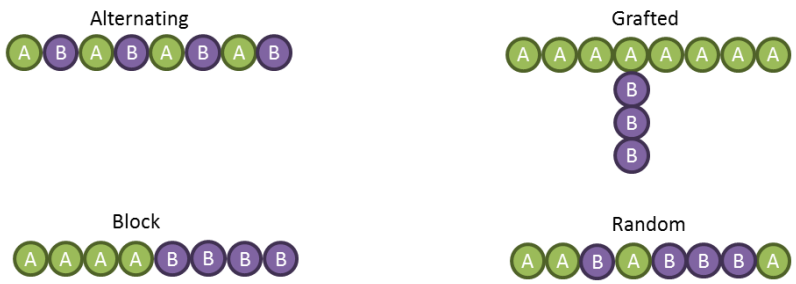

Figure 2 Copolymer classification

To better understand the mechanical and physical properties of a polymer, it is necessary to calculate the molecular weight of the compound. Polymers are generally composed by chains of various lengths and for this reason it is possible to represent a distribution of molecular weights related to the number of moles of each species, as shown in Figure 3.

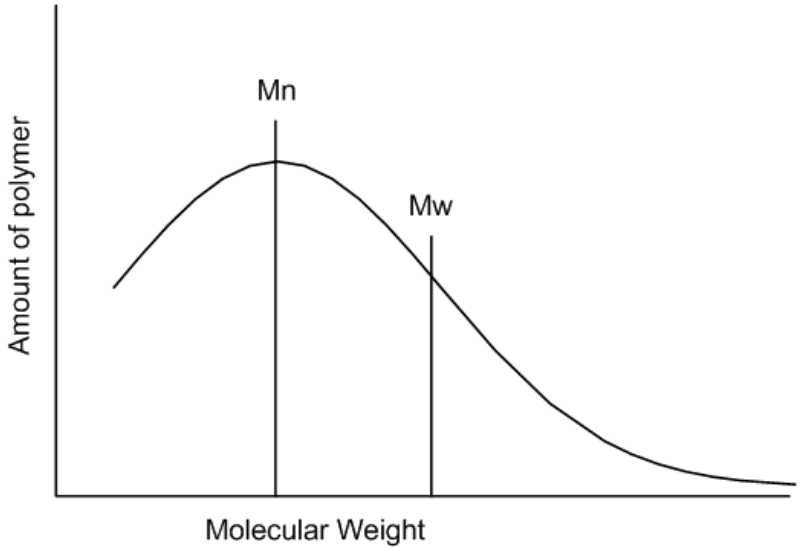

Figure 3 Molecular Weight Distribution

The number average molar mass (M_n) is the weighted average with respect to the number of moles, where N_i is the number of moles of the polymer with a molecular weight M_i:

$$M_n = \frac{\Sigma(N_i * M_i)}{\Sigma(N_i)}$$

The mass average molar mass (M_w) is the average with respect to weight of the species, where Wi is the weight of the polymer with a molecular weight M_i (W_i=M_i*N_i):

$$M_w = \frac{\Sigma(W_i * M_i)}{\Sigma(W_i)}$$

Another important characteristic parameter of a polymer is the polydispersity index which allows to understand if a material is homogeneous (D approximately 1) or it has a wide distribution of chain lengths (D>>1):

$$D = \frac{M_w}{M_n}$$

The molecular weight influences the mechanical properties and the workability of a material. Moreover, the processability of a polymer is closely linked to the solubility of the material: the higher is the solubility and the easier is the material to process. For these reasons, it is important to obtain a molecular weight that can satisfy the required mechanical and process qualities and usually the optimum interval is from 20000 g/mol to 200000 g/mol.

2.2 Hydrogels

The term “hydrogel” defined a hydrophilic three-dimensional polymeric network able to absorb a large amount of water or biological fluids. It is possible to classify these kinds of materials considering their physical structure (amorphous or semi-crystalline), their electrical charge (neutral, charge or amphoteric), their stimuli-responsiveness (i.e., the ability to change their characteristics in response to external cues such as pH, temperature or other), their origin (natural, synthetic or bioartificial) or their crosslinking type and degree. This last classification allows to distinguish two types of hydrogels: i) chemically crosslinked hydrogels, which present covalent bonds among the chains (permanent or chemical gels) and ii) physically crosslinked hydrogels, which transition from the sol to the gel state is based on the formation of physical interactions among the polymer chains, such

as hydrogen bonds, ionic interactions, hydrophobic interactions or molecular entanglements (non-permanent or reversible gels). Obviously, permanent and non-permanent gels have very different characteristics because of their intrinsic structure.

Chemically crosslinked hydrogels are called “permanent” because their chains are held together by strong bonds (i.e., covalent bonds) that provide the resulting materials with good stability. The ability of chemical hydrogels to swell depends on the characteristic crosslinking density. However, it is necessary to consider that even permanent hydrogels are not homogeneous in their structure: this kind of materials could present regions called ‘’clusters’’ with higher crosslinking density and therefore less swelling capacity due to a further hydrophobic aggregation of crosslinking agents. Permanent hydrogels can be obtained using different methods: starting from monomers or macromers having double reactive sites, a crosslinking agent is added and a radical polymerization occurs directly in the mould used. The same process can be followed from monomers and polymers that are bi-functional, polyfunctional or that have pendant groups that bind covalently in order to obtain the hydrogel network.

Physical hydrogels do not show homogeneity in their structure since they are organized into clusters of ionic bonds, molecular twists or hydrophobic domains. Any interaction in a reversible gel can be destroyed by external stimuli like pH, application of stress, temperature or addition of specific solutes [1]. The capability of these systems to degrade or disintegrate and dissolve in aqueous environment makes them an interesting alternative for biomedical applications as in that way the material does not remain for long periods of time inside the body. Additionally, this property allows them to release drugs or even cells. Hence, they are preferred to chemical hydrogels in some biomedical applications, such as for drug release as they do not contain toxic substances (e.g., photoinitiators, crosslinking agents, …) which may affect the biocompatibility of the system. There are different kinds of physical hydrogels including pH sensitive hydrogels, ionic crosslinked hydrogels and thermosensitive hydrogels. Considering those sensitive to the pH, they expose acid (e.g., COOH) or basic groups (e.g., NH_2) that release or accept protons in response to changes in environmental pH and for that reason they may have a reversible phase transition depending on the external conditions. As regards to hydrogel characterised by ionic crosslinking, their forming materials expose acid and/or basic groups that, depending on

the pH, become polyelectrolyte by exposing a charge. In these conditions, the addition of an electrolyte with opposite charge will lead to gelation with the formation of ionic bonds among the chains. Finally, a thermosensitive hydrogel is composed of an alternation of hydrophilic and hydrophobic blocks (amphiphilic). When this type of polymer is solubilized in an aqueous solution, its chains tend to form micelles that expose hydrophilic groups to the outside and keep the hydrophobic blocks inside, thus minimizing the interactions between hydrophobic blocks and water molecules. In this case, temperature results to be the stimulus that allows to change the physico-mechanical properties of the hydrogel; indeed, at a precise temperature a phase transition from solution to gel occurs. A thermosensitive hydrogel can show one of the two following behaviours during the phase transition: lower critical solution temperature (LCST) and upper critical solution

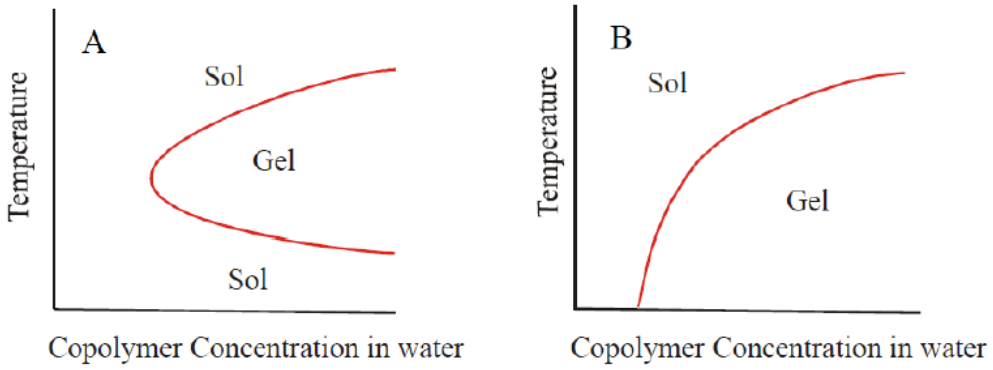

Figure 4 (A) Lower critical solution temperature behaviour; (B) Upper critical solution temperature behaviour

temperature (UCST) (Figure 4).

In both cases, a minimum concentration (critical gelation concentration CGC) of polymer must be reached to obtain gelation. For samples that are characterized by a LCST behaviour it is possible to observe gelation at a temperature above the lower critical gelation temperature (LCGT) and below the upper critical gelation temperature (UCGT), while for UCST hydrogels the phase transition is obtained at a temperature lower than a critical value. Having regard to the application in the biomedical field, systems with an LCST behaviour are preferred for their ability to encapsulate both cells and very sensitive and critical molecules (e.g., growth factors) in mild conditions.

Hydrogels are characterized by three important properties to consider:

1. **Water content**: it is important to understand how much water can enter in the network and how much the hydrogel can maintain its shape while swelling.

Initially, the hydrogel absorbs water that is attracted by hydrophilic domains and so bonds are formed between the hydrophilic parts of the material and water inlet (primary bound water). Additionally, the gel also exhibits non-hydrophilic groups and water continues to interact also with them (secondary bound water). After these two kinds of interactions, still a part of liquid enters in the network due to the osmotic effect (free water) and occupies the empty spaces among the chains, large pores, macropores and voids. Only when a balance is established, the chains will begin to oppose to the entrance of fluids (equilibrium swelling level).

If the gel does not show good stability, as physical hydrogels, it will physically degrade and dissolve, showing a deswelling (wet weight loss). On the contrary, a stable gel will tend to swell keeping its internal network intact.

In order to understand the amount of water content in a hydrogel, the wet weight of the sample must be measured. So, first of all, it is necessary to measure the weight of the sample at zero time (W_0), then incubate it in contact with a water-based medium and finally keep it in the medium for different time intervals (t_i). At each time point (t_i), hydrate samples are withdrawn and their wet weight is measured (W_{ti}). The following formula allows to calculate the absorption of water-based media by a hydrogel system:

$$Water\ absorption(\%) = \frac{W_{ti} - W_0}{W_{ti}} * 100$$

By observing the samples for an appropriate number of time intervals, it is possible to obtain a curve until equilibrium is reached. When the hydrogel swells:

- Superficial chemistry changes;
- Mechanical properties vary;
- Encapsulated drugs could be better released as the relaxation of the network is occurring.

It is very reasonable that the hydrogel loses weight during the absorption of water, and this is estimated using the same method explained above but for each time step it is necessary

to dry the samples, in order to eliminate the residual water ($W_{freeze\ dried\ gel\_0}$ and $W_{freeze\ dried\ gel\_i}$). Based on these data, hydrogel weight loss can be calculated according to the following equation.

$$Hydrogel\ weight\ loss(\%) = \frac{W_{freeze\ dried\ gel\_0} - W_{freeze\ dried\ gel\_i}}{W_{freeze\ dried\ gel\_0}} * 100$$

Weight loss occurs when many hydrolysable groups are present in the sample, or when some chains are not properly bonded (they can be released), or when the crosslinking is not permanent (as for physical hydrogels).

2. **Mesh size:** the mesh width of the network plays a key role in drug delivery applications and in the diffusion of nutrients and catabolites when cells are encapsulated into a hydrogel. Considering a system for drug release, when the dimensions of the mesh are like those of the encapsulated molecule, the diffusion will be slow. If the molecules are larger than the mesh of the network, the hydrogel must degrade, swell or it must be mechanically deformed to allow the release. Instead, if the drug is smaller than the mesh size, the release is very fast (Figure 5 [2]).

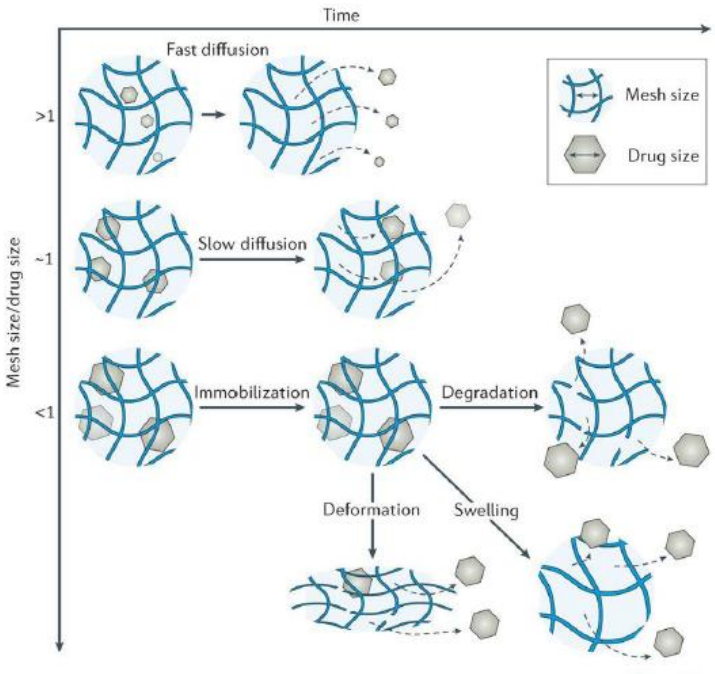

Figure 5 Drug release and mesh size

In the event that cells are encapsulated inside the hydrogel, the mesh size of the network shall ensure the entrance of nutrients and the spillage of catabolites.

It is possible to estimate the mesh size by measuring the release of labelled molecules with different size encapsulated inside the hydrogels. One of this kind of compounds is fluorescein isothiocyanate-dextran (FTIC-dextran, FD) that is available with different molecular weight to mimic molecule with different dimensions. FTIC-dextran has the advantage of being easily detected by optical spectroscopy in the range from 350 nm to 600 nm with the main absorption peak at 493 nm. Firstly, it is necessary to select a hydrodynamic diameter dimension of the dextran to be investigated (i.e., a molecular weight) and insert a precise number of molecules into the sample. Using Uv-visible spectroscopy, it is possible to obtain the release curve that allows to understand the release kinetics, which is related to the mesh size: when the dimensions of dextran are smaller than the dimensions of the network, it is possible to obtain a burst or enhanced release.

Using the same molecule, it is possible to comprehend the FD diffusion coefficient using the method offered by Sultana and Khan [3]: the permeability of the sample can be estimated by selecting a specific size of the probe molecule and the nutrients transport through the sample is also evaluated. After the gelation of the hydrogel, a solution of phosphate buffered saline (PBS) and FD is added to the gel and then the sample is incubated at 37 °C. At selected time steps, the residual PBS/FD solution is collected, and its absorbance is analysed using UV-visible spectroscopy. A calibration curve based on FD/PBS standards at precise concentration is used to residual amount of FD in the elute. Knowing the initial FD (FD_0) content within the solution added to the sample, it is possible to understand the amount of FD absorbed into the hydrogel by calculating the difference of FD_0 and the residual FD. The following formula is used for the estimation of FD diffusion coefficient (D):

$$\frac{w_t}{w_\infty} = 2\left(\frac{Dt}{\pi l^2}\right)^{1/2}$$

where w_t is the amount of FD at time t that is the considered absorption time, w_∞ corresponds to FD_0 and l is the distance between the free surface and the surface in contact with the hydrogel of the FD solution in PBS [4].

A more sophisticated method to characterize the mesh size is the Flory-Rehner equation that can be used to analyse hydrogels without ionic domains. This formula describes the mixing of polymers and liquid molecules. According to this theory, the changes in total free energy involved in the mixing of pure solvent with a crosslinked sample (ΔG_{tot}) can be calculated by the difference between the elastic free energy derived from the elastic forces of the extension of polymeric chains ($\Delta G_{elastic}$) and the variations of free mixing energy (ΔG_{mixing}).

$$\Delta G_{tot} = \Delta G_{elastic} + \Delta G_{mixing}$$

The size of the pores is defined as the linear distance between two neighbour crosslinks (ξ):

$$\xi = \alpha({r_o}^2)^{1/2}$$

$$\alpha = \upsilon^{-1/3} \qquad ({r_o}^2)^{1/2} = l(C_n N)^{1/2} \qquad N = {}^{2M_c}/_{M_r}$$

where α is the elongation ratio of the polymer chains, r_o is the distance between two polymer chains in an unperturbed situation, υ is the volume fraction of the swollen polymer ($V_{polymer}/V_{total}$), C_n is the Flory characteristic ratio (4<C_n<10), N is the number of links per chain, M_c is the molecular weight between adjacent crosslinks and M_r is the molecular weight of the polymer units. Based on these formulas, the mesh size ξ can be calculated as:

$$\xi = Q^{1/3} l(Cn \frac{2M_c}{M_r})^{1/2}$$

where l is the bond length along the polymer backbone and Q is the volumetric swelling ratio $V_{total}/V_{polymer}$.

In the case of $Q > 10$ it is possible to use the simplified Flory-Rehner-equation:

$$M_c = \frac{Q^{5/3} V_1}{((\frac{1}{2} - 2\chi_1)\upsilon}$$

where υ is the specific volume of the polymer, V_1 the molar volume of water (18 cm^3/mol) and χ_1 is the Flory Rehner interaction parameter.

3. **Character of water** (''free water'' or ''bound water''): small probe molecules or Differential Scanning Calorimetry (DSC) are used to characterize the water inside the hydrogel. DSC analysis characterizes the thermal properties of the material considering that if a sample is frozen only the crystals of free water will be formed. According to this test, the amount of bound and free water is calculated by heating the investigated hydrogel and a reference sample: the appearing endothermic peak in the thermogram represents the melting of free water presents in the hydrogel and the fusion enthalpy is calculated by the area under the curve. In that way it is possible to measure the amount of free water: the amount of bound water is obtained by a simple difference between the total water present in the sample and the calculated free water. As mentioned above, another method for understanding the character of the absorbed water is the use of a probe molecule which is dissolved in a solution where the dried hydrogel is inserted. When the swelling balance of the material is reached, the solution in contact with the polymer is analysed and the absorbance of the present probe molecule is assessed by Uv-visible spectroscopy. Using a calibration curve, it is possible to calculate the amount of the non-entering probe molecule inside the material and also how much has entered inside the sample. In that way the amount of free water is calculated, assuming that the probe solute is dissolved in the gel only by free water.

Based on the aforementioned characteristics of hydrogels and their huge potential and versatility, one of the many applications of gelling systems is in tissue engineering/regenerative medicine.

2.2.1 Hydrogels in Regenerative Medicine

Regenerative medicine aims to regenerate damaged tissues and replace them with healthy ones or by stimulating healthy tissue growth [5]. This approach gives the possibility to have an alternative to tissue transplantations which can have unpleasant consequences: for example, a xenograft can cause an inflammatory response and a rejection from the body where it has been implanted; an allograft can also activate the inflammatory response and in addition donors are few compared to the request. Therefore, alternative methods are sought with tissue engineering: it is necessary to find materials that are biocompatible, biodegradable and also bioactive in order to give the correct stimuli for the regeneration of a healthy tissue [6][7]. In this way, a biomaterial studied "*ad hoc"* can give support, stimuli, send cells, genes or drugs in such a way as to properly stimulate the surrounding tissue and start the production of the healthy one. Among the many materials that are used in this innovative field of medicine, hydrogels are excellent candidates for the different functions that they can exert. This class of materials has structures and compositions that are very similar to the native extracellular matrix of tissues; hence, they can also be used for cell migration, adhesion and proliferation. Some of their applications in tissue engineering are:

1. Scaffolds: it is a platform that allows to best regenerate the structure of the n native extracellular matrix of a tissue. In many studies, synthetic hydrogel forming materials material have been used in combination with biological materials that allow a better biomimetic behaviour of the framework and a better cellular adhesion. For instance, RGD is a peptide sequence that increases cell adhesion upon exposure on the hydrogel surface: in this way the cells tend to colonize it and reconstruct the characteristic extracellular matrix of the tissue while the scaffold initially acts as a support and then degrades [8]. For these applications the kinetics and the nature of the products of degradation of the hydrogel are essential to monitor because degradation kinetics should be in line with the tissue growth and the resulting degradation products must be biocompatible.

2. Barriers: in some cases, hydrogels are used as thin coatings of vessels or as coatings of organ surfaces (e.g., peritoneal surface) to avoid adhesion of unwanted cells or tissues. For instance, a hydrogel suitable for photopolymerization on the wall of a

blood vessel has been developed to avoid the adhesion of platelets, coagulation, thrombosis and intimal thickening [9].

3. Drug Delivery: much attention was paid to the application of hydrogels as carrier for drugs and proteins. Because of their high hydrophilicity and biocompatibility, hydrogels can be formulated to finely regulate the release kinetics of molecules that are encapsulated inside them. In order to obtain a controlled release, swelling kinetics, degradation rate and cross-linking density of the biomaterial should be properly controlled.

4. Cell Encapsulation: hydrogels also give the possibility to encapsulate cells and then, the whole system can be transferred inside the human body. The typical hydrogel structure and hydrophilic nature make cell encapsulation feasible, allowing nutrients to enter, and metabolic wastes of the cells to be released.

Among all these fields of application, one of the most investigated is the use of hydrogels as carriers of molecules and drugs. For this specific application, strict requirements exist concerning biocompatibility of the system and of its degradation products, as well as hydrogel mechanical, chemical and physical properties of degradation and swelling. In addition, it is necessary to obtain a system that can release its payload in a controlled and effective way for the treatment but at the same time that has a controlled transition from solution to gel. Thermosensitive hydrogels could meet all these characteristics thanks to their ability to become gel from an easy injectable solution under certain thermal conditions.

2.2.2 LCST Hydrogels for biomedical applications

A system designed for the transport of molecules must have specific properties. Firstly, the system has to protect the transported payload against the surrounding environment that could denature proteins or damage drugs. Another indispensable characteristic is to be able to control the response of the body, in order to avoid a marked inflammatory response or a possible kind of toxicity. In addition, it must succeed in delivering the drugs in a controlled manner, avoiding a rapid release if not necessary and maintaining an appropriate dose of medicine in the treated area. Focusing on these important characteristics, the systems that can satisfy them are those made by gels able to react and change their structure after receiving an external stimulus. In fact, as reported above, Lower Critical Solution Temperature Hydrogels (LCST) are used in the biomedical field thanks to their gelation properties and their ability to transport different compounds. Using these kinds of materials, chemically cross-linked hydrogels can be avoided. Thermosensitive gels can be simply combined with drugs by mixing the two components and, considering LCST hydrogels, at room temperature they are easily injectable polymeric solutions/semi-gels while, once administered into the human body (37 °C), they will become gels able to release the encapsulated medications in a controlled way.

LCST hydrogels are formed thanks to the entropy (S) of the two phases (i.e., polymer and water): when the variation of enthalpy (ΔH) is less than the entropy (which is positive), a negative free energy (ΔG) according to the following formula:

$$(\Delta G) = (\Delta H) - T(\Delta S)$$

In these conditions association in favourite. This thermodynamic phenomenon can be chemically explained by the formation of hydrophobic interactions and hydrogen bonds between different polymeric chains. As a consequence of these physical changes, a different degree of swelling can be achieved, which could be exploited for the design of drug releasing systems. In fact, there are several methods to take advantage of swelling in drug release, as shown in figure 6. A Fickian release for hydrophilic drugs is achieved below LCST value because the hydrogel is swollen and the drug can exit from the polymeric network (Figure 6 A, [10]). Contrarily, when the temperature is above the LCST, there is a Fickian diffusion (for hydrophobic drugs) with the hydrogel undergoing shrinkage and the resulting pressure tending to throw out the drug molecules (Figure 6 B). Another method is to use a porous membrane with inside the hydrogel containing the drug. When the temperature is below the LCST, the polymer is swollen, and the pores are closed, but when the hydrogel is gelled (T>LCST) then the pores are opened and it is possible to spread out the encapsulated medicine (Figure 6 C). The last system described and shown in Figure 6 D is a heterogeneous hydrogel where, above the LCST, only the surface becomes gel, leaving the core swollen [10].

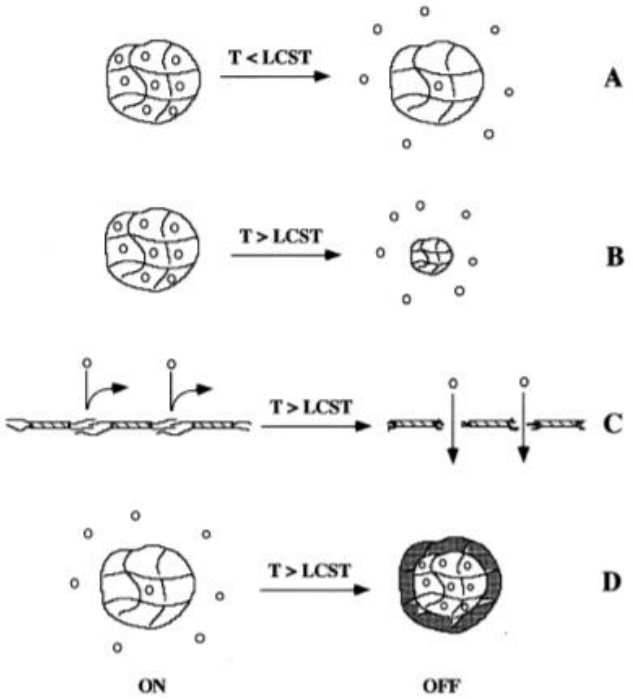

Figure 6 Drug delivery of LCST Hydrogels

Among the most widely used materials for their LCST behaviour and for their drug carrying capabilities there are block-copolymers called Pluronics® or Tetronics®, that are formed by poly(ethylene oxide) (PEO) and poly(propylene oxide) (PPO) domains (Figure 7 [11]). Their

used in the biomedical field has been approved by United States Food and Drug Administration (FDA) and Environmental Protection Agency (EPA).

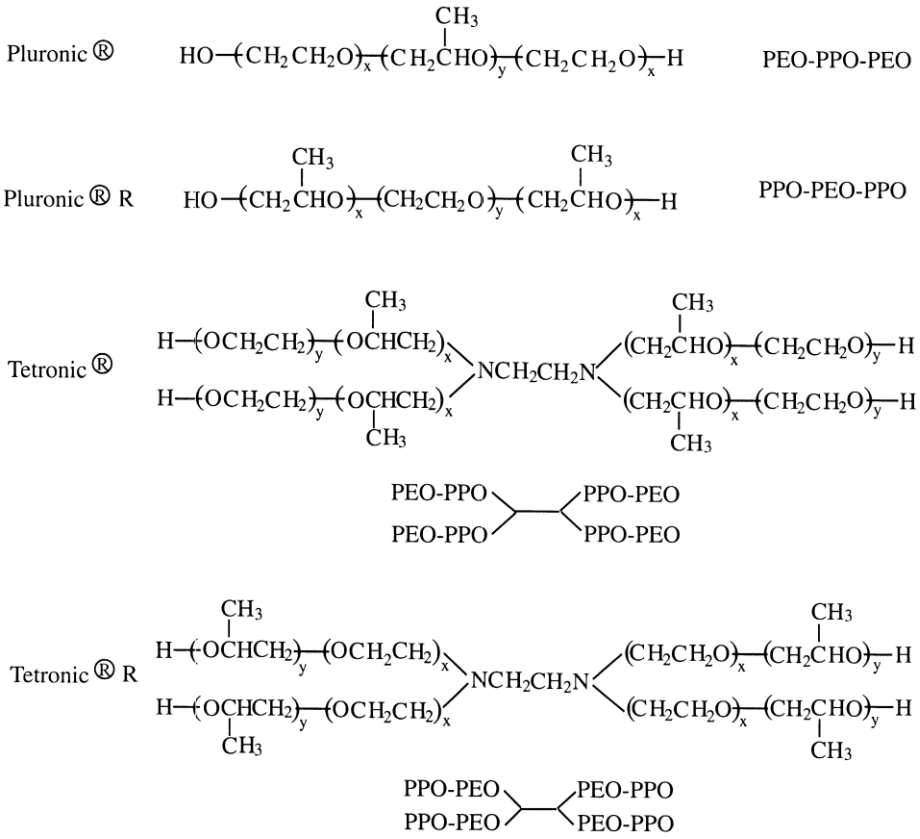

Figure 7 Copolymers formed by PEO and PPO groups

2.2.3. Pluronic®

Pluronics® (or also called Poloxamers®) are PEO-PPO-PEO triblock copolymers. They are commercially available with different lengths depending on the number of groups that compose them. Due to the presence of an alternation of hydrophilic (PEO) and hydrophobic (PPO) blocks, these polymers show an LCST behaviour characterised by the formation of micelles.

The formation of micelles occurs when the Critical Micelle Concentration (CMC) is exceeded: below this there are only single copolymer units (called unimers) which begin to self-assemble when this concentration is reached. Maintaining a constant temperature, the CMC depends on the balance between EO (ethylene oxide) and PO (propylene oxide) domains so that it increases if the length of the EO block increases and it decreases if the

length of the PO block increases. Instead, with an increase of temperature, CMC tends to diminish [12]. To calculate it, some of the most used methods are chromatography, light scattering and fluorescent assay exploiting fluorescent probes.

Another important parameter is the Critical Micelle Temperature (CMT) which defines the temperature of the onset of micellization. Indeed, at this temperature DSC thermograms report an increase of the endothermic heat proportional to the length of the PO-based block as the phenomenon of micellization progresses over temperature. This behaviour can be explained by surface tension measurements, making it clear that with the increase of temperature, PO groups dehydrate, enhancing hydrophobicity and promoting the formation of micelles [12]. Therefore, it is important that both CMC and CMT are reached for micelle formation.

Considering the phase transition diagram reported in Figure 8, when the Critical Gelation Concentration (CGC) is reached, it is possible to observe a Sol-Gel transition maintaining the temperature between the Lower Critical Gelation Temperature (LCGT) and the Upper Critical Gelation Temperature (UCGT). All these temperature parameters can be modified: LCGT decreases when the hydrophobicity and/or the concentration of the polymeric solution increase. Moreover, the LCGT can be reduced also by adding some additives (e.g.,

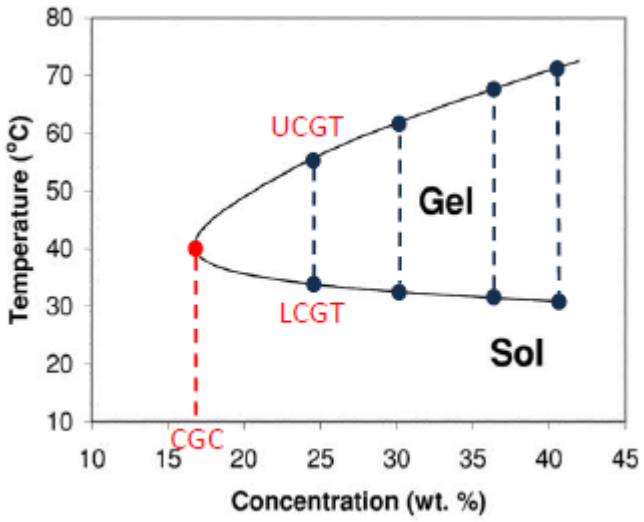

Figure 8 Phase Diagram of LCST sol-gel system

NaCl) or using a saline solution to solubilize the material instead of pure water.

The Solution to Gel transition is possible thanks to the formation of micelles characterized by a hydrophobic core (composed by PPO groups) and an hydrophilic shell (made of PEO

groups): at a temperature below the LCGT and at a concentration above the CGC, polymeric micelles are formed and there is a prevalence of hydrogen bonds between water and hydrophilic groups; as the temperature increases (when it is greater than LCGT), hydrophobic bonds begin to form between the PPO groups of different micelles, overcoming hydrogen bonds. By increasing the temperature, the size of the micelles increases (thanks to the new formed bonds) and a compact gel is finally obtained. However, when the temperature is higher than the UCGT, the transition from gel to solution will be observed (Figure 9,[13]).

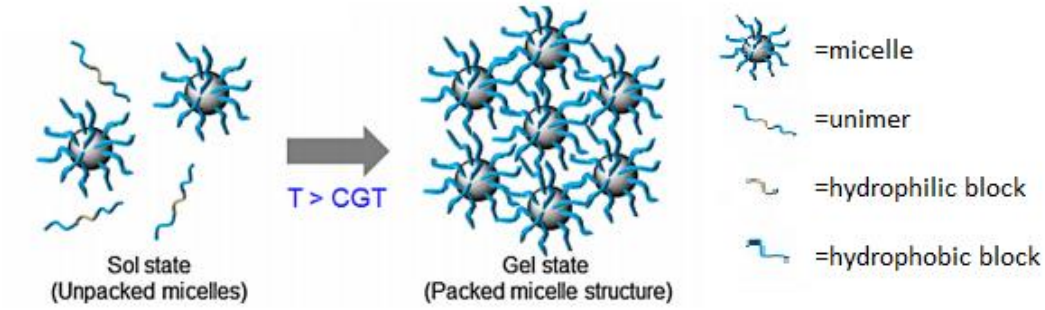

Figure 9 Sol-Gel Transition of an amphiphilic polymer showing LCST behaviour

These hydrogels are easily obtainable through simple solubilization of Pluronic powder in aqueous solutions, at a selected concentration. Dissolution should take place at low temperatures (3°C-5°C) so that the gelation process does not start.

Taking advantage of the formation of micelles, it is possible to exploit these materials as carrier for molecules. The core of the micelles repels water because it is composed of hydrophobic groups and it is completely enclosed by a hydrophilic shell, formed by PEO groups. Hence the micelle core or the interstitial space among micelles could be exploited to load compounds such as drugs, genes or diagnostic reagents [14]. In this way, also slightly soluble molecules, poorly stable in physiological environment or with an unsatisfactory pharmacokinetics can be transported and released in the area of the body to be treated. In this regard, it is essential to estimate the size of the micelles because if they are bigger than 200 nm they are taken from the spleen and then phagocytized; instead, if their diameter is smaller than 5-10 nm, they are rapidly excreted by the kidney. The micellar dimensions are strongly dependent on the composition of the copolymer blocks: keeping constant the number of PO groups and increasing the length of the EO blocks, the aggregation capacity and the size of micelles decrease. Therefore, depending

on the Pluronic used, micellar diameters between 20 nm and 80 nm have been observed as an excellent range for biomedical applications [15].

Exploiting the properties of these thermosensitive hydrogels, it is possible to form a system capable of encapsulating the drug in micelles and which can be injected, considering the fact that at room temperature it appears to be in solution/semi gel state while it gels inside the body.

For instance, Al Khateb et al. used Pluronic F127 alone and mixed with Pluronic F68 to design a drug delivery system capable of gelling on the cornea. Differential Scanning Calorimetry, Dynamic Light Scattering and Rheological Measurements evidenced that gelation occurs at higher temperatures than body temperature for systems containing also F68. In fact, only 20 wt% of F127 compound formulation containing fluorescein sodium turned out to be able to gel over the cornea and improve drug residence [12].

With Poloxamers it is possible to encapsulate Curcumin, that is highly hydrophobic, inside micelles. L. Zhao and co-workers studied the possibility to form a system based on two Pluronics which contain the drug molecules in their micelles. The two Poloxamers chosen are the P123, characterized by a large number of hydrophobic groups PO, and the F68 that contains many hydrophilic groups. In this way it is possible to obtain micelles that have the possibility of encapsulating the curcumin molecules in their hydrophobic interior. As evidenced by the solubility tests, it is possible to observe a clear solution when the polymer micelles are filled with drug while a cloudy solution is obtained when the curcumin is dissolved alone in a water solution. To obtain the micelles of P123 and F68 loaded with curcumin, it is firstly necessary to dissolve the three reagents in dichloromethane (CH_2Cl_2). Then they proceed with the evaporation of the solvent by rotary vacuum evaporation in order to obtain a thin film composed of polymer and drug which was dried overnight. To have the formation of micelles it is hydrated with double distillate water, dispersed using ultrasonication and the unreacted curcumin is separated by a filter (Figure 10, [16]). As regards drug release, it is noted that it is better when curcumin is encapsulated in polymer micelles: in this way it increases its pharmaceutical power, its bioavailability and the possibility of solubilization [16].

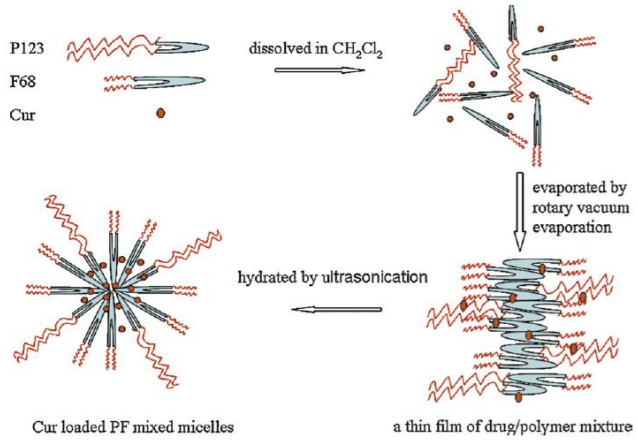

Figure 10 Schematic drawing on the production of micelles formed by P123 and F68 and loaded with curcumin

The use of Pluronics is not confined only to drug release but also to the encapsulation of cells. However, the work of Sarwat F. Khattak et al. showed that F127 cannot be used alone for this purpose. In fact, the concentration necessary for the formation of gels composed of F127 at 37 °C is not biocompatible, as assessed using different cell types. In order to overcome this drawback, some stabilizers of the cell membrane (such as hydrocortisone) should be added to allow cell encapsulation within P407 hydrogels with no detrimental effects on their viability.

Unfortunately, there are also some disadvantages in the use of hydrogels based on Poloxamers that limit their application in the biomedical field: they do not possess excellent mechanical properties, they tend to quickly dissolve in aqueous environment, and they are permeable in watery environment. In addition, as mentioned above, the LCST behaviour is achieved by solubilizing these materials at high concentrations, which is not compatible with a good cell viability. For these reasons, Poloxamers are commonly used as macrodiol in the design of polyurethanes which aqueous solutions can show improved gelation and mechanical properties, as well as residence time in aqueous media.

2.2.4. Polyurethanes

Polyurethanes are characterized by urethane groups (Figure 11) and they are composed of a macrodiol, a diisocyanate and a chain extender which bind each other in a predefined order during a two-step poly-addition reaction.

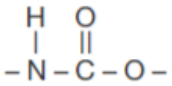

Figure 11 Urethane group

During the first step of the reaction, the hydroxyl groups of the macrodiol bind with the isocyanate terminal groups of the diisocyanate, to form the urethane bonds that constitute the prepolymer (Figure 12). This process is a staged polyaddition in the presence of a catalyst.

During the second step of the reaction, the chain extender is added to the prepolymer

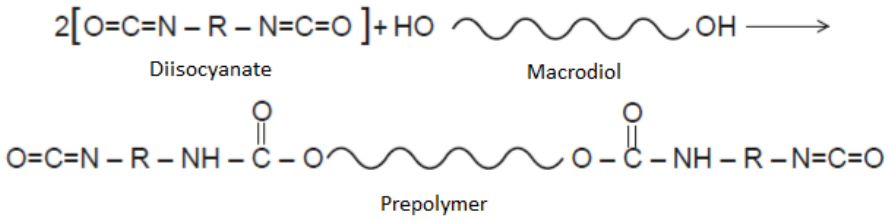

Figure 12 Synthesis of prepolymer from macrodiol and diisocyanate

solution in order to finally obtain a chain-extended polymer. Both diols or diamines can be used as chain extender, obtaining poly(urethane)s or poly(urethane ureas)s, respectively.

Being synthetic multiblock copolymers, the properties of polyurethanes can be finely modulated through a proper selection of their building blocks. In addition to the great chemical versatility that is achieved using different components, also the mechanical and thermal properties, surface characteristics, biocompatibility and biodegradation can be tuned in the same way. For example, it is possible to modify the hydrophobic/hydrophilic balance using different macrodiols: Pluronics can be selected depending on the number of EO and PO groups, where an increase in ethylene oxide groups promotes greater hydrophilic properties of the material while a higher amount of propylene oxide groups induces an increase in hydrophobicity. Tuning this balance also varies the speed and temperature of gelling and the ability to resist in aqueous environment. Polyurethanes can

contain building blocks that have the ability to graft biomolecules. To obtain this specific feature, for example, N-Boc serinol can be used as chain extender so that, after deprotection, the resulting polyurethane exposes free primary amino groups which can be exploited for their antibacterial potential [17], but also to open the way to the possibility to graft other chemical groups or biomolecules to the polymer backbone.

With regard to the antibacterial potential of exposed amino groups, M. K. Calabretta and co-workers compared the effects of poly(amidoamine) dendrimer (PAMAM) (unmodified or partially decorated with PEG) and antimicrobial peptides on different bacteria. Amino groups exposed by PAMAM made it able to show higher toxicity effect on Gram-negative bacteria compared to the investigated antimicrobial peptides [17].

However, as a result of their high compositional versatility and, as a consequence, the high variety of physico-chemical properties that can be achieved, polyurethanes biomaterials can find widespread application in the biomedical field. For instance, rigid polyurethane scaffolds can be used for bone reconstruction [18], while softer polyurethanes can be applied in the reconstruction of soft tissues or the design of drug/cell delivery systems [19].

Hence, designing hydrogels from custom-made polyurethane can open the way to the possibility to overcome the limitations of commercially available sol-gel systems. For instance, Boffito et al. compared the properties of hydrogels based on F127 (or P407) with those of hydrogels with the same composition (i.e., polymer concentration) and prepared starting from an amphiphilic polyurethane containing F127 as building block [4]. P407-based hydrogels showed higher CGC, worst mechanical properties, slower gelation kinetics and poor stability under physiological conditions (i.e., aqueous environment and 37 °C) compared to NHP407-based hydrogels, which also resulted to be injectable, biocompatible and able to retain their shape. In addition, a wide plethora of hydrogels with different properties was easily designed by simply chaining polyurethane concentration within the formulations, thus making the developed sol-gel systems suitable for a variety of different applications, such as drug delivery and scaffold bioprinting. For instance, C. Pontremoli, M. Boffito et al. designed hybrid injectable formulations based on a F127-based polyurethane and mesoporous bioactive glasses doped with copper, for the localized, sustained and prolonged release of copper species which exert antibacterial activity and are great for stimulating new bone formation and angiogenesis. Particle loading within thermosensitive

hydrogels did not affect their gelation properties. Hence, injectable and fast gelling hydrid sol-gel systems were successfully designed showing a long-lasting ion release and a significantly lower burst release compared to the particles as such [20].

Amphiphilic polyurethanes can find application also in the design of injectable supramolecular hydrogels. In this case, polyurethanes are used as synthetic component of bioartificial gels which gelation is driven by supramolecular physical interactions occurring between polyurethane chains and commercially available cyclodextrins.

2.3 Cyclodextrins

The era of cyclodextrins (CDs) began in 1891 with the pioneering work carried out by Villiers, who observed and studied the characteristics of the crystals obtained from starch produced from an impure bacterial cultivation [21]. However, the real founder of cyclodextrin chemistry was Schardinger, who, in his works from 1903 to 1911, isolated the bacterium responsible for the synthesis of these molecules [22][23][24]. In the following years new studies were carried out and nowadays cyclodextrins are used also in the biomedical and pharmaceutical fields, thanks to the in-depth knowledge obtained until now and also to all their advantageous features [25] [26] [27]. As mentioned before, CDs are derived from starch and they have also been included in the FDA's GRAS list. Indeed, cyclodextrins can be used in drugs, cosmetics or foods because of their high biocompatibility. Their production is not dangerous for the environment and simple, thus making them quite cheap.

Cyclodextrins are natural cyclic oligosaccharides, formed by D(+)-glucopyranose monomers joined together by glucosidic α,1-4 binding and ring closed. Depending on the number of monomers present in the ring, α- (6 monomers), β- (7 monomers) and γ-cyclodextrins (8 monomers) can be differentiated. In addition to compositional differences, the three different cyclodextrins also differ in terms of dimensions and water solubility (Table 1, [26]). Using different synthesis methods, cyclodextrins can also be functionalized in order to

obtain even more specific properties for every need. For instance, polymethacrylate cyclodextrin can be obtained using click chemistry reactions [28].

Table 1 Main Characteristics of α-,β-,γ-Cyclodextrins

	α	β	γ
no. of glucose units	6	7	8
mol wt	972	1135	1297
solubility in water, g 100 mL^{-1} at room temp	14.5	1.85	23.2
$[\alpha]_D$ 25 °C	150 ± 0.5	162.5 ± 0.5	177.4 ± .5
cavity diameter, Å	4.7–5.3	6.0–6.5	7.5–8.3
height of torus, Å	7.9 ± 0.1	7.9 ± 0.1	7.9 ± 0.1
diameter of outher periphery, Å	14.6 ± 0.4	15.4 ± 0.4	17.5 ± 0.4
approx volume of cavity, $Å^3$	174	262	427
approx cavity volume in 1 mol CD (ml)	104	157	256
in 1 g CD (ml)	0.10	0.14	0.20
crystal forms (from water)	hexagonal plates	monoclinic parallelograms	quadratic prisms
crystal water, wt %	10.2	13.2–14.5	8.13–17.7
diffusion constant at 40 °C	3.443	3.224	3.000

The three-dimensional structure of cyclodextrins can be schematized as a truncated cone that presents on the narrower end the primary hydroxyl groups while on the wider extremity the secondary ones (Figure 13, [29]).

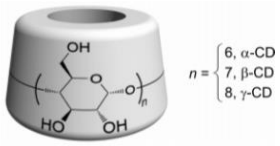

Figure 13 Drawing of Cyclodextrin

Another important characteristic is that they have a hydrophilic outer surface and a hydrophobic inner cavity: this allows them to host and transport molecules such as drugs through the formation of inclusions complexes. These complexes can also be formed between cyclodextrins and chains of linear and aliphatic polymers and, in this case, poly(pseudo)rotaxanes are obtained. Exploiting the possibility to form hydrogen bonds through the external surface of the cyclodextrins that make up the poly(pseudo)rotaxanes, it is possible to obtain further supra-molecular complexes when more structures spontaneously come in contact.

2.3.1 Cyclodextrins Inclusion Complexes

Cyclodextrins can be used for their ability to accommodate molecules inside the hydrophobic cavity, thus forming inclusion compounds. The forces that allow to have links between host and guest are mainly hydrophobic and Van der Waals interactions, although in some cases hydrogen bridges and electrostatic interactions can play a key role in the design of complexes [30]. A necessary condition for obtaining the inclusion complexes is that the size of the molecule is compatible with the smaller diameter of the cyclodextrin cavity (Figure 14, [29]); if the molecule is larger than the minimum size of the cavity, it cannot enter and no complexes can be formed.

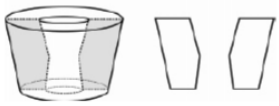

Figure 14 Drawing and section on cyclodextrin axis

Different type of compounds can be formed depending on the molecule entering the cavity[29]:

1. Channel-like Inclusion Compounds: when the guests are hydrophobic, they are stabilized by the cyclodextrins that align forming an interconnection between the cavities. The optimal arrangement of the cyclodextrins to obtain the channel is head-to-head because hydrogen bonds are better formed between two primary hydroxyl groups and two secondary hydroxyl groups, which is not the case with head-to-tail positioning. These compounds tend to pack in such a way as to obtain crystals that are insoluble in water and dissolve only in highly polar organic solvents (Figure 15, [29]).

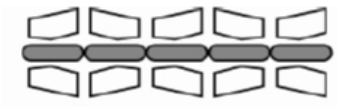

Figure 15 Channel Inclusion Compounds

2. Inclusion Compounds of Amphiphiles: for amphiphilic guests, complexes do not position in order to create a channel but remain single, maintaining a 1:1 stoichiometry of CD/guest (Figure 16 a, [29]). In this case, the hydrophobic part of the molecules is placed inside the cavity of the cyclodextrin while the hydrophilic head remains outside, in order to not lose its contact with the surrounding aqueous environment. Aggregation with other complexes is impossible because of the

repulsive forces given by head groups. Only in one case a 2:1 stoichiometry of CD/guest can be achieved: when the hydrophobic tail of the molecule is long, a cyclodextrin completely penetrate, allowing another cyclodextrin to interact with the first, ensuring that its secondary hydroxyl groups interact with secondary hydroxyl groups of the other cyclodextrin (Figure 16 b, [29]).

Figure 16 Inclusion of Amphiphiles a) 1:1 b) 2:1 stoichiometry of CD/guest

3. Inclusion Complexes of Bola-Amphiphiles: the guest molecule in this case has the hydrophobic tail with two hydrophilic heads and therefore the formation of complexes will be slower because the hydrophilic end must pass the whole cavity of the cyclodextrin and position toward the exterior, spending a lot of energy. However, with regard to the disposition of molecules and cyclodextrins, complexes that are formed have a 1:1 or 2:1 stoichiometry of CD/guest, depending on the length of the hydrophobic part (Figure 17, [29]).

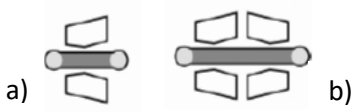

Figure 17 Inclusion of Bola-Amphiphiles a) 1:1 b) 2:1 stoichiometry of CD/guest

For pharmaceutical applications, cyclodextrins are used as carriers for lipophilic and poorly water-soluble drugs. Indeed, cyclodextrins and drug molecules form inclusion complexes in watery environment when the drug molecule has the appropriate size and characteristics to enter the cavity of cyclodextrins. For the formation of the compounds it is necessary to achieve in the solution a dynamic balance between free cyclodextrins, free drug molecules and complexes. The binding constant (or stability constant, $K_{m:n}$) can be calculated because the formation of inclusion compounds (D_mCD_n) is a reversible process where the stoichiometric ratio is *m:n* (the drug molecules (D) are represented with *m* and *n* is associated with cyclodextrins (CD)):

$$K_{m:n} = \frac{[D_m CD_n]}{[CD]^n \cdot [D]^m}$$

$$m \cdot D + n \cdot CD \overset{K_{m:n}}{\rightleftarrows} D_m CD_n$$

where molar concentration is denoted by square brackets [25].

Hence, the use of cyclodextrins with drugs brings excellent advantages, such as an increase in the solubility of the molecule in aqueous environment, its stability and bioavailability. Curves reporting the variation of drug solubility as a function of the concentration of drugs and cyclodextrins can be also obtained as reported in the illustrative graph in Figure 18 [27]. In the solubility diagram of drug-CD complexes two types of complexes can be identified: red lines indicate soluble drug-cyclodextrin complexes, while blue lines identify insoluble ones. These different behaviours depend on the type of complexes formed and the stoichiometry [27].

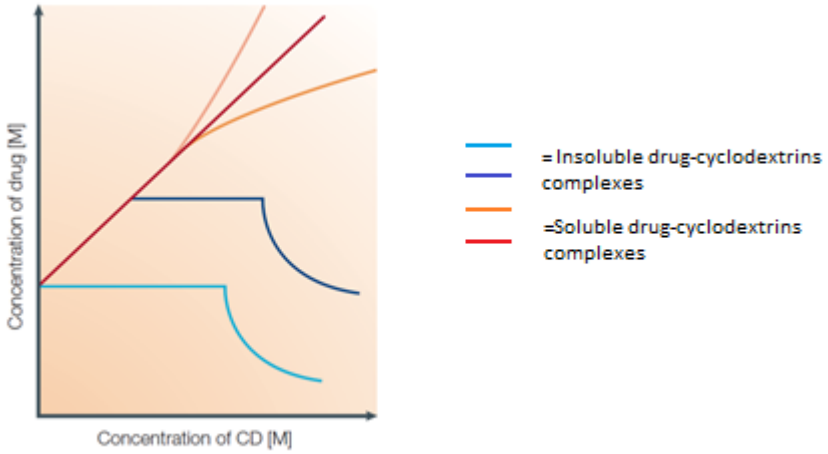

Figure 18 Solubility Diagram of drug-CDs complexes

An example of drug that could improve its properties with the use of cyclodextrins is curcumin (CUR). Curcumin has many healing and beneficial qualities, without showing any toxicity. Among the various pharmacological effects there are antioxidant, anti-inflammatory, anticancer, antimicrobial and promotes healing of wounds. The other biological assets are shown in the figure below [31].

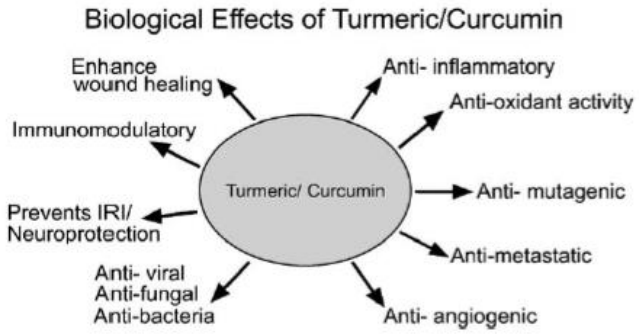

Figure 19 Biological effects of curcumin

However, curcumin administered as oral use is largely excreted by faeces and urine and it is poorly absorbed by the intestine. Hence, Ying-Jan Wang and co-workers studied the stability of this molecule in different physiological matrices and at different pH using the HPLC analysis. In addition, they evaluated species in which it degrades. They have obtained as a result that curcumin is more stable in a mix of culture medium and bovine serum (10%) and in human blood than in a phosphate buffer or in a simple culture medium. Additionally, at acids pH the molecule degrades less than when it is at basic or neutral pH. Another important result is that obtained on degradation products: they noted that after a long-lasting incubation in a 37°C buffer curcumin tends to degrade largely into vanillin. This degradation product shows excellent biological activity: it is antimutagenic, inhibits lipid peroxidation and formation of free radicals [32].

Unfortunately, also this drug is poorly soluble in water and therefore does not have the possibility to be very bioavailable in the site to be treated. Hence, many studies have been completed to understand how curcumin can be dissolved in aqueous solvent and one of these has been described above.

Nagaraju M. Patro et al. have studied the main advantages in the use of cyclodextrins with curcumin, comparing the results with the use of the drug as such. Curcumin is a drug difficult to solubilize in an aqueous environment (0,002 mg/mL [33]) and suffers for poor

bioavailability. The authors reported that the highest amount of complexes can be achieved using α-cyclodextrins, with a great increase in both the solubility and the stability of curcumin. In order to avoid the degradation of the drug, they used the co-grinding method to form the inclusion complexes, that finally resulted in an enhanced drug release (given by the increased solubility) and a greater amount of curcumin available for the treatment [33].

A study on the formation of inclusion complexes composed of β-cyclodextrins and curcumin in an aqueous solvent was also conducted by Murali Mohan Yallapu and co-workers and they applied these compounds to prostate cancer cells. In this case the β-cyclodextrins were used and the solvent evaporation technique was used to obtain the CDs/CUR inclusion complexes (Figure 20, [34]). Therefore, by many analysis techniques such as FTIR, ^{1}H-NMR, XRD, DSC and microscopic studies, the formation of complexes has been confirmed. Increasing the amount of curcumin also increases the potentialities in encapsulation of cyclodextrin and these formed complexes are more effective on prostate cancer cells than the drug molecules used alone [34].

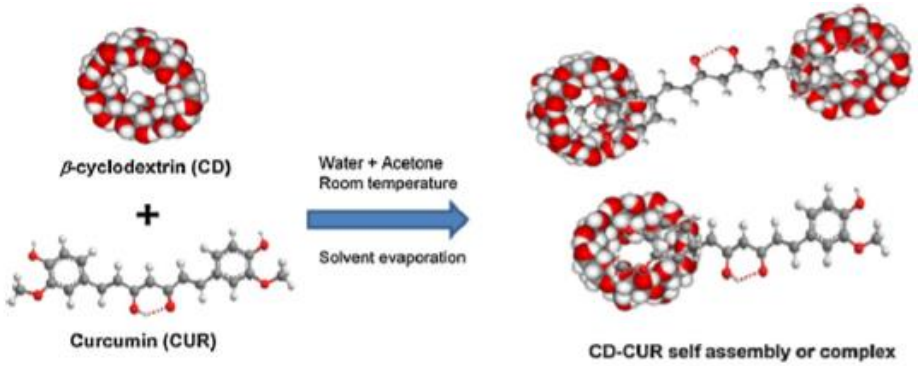

Figure 20 Solvent evaporation Techniques for the formation of CDs and Curcumin complexes

2.3.2. Cyclodextrins-based Poly(pseudo)rotaxanes

Cyclodextrins have the ability to accommodate inside their hydrophobic inner cavity not only molecules such as drugs but also polymeric chains and, in this case, the formed compounds are defined as Poly(pseudo)rotaxanes (PPRs). Schematically, these structures are formed by the threading of cyclodextrins onto the polymeric chains and the length of the latter will defined the length of the resulting poly(pseudo)rotaxane (Figure 21 [29]).

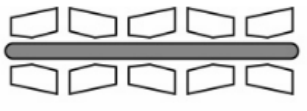

Figure21 Drawing of PPR

Poly(pseudo)rotaxanes are obtained when the binding enthalpy is lower than zero and this is ensured during the formation of bonds between cyclodextrins and the polymer chains. Van der Waals and hydrophobic bonds are formed between the polymer and the inner cavity of cyclodextrin molecules, while hydrogen bonds will appear between two adjacent cyclodextrins. To obtain a good stability it is necessary that the cyclodextrin cavity is completely filled and for this reason the three types of cyclodextrins (i.e., α, β and γ CDs) can accommodate different chains. For example, poly(ethylene oxide) (PEO) is hosted by α-cyclodextrins, while γ-cyclodextrins, due to their larger dimension, can contain two chains of the same polymer. In any case, if the polymer chain is larger than the internal diameter of cyclodextrin molecules, the complex cannot be formed. In addition, a maximization of hydrogen bonds between adjacent cyclodextrins is required to have a greater stability and a highly ordered structure. From this point of view, the head-head and tail-tail have resulted to be better packing conditions.

All these properties and information about the formation of poly(pseudo)rotaxanes were first studied by Akira Harada et al.. They were the first to report the preparation of complexes based on poly(ethylene glycol) (PEG) and α-cyclodextrins and to investigate their properties. In order to obtain the complexes, the authors added an aqueous solution of cyclodextrins to an aqueous solution of PEG and the resulting turbidity confirmed the formation of complexes. In addition, they noted that the stoichiometry of the compounds turns out to be 2:1 (EG:α-CD) and that the formed bonds were not ionic but as described above [35].

Many methods can be adopted to assess the formation of poly(pseudo)rotaxanes. First of all, X-ray structure analysis allows to separately identify free and tied cyclodextrins and for the latter head-head and tail-tail positioning can be distinguished from the head-tail packing. Unfortunately, single and large crystals are needed in order to carry out this analysis. In addition, in the case of β-cyclodextrins it is not possible to distinguish between free and packed CDs because of the poor symmetry that does not provide clearly evident peaks. Nuclear Magnetic Resonance spectroscopy (NMR) can be another analysis tool to evaluate the structure of the crystalline complexes formed by cyclodextrins. In fact, ^{1}H NMR allows to distinguish between free and occupied cyclodextrins and between coated and naked polymer chains. Instead, in order to visualize them through microscopic images Transmission Electron Microscopy (TEM), Scanning Tunnelling Microscopy (STM) and Atomic Force microscopy (AFM) could be exploited [29].

The formation of poly(pseudo)rotaxanes results in the development supramolecular structures such as hydrogels based on the self-assembly of the polymer chains covered by cyclodextrins.

2.4 Supramolecular Hydrogels formed by poly(pseudo)rotaxanes based on Cyclodextrins and homopolymers

Supramolecular structures are characterized by multiple levels of interactions between different molecules. For instance, in the case of poly(pseudo)rotaxanes the first interactions to appear are those between cyclodextrins and the polymer chains (consisting of a single block (homopolymer) or several blocks with different properties (copolymer)) followed by the bonds between cyclodextrins of two different poly(pseudo)rotaxane chains. Cyclodextrins that are threaded onto different polymer chains can interact through hydrogen bonds, leading to supramolecular crystals based on physical crosslinks. In that way the use of chemical crosslinking agents is not required, thus limiting the risk of issues regarding cytocompatibility and the presence of residual unreacted reagents. In addition, all of these structures have thixotropic and reversible properties, which make them a valuable choice to design new injectable drug carriers. Moreover, the cyclodextrins forming the poly(pseudo)rotaxanes can progressively dissolve in a watery environment, leading to the release of biocompatible molecules. From a technical point of view, CDs are not expensive and the preparation of poly(pseudo)rotaxanes-based crystals is simple.

Starting from the work of Harada's group, supramolecular structures based on poly(pseudo)rotaxanes formed by PEG and α-cyclodextrins have been described in literature [35]. Later, Jun Li et al. proposed the same composition of hydrogels (α-CDs and PEG) and studied their supramolecular structures using X-ray diffraction, confirming the assembly of supramolecular systems (Figure 22, [36]).

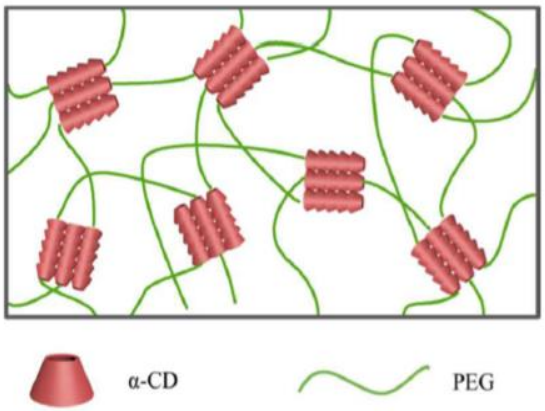

Figure 22 Supramolecular Hydrogel formed by PEG and α-CDs

Rheological characterization evidenced an increase in the viscosity of the hydrogel at the time of the gelation followed by a decrease upon application of a shear, confirming its thixotropic behaviour. In addition, upon removal of the applied shear, the viscosity tended to increase again leading to the initial structure, as a consequence of the self-healing behaviour of these systems. Thixotropy and reversibility of the structures address the application of supramolecular gels in the field of drug release as injectable systems. In fact, hydrogel injection through a small needle into the body is made possible by thixotropic properties, meanwhile reversibility allows the gel to recover its initial characteristics upon injection, becoming a system that controls the release of the drug it contains. The release rate can be controlled depending on the molecular weight and cyclodextrin concentration that characterize the system and it does not depend on the type of molecule that is encapsulated [37].

Maintaining the same supramolecular system of Harada and Li, Higashi et al. studied the encapsulation and the kinetics release of an enzyme, lysozyme. In this work, they compared two PEG structures based on α-CDs and γ-CDs, respectively. Gelation resulted to be faster for the systems containing α-CDs. X-Ray Diffraction analysis confirmed the formation of poly(pseudo)rotaxanes and their supramolecular crystals. Moreover, the PPRs formed by PEG and α-CDs showed hexagonal columnar necklace-like inclusion complexes-based crystals, whereas those formed by PEG and γ-CDs contained tetragonal columnar channels (Figure 23, [38]). This difference in the arrangement of the complexes affected the behaviour of the two different hydrogels: swelling ratio and viscosity were higher for the PEG and α-CDs systems, probably as a consequence of the hexagonal columnar structure that allows a tighter packaging.

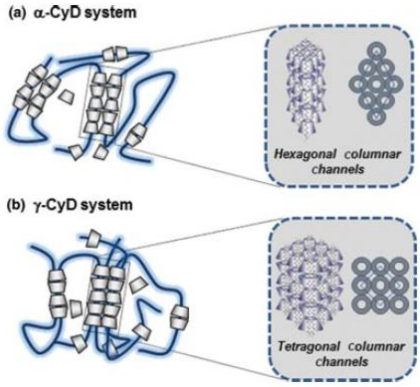

Figure 23 Scheme for the PPR of (a) PEG and α-CDs hydrogel (b) PEG and γ-CDs hydrogel

The study of enzyme release revealed a dependence of the release profile over the volume of releasing medium surrounding the hydrogels. No differences in release method were observed between the two different systems. In addition, the enzyme was released in its functional form (i.e., not-denaturated). Hence, for all these results, the supramolecular hydrogels formed by PEG and α-CDs or γ-CDs are not only excellent carriers for drug molecules, but also manage to transport proteins and enzymes without affecting their functionality [38].

Studies on supramolecular hydrogels based on homopolymers and cyclodextrins have led to excellent results for biomedical applications but show several drawbacks. For example, the use of poly(ethylene)glycol allows to obtain a good drug encapsulation but the release kinetics is very fast due to its hydrophilicity. In addition, in order to achieve good stability in aqueous environment, high molecular weights are required with the risk of exceed renal clearance capability. Hence, in the last decades, the focus has shifted towards the

development of systems based on multi-block polymers that can interact with cyclodextrins but at the same time possess suitable domains to interact each other, with a consequent enhancement in mechanical properties and residence time in watery environment.

2.4.1 Supramolecular Hydrogels formed by poly(pseudo)rotaxanes based on Cyclodextrins and Pluronics

Poloxamers®, as mentioned before, are triblock copolymers characterized by poly(ethylene oxide) and poly(propylene oxide) groups that interact with α-cyclodextrins via PEO groups and with each other with hydrophobic interactions formed between the uncovered PPO groups.

Jun Li et al. were the first to hypothesize and study the development of a supramolecular system based on cyclodextrins and a triblock copolymer (Pluronic®). They compared the gelation kinetics of different Pluronics with and without cyclodextrins and observed that, using α-cyclodextrins, gels can be obtained at low Pluronic concentration (the gelation of 13 wt% of Pluronic has happened only in the case in which 9,7 wt% of α-cyclodextrins have been added). This happens thanks to the formation of poly(pseudo)rotaxanes resulting from the penetration of α-cyclodextrins through the polymer chains and their interactions with EO groups. These poly(pseudo)rotaxanes can also interact each other through the self-assembly of the α-cyclodextrins of different PPRs and the hydrophobic interactions between the exposed PPO parts of the chains (Figure 24,[39]).

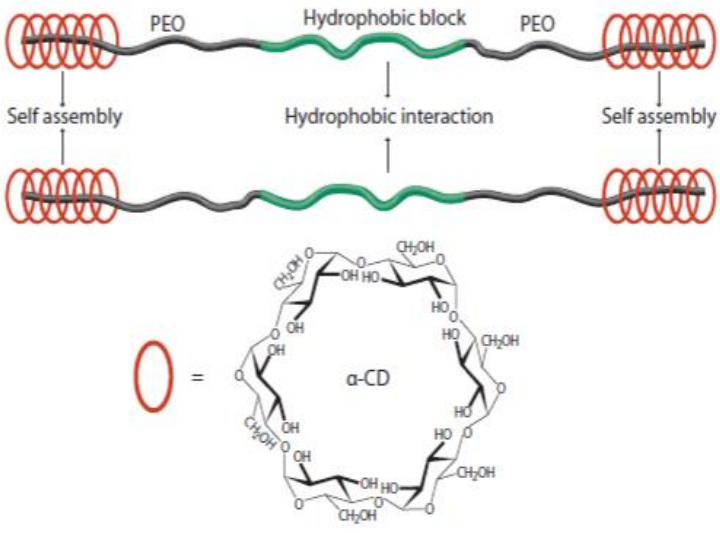

Figure 24 Supramolecular system based on Pluronic and α-CDs

Interestingly, no gelation was observed at 4°C, suggesting the key role exerted by hydrophobic interactions in the gelation properties. Hence, the balance of ethylene oxide and propylene oxide groups in the Pluronic selected for the formation of the hydrogel play a pivotal role in determining the properties of the resulting systems [40]. In this regard, Clementine Pradal and co-workers studied the gelation behaviours of two different Pluronics, F127 (or P407) ($PEO_{100}PPO_{65}PEO_{100}$, Mw = 12600 $g \cdot mol^{-1}$) and F68 ($PEO_{76}PPO_{29}PEO_{76}$, Mw = 8400 $g \cdot mol^{-1}$), and compared the results obtained with and without the use of cyclodextrins. Using different analysis techniques as Rheology, Dynamic Light Scattering (DLS) and Small-Angle X-ray Scattering (SAXS), they were able to understand the kinetics of gelation, which depends on the kind of Pluronic used, its concentration and the concentration of cyclodextrin added. Three different types of gelation have been hypothesized (Figure 25, [41]). Figure 25A represents the gelation of a Pluronic that interact with cyclodextrins without the formation of micelles: this behaviour is characteristic of polymeric solutions at low concentrations that, without the help of a

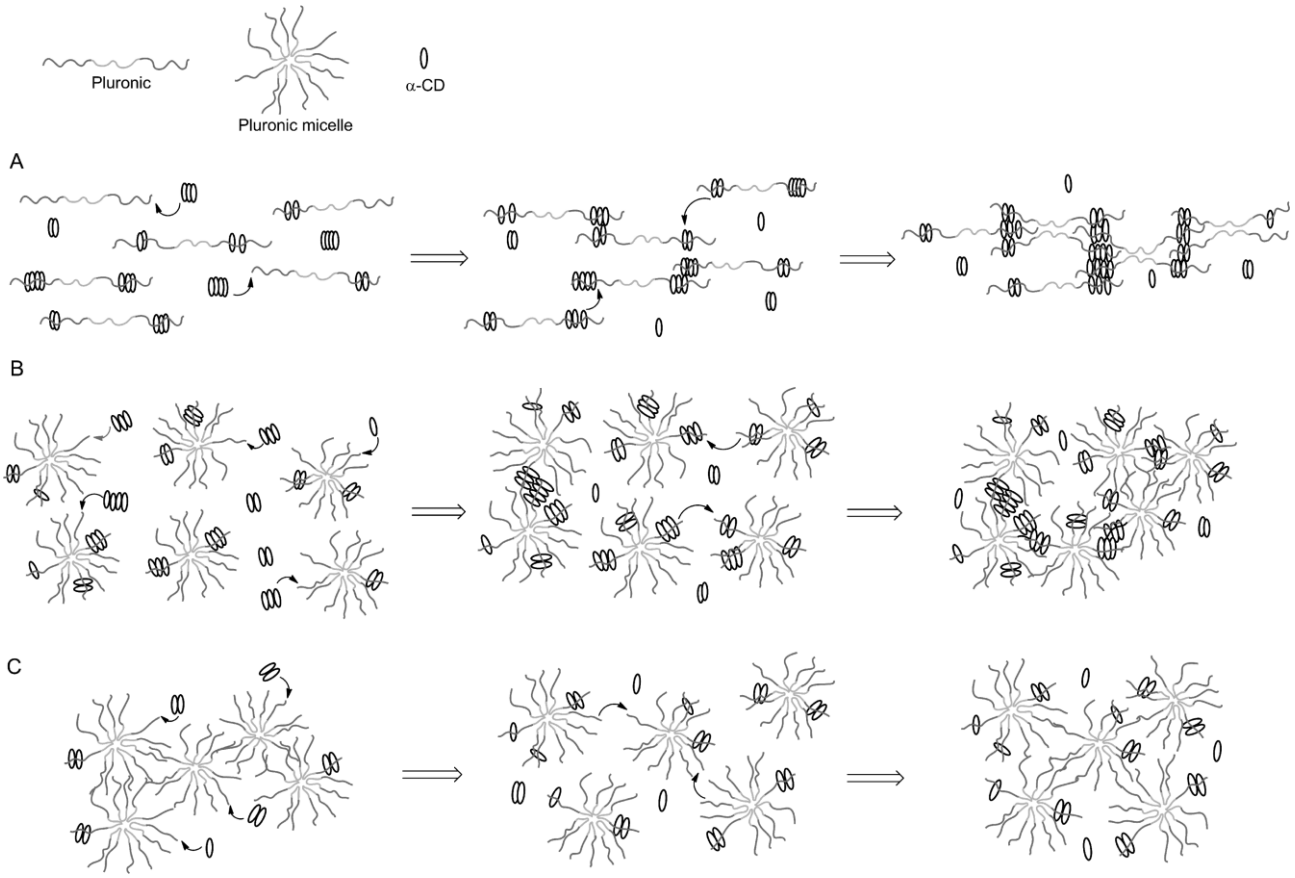

Figure 25 Different Kind of Gelation of Supramolecular Hydrogel formed by Pluronic and Cyclodextrins

supramolecular structure, would not have the sol-gel transition (for example F68 at the concentration of 10% w/v and 20%w/v).

In the absence of micelles, cyclodextrins interact more easily with the linear polymeric chains; hence, gelation time decreases with increasing their concentration. Hence, the driving forces of the transition are those established between the poly(pseudo)rotaxanes formed between the cyclodextrins and the ethylene oxide groups, but the network is more stabilized thanks to the hydrophobic interactions present between the groups of propylene oxide, even if they do not form micelles. In any case, a minimum cyclodextrin concentration must be reached in order to obtain the necessary interactions to enable the transition to take place. In the second kinetics of gelation described by the drawings (Figure 25B), the concentration of the polymer is high enough to induce micelle formation, but not yet optimal to allow the transition from solution to gel without the use of cyclodextrins (for example F127 at the concentration of 10% w/v). In that case, cyclodextrins take longer time to insert into the Pluronic chains because this is present in its micellar form but, when they enter, they succeed in forming poly(pseudo)rotaxanes and establish those supramolecular interactions necessary for the formation of the hydrogel. Also, for this kinetics, the cyclodextrins must reach a minimum concentration that allows the achievement of supramolecular interactions ensuring the gelation. As regards the last situation described in figure 25 (Figure 25C), the concentration of the synthetic part is high enough for the formation of micelles and the transition from solution to gel without the intervention of cyclodextrins (for example F127 at the concentration of 20% w/v). In this case, if the cyclodextrin concentration is low (cyclodextrins coverage of 1%) they will only interfere in the interactions between the different micelles, without being able to give the supramolecular contribution and even prolonging the transition time. Instead, if the concentration is high enough (cyclodextrins coverage of 9%), supramolecular interactions will overwhelm those between the micelles and there will be the formation of a hydrogel thanks to the formed bonds between the poly(pseudo)rotaxanes [41].

As regards the applications of supramolecular hydrogels formed by Pluronic and cyclodextrins, Simões et al. developed a system based on Pluronic F127 and α-cyclodextrins that aimed to release vancomycin in a controlled way, without degrading it. Comparing the hydrogels containing cyclodextrins with those containing only Pluronic F127, differences in

the release kinetics were observed, with systems based on supramolecular structures (composed by F127 and α-cyclodextrins) showing much more controlled drug release than those containing only Pluronic. Additionally, a decrease in vancomycin diffusion coefficient was observed with increasing CD content within the gel, while the amount of Pluronic turned out not to interfere with the release of drug. In addition, the authors showed that released vancomycin retained its antibacterial properties [42].

2.4.2 Supramolecular Hydrogels formed by poly(pseudo)rotaxanes based on Cyclodextrins and Polyurethanes

Polyurethanes have very different characteristics and properties compared to Poloxamers as such. Additionally, the wide versatility of polyurethane chemistry allows to design materials with the optimal properties to obtain interactions between the chains and the cyclodextrins.

A first supramolecular system based on polyurethanes and cyclodextrins was studied by Isao Yamaguchi and co-workers. They used 1,4-Bis(7-hydroxy-1-oxaheptyl)benzene (BHHB) as aliphatic linear diol and methylenediphenyl-4,4'-diisocyanate (MDI) that formed a polyurethane for polyaddition in the presence of permethylated α- or β-cyclodextrin (PM-α-CD and PM-β-CD) in dimethylformamide (DMF) solution. Proton nuclear magnetic resonance (^{1}H-NMR) analysis evidenced the formation of inclusion complexes between PM-β-CDS and benzene in the polyurethane chain and the presence of interactions between the hydrogens of the PM-α-CDS and the polymethylene groups. Hence, using this method and these elements, poly(pseudo)rotaxanes were successfully formed but, depending on the cyclodextrins used, interactions were obtained with different moieties of the polyurethane chain. In fact, the dimensions of the inner cavity of the PM-α-CD do not allow to receive the benzene ring but allow polymethylene group entry [43].

Another important study on the characterization of polyurethanes interacting with cyclodextrins was conducted by Erol A. Hasan and co-workers. They synthesized a polyurethane composed by blocks of polyethylene glycol (Mw = 400 Da) and 1,6-hexamethylene diisocyanate in order to obtain chains composed by hydrophobic and hydrophilic parts that could interact with α-cyclodextrins. They demonstrated the formation of inclusion complexes using different techniques. First, thanks to the phase

diagram, they evidenced that depending on the amount of cyclodextrin and polyurethane, three different situations can be obtained: phase separation of the components, a solution or a gel. When the amount of cyclodextrins is too low (12,9 mM and 25,7 mM), inclusion complexes are not formed and a solution is achieved, while when cyclodextrins have an adequate concentration (greater than 51,4 mM), inclusion complexes are formed and interact with each other using these oligosaccharides as physical crosslinking, thus forming a gel. Phase separation is achieved when cyclodextrins are threaded onto the polymeric chains, but these are not enough to form the physical crosslinks needed to obtain a gel. By studying the stoichiometry of the inclusion complexes formed between the different parts of the polyurethane chain and cyclodextrins, they also noticed that polyurethane chains were almost completely covered by cyclic oligosaccharides, observing the formation of root canal structures between polyurethane and cyclodextrins through ^{1}H NMR shift titration method. Finally, they studied the morphology of these complexes through AFM and SEM, highlighting the achievement of highly ordered canal structures [44].

No other examples of supra-molecular hydrogels based on cyclodextrins and polyurethanes have been reported in literature.

3. Thesis Goals

The main purpose of this thesis work is to design and characterize bioartificial systems able to transport and release drugs in a controlled way and precisely in the zone to treat. These systems may have different uses depending on the encapsulated drug, such as anti-inflammatory or anticancer. To this purpose, polyurethanes will be chosen as a synthetic material and α-cyclodextrins will be used as a biological part. During this thesis work, a library of bioartificial supramolecular hydrogels will be developed, containing all the different types of synthetized polyurethanes in combination with cyclic oligosaccharides which, depending on the properties obtained, could be used for different purpose in the field of regenerative medicine.

Using different components, polyurethanes with different characteristics will be designed thanks to the great versatility of the synthesis process. Five polyurethanes will be synthesized and characterized in order to specifically interact with cyclodextrins in aqueous solutions and the differences induced from their compositions will be studied. Therefore, it will be necessary to properly choose the reagents for the composition of the different polyurethanes focusing on how the chains can interact with each other and with the cyclodextrins. This hierarchical process of self-assembly will lead to the formation of specific structures, known as poly(pseudo)rotaxanes, which will compose engineered supramolecular hydrogels. First, it will be useful to assess the importance of the choice of the macrodiol that will compose the synthetic material and different Poloxamers will be used to this purpose. Two different Pluronics will be chosen, F68 and P407 which differ in the molecular weights and the length of poly(ethylene oxide) and poly(propylene oxide) domains (M_n=8400 Da, 80% PEO and M_n=12600 Da, 70% PEO, respectively). A linear and aliphatic diisocyanate (1,6-examethylene diisocyanate) will be used to form urethane bonds. This particular molecule will be also chosen in order to enhance the stability of the polyurethane-based complexes. In addition, different chain extenders will be used, in order to evaluate if the linearity of the chain could help the interactions with the cyclodextrins. Therefore, for this purpose, N-Boc serinol and 1,4-cyclohexane dimethanol will be used as different chain extenders. Using N-Boc serinol groups, it will be also possible to obtain a different form of polyurethane: in fact, using a specific protocol, Boc groups will be eliminated and the material will expose amino groups for further functionalizations (e.g.

through carbodiimide chemistry). Therefore, the different polyurethanes will be coded with regard to their chemical composition. NHP407 and NHF68 polyurethanes will be formed by N-Boc serinol as chain extender and 1,6-Hexamethylene diisocyanate as diisocyanate but, for what concern the macrodiol, P407 and F68 will be used, respectively. SHP407 and SHF68 will be obtained after the deprotection of N-Boc serinol groups of NHP407 and NHF68, respectively. CHP407 will be composed of P407 as macrodiol, 1,6-Hexamethylene diisocyanate as diisocyanate and 1,4-cyclohexane dimethanol as chain extender.

Therefore, the aim of this project is to chemically and physically characterise these different synthetic compounds and evaluate their supramolecular behaviour when cyclodextrins will be added to the polymeric solution. The resulting systems would be cytocompatible, easily injectable, easy to produce, economical and carrier for molecules and drugs.

In addition, it will be possible to form blends of synthetic materials, which combine the properties of both involved polyurethanes: a wide platform of novel supramolecular systems will be obtained and characterized working on different concentrations of the added polyurethanes and the addition of α-cyclodextrins.

Considering the application of the designed and characterized supramolecular hydrogels, they will have important properties including thixotropy and self-healing behaviour that will be evaluated with rheological characterizations. These peculiarities will be exploited with respect to the design of biomedical systems that could have the ability to transport drugs and, at the same time, that could be injected through a syringe with a thin needle. Therefore, the possible applications will turn out to be multiple precisely because any type of needle could be used. For example, G21-G23 (about 0,64 mm of diameter) needles are used for intramuscular injections, G13 (2,41 mm of diameter) needles are used for intra-bone injections while for topical applications (such as infected wounds) no special dimensions are required. In addition, changing the drug or molecule that is transported by the supramolecular hydrogel, it will be also possible to act on different issues, such as infection, inflammation, cancer therapy or also medical imaging.

For this thesis project, curcumin will be chosen as incapsulated drug. Among the various properties, this is an anticancer and anti-inflammatory drug but also a very hydrophobic molecule, that results difficult to solubilize. Using α-cyclodextrins, it will possible to

increase solubility and chemical stability of curcumin and also to incapsulate this molecule into polyurethane-based supramolecular hydrogels. Therefore, the higher the solubility of curcumin will be obtained and the higher the amount of curcumin will be encapsulated inside the hydrogel and released in the treated area. Release tests will be performed in order to evaluate release kinetics from the designed supramolecular hydrogels.

Another application of these supramolecular hydrogels will be to encapsulate them inside poly ε-caprolactone-based (PCL) porous scaffolds, useful for tissue regeneration. Scaffolds will be produced using the porogen leaching method with PCL and sodium chloride as porgen agent. A formulation of supramolecular hydrogel containing a model molecule (Fluorescein isothiocyanate–dextran, FD4, 4000 Da) will be inserted inside porous scaffolds in order to evaluate mechanical properties and release kinetics of molecules from the resulting system. Therefore, it will be possible to generally understand how the hydrogel could be loaded into a previously developed porous structure, that will potentially retrace the tissue defects of patients while treating a disease.

In conclusion, the principal aim of this work of thesis will be the design and characterization of supramolecular hydrogels composed of custom-made polyurethanes and α-cyclodextrins in order to obtain versatile systems characterised by low amount of synthetic material, high cytocompatibility, thixotropic and self-healing characteristics, with the target to encapsulate and release different drugs in the field of regenerative medicine.

4. Materials and Methods

4.1.1 Synthesis of materials

In this thesis work three different polyurethanes differing in their composition but not in the synthesis protocol were synthesized. The process was conducted in two steps under inert atmosphere. Anhydrous 1,2-dichloroethane (DCE) was used as solvent, dibutyltin dilaurate (DBTDL) as catalyst and 1,6-hexamethylene diisocyanate (HDI) as diisocyanate. The synthesized polyurethanes differed for their macrodiol and chain extender: Kolliphor P188 (F68, M_w=8400 Da, $PEO_{80}PPO_{20}PEO_{80}$) and Kolliphor P407 (P407, M_w=12600 Da, $PEO_{70}PPO_{30}PEO_{70}$) were used as macrodiol, while N-Boc serinol and 1,4-ciclohexane dimethanol were used as chain extenders. The solvents were purchased from Carlo Erba while the other reagents mentioned above were purchased from Sigma-Aldrich (Milan, Italy). The chain extenders are commonly stored in a dryer under vacuum (c.a. 50 mbar), while the diisocyanate is periodically purified through distillation at low pressure (less than 1 mbar) and kept in a desiccator. The day before the synthesis, residual water present in Kolliphor was removed by dynamic vacuum cycles: the material was put at 100 °C under vacuum (150 mbar) for 8 h and then the temperature was lowered to 40 °C.

In order to synthesis the polyurethane composed of F68 as macrodiol, HDI as diisocyanate and N-Boc serinol as chain extender, Poloxamer F68 was first dissolved in DCE at 20% w/v and equilibrated at 80 °C under nitrogen atmosphere. During the first step of the synthesis F68 and diisocyanate (HDI) reacted so as to obtain an isocyanate-terminated prepolymer. To this aim, HDI was added to the F68 solution at a molar ratio of 2:1 with respect to F68, and they were left to react in the presence of dibutyltin dilaurate catalyst (DBTDL, 0.1% w/w with respect to F68) for 2 hours and 30 minutes at 80 °C under stirring. The second step was characterized by the addition of the chain extender N-Boc serinol which was previously weighed with a molar ratio of 1:1 with respect to F68 and dissolved in DCE at 3% w/v. This second part of the process lasted 1 hour and 30 minutes and took place at a temperature of 60 °C under stirring. Then, the reaction system was cooled down to room temperature and methanol was added (6 mL for every 16 g of theoretical polymer) to passivate the residual isocyanate groups. After the synthesis, the solution containing the

synthesized polyurethane was precipitated in petroleum ether (4:1 volume ratio with respect to total DCE) under stirring at room temperature. The precipitated polymer was separated from supernatant and maintained overnight under a fume hood to dry. Then, a further purification process was performed to remove impurities from the obtained synthetic material. To this aim, the polyurethane was re-solubilized in DCE (20% w/v) and precipitated in a mixture of diethyl ether and methanol (98:2 v/v, 5:1 volume ratio with respect to DCE used for the re-solubilization). Centrifuges were then run at 0 °C for 20 minutes at 6000 rpm to collect the polymer which was finally dried overnight under a chemical hood. The synthesized polymer was stored at 5 °C under vacuum until use. The obtained polyurethane was identified with the acronym NHF68 where each letter corresponds to its components: N refers to the chain extender N-Boc serinol, H identifies the presence of HDI and F68 corresponds to Pluronic F68 (i.e., Kolliphor P188).

The other two synthesized materials also followed the same synthesis protocol but, as mentioned above, they differed in composition from NHF68. The first was based on the same chain extender (N-Boc serinol) and diisocyanate (HDI), but differed in the macrodiol which was P407; its acronym was coded as NHP407 [4]. The last polyurethane used in the present work was composed of HDI as diisocyanate, P407 as macrodiol and 1,4-cyclohexane dimethanol (CDM) as chain extender. Its defined acronym was CHP407 where C refers to CDM [20].

4.1.2 Chemical treatment of NHF68 and NHP407 to expose Boc-protected amines

The presence of N-Boc serinol as chain extender in NHF68 and NHP407 polyurethanes gives the possibility to remove the Boc caging group so as to expose pendant primary amines. Polyurethanes with these hanging groups have the potential of being functionalized with carboxylic group-containing molecules by carbodiimide chemistry, for example.

In order to perform the deprotection reaction, 10 g of polyurethane were first dissolved in 225 mL of chloroform (CF) for 2 hours at room temperature under stirring. Then, trifluoracetic acid (TFA) was added a 90:10 v/v ratio (CF:TFA). The resulting solution was then stirred for 1 hour at 250 rpm at room temperature. After the reaction was completed,

the solvent was evaporated under reduced pressure using a rotary evaporator (Büchi Rotavapor R-210, USA). After the first evaporation, the polyurethane was washed twice through solubilisation in 100 mL of chloroform followed by evaporation using the rotary evaporator. Upon completion of solvent evaporation cycles, the polyurethane was dissolved in 200 mL of bi-distilled water and stirred at 250/350 rpm overnight at 5 °C. Then, the polymer solution was poured into dialysis bags (cut-off 10000-12000 Da, Sigma Aldrich, Milan, Italy) and dialyzed in distilled water for two days at 5 °C (complete dialysis medium refresh three times/day). Dialysis was required to remove any residual molecule of TFA, CF and cleaved Boc groups. Subsequently, the dialysed solution was freeze-dried (Alpha 2—4 LSC, Martin Christ, Germany) for two days. Then, using a Buchner filter, the last remaining TFA residues were removed by washing the freeze-dried polymer with diethyl ether. Washed polymer was dried for 3-4 hours under chemical hood and finally stored under vacuum at 5 °C.

As specified above, the deprotection treatment was carried out on NHP407 and NHF68 polyurethanes thus obtaining SHP407 and SHF68, respectively.

4.2 Chemical Characterization of Polyurethanes

4.2.1 Attenuated Total Reflectance Fourier Transformed Infrared (ATR-FTIR) Spectroscopy

Vibrational Infrared Spectroscopy (IR) is an analysis technique that evaluates the vibrational states of the bonds that compose the analysed sample. Samples can be solids, liquids, gases, powders and even thin films.

When a molecule is excited by an infrared photon, it switches to an excited vibrational state and a transition between vibrational energy levels is obtained. Hence, it is necessary to understand how atoms interact with infrared waves and for this purpose the law of Lambert-Beer (Equation 1) is used to calculate the absorbance (A) of energy:

$$A = Log(\frac{1}{T}) = Log(\frac{I_0}{I}) = \varepsilon C d \qquad \text{(Equation 1)}$$

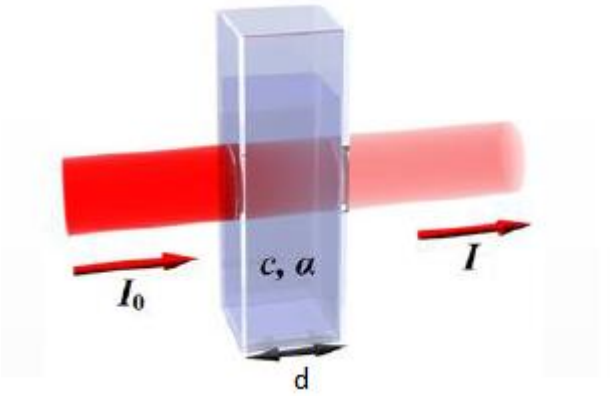

Figure 26 Outline of the law of Lambert-Beer

Where T is the Transmittance, I_0 is the incident infrared radiation, I is the output infrared radiation, ε is the Coefficient of molar absorption (cm^{-1} mol^{-1}), C is the concentration (M) and d is the optical path (cm) (Figure 26).

The Attenuated Total Reflectance Fourier Transform infrared (ATR-FTIR) spectroscopy is a type of infrared analysis which is based on changes in intensity associated with the total reflection of an infrared ray coming in contact with the sample. This is possible because the IR ray is directed on a crystal with high refractive index: in this manner, an evanescent wave

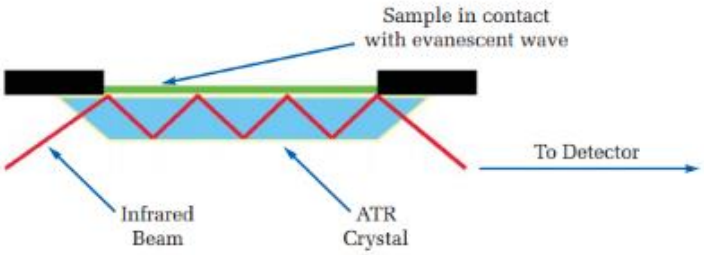

Figure 27 ATR crystal and IR wave operation scheme

is formed by reflection and it enters the sample perfectly positioned above the crystal. The absorbance result is obtained because the evanescent wave that is formed is attenuated only at the points where the sample has absorbed (Figure 27).

To ensure that the ATR technique is applied correctly, certain requirements must be met. First of all, it is important that the sample is placed in contact with the ATR crystal because the evanescent wave has an extension of 0.5-5 µm (for this reason the analysis gives superficial information). Another important aspect is that the refractive index of the ATR crystal must be much higher than that of the sample. Finally, comparable absorbance or transmittance spectra are only those with the same incidence angle.

FTIR spectrometer is a tool that brings many advantages to the less recent dispersion spectrophotometry. In fact, this kind of spectrometer allows to obtain a high precision of analysis, improves the signal/noise ratio, has very simple optics and also allows to obtain results quickly because it simultaneously records the spectra at the various wavelengths. With regard to the operation of the FTIR spectrometer, from the infrared source a radiation is sent on the beam splitter which divides it into two parts: a half of radiation is reflected on the static mirror while the remnant is transmitted to a moving mirror. The two parts of radiation join again on the beam splitter, are transmitted to the sample and then the radiation is captured by a detector. If the distance between the stationary mirror and beam splitter is identical to that between the moving mirror and the beam splitter, then a constructive interference is obtained, otherwise it will be a destructive interference. Whereas the IR wave is polychromatic, and each wavelength generates a cosine, the detector has a sum of cosines as input. This summation is analysed by the interferogram that produces a signal in the time domain and therefore, with the help of the Fourier

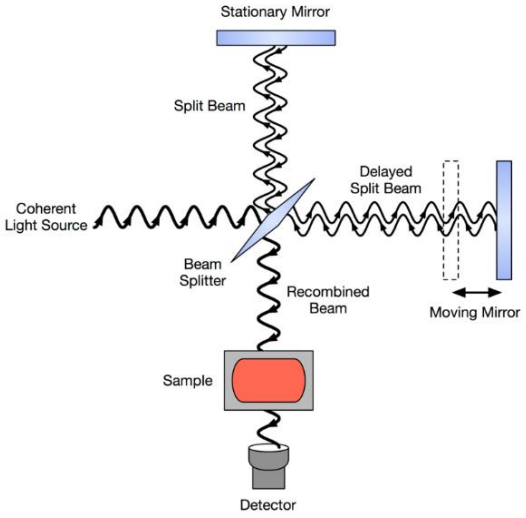

Figure 28 Functioning Diagram of spectrometer FTIR

transformation, it is converted into a spectrum in the domain of frequencies (Figure 28). Spectrum peaks refer to certain frequencies to which the infrared wave is absorbed by the various chemical groups forming the sample material.

The spectra reported in this work of thesis were obtained from polymer powder through to the use of a Perkin Elmer (Waltham, MA, USA) Spectrum 100 including an ATR accessory (UATR KRS5) with diamond crystal. Each spectrum resulted from sixteen scans with a

resolution of 4 cm^{-1}, registered at room temperature. Perkin Elmer Spectrum software was used for data analysis.

4.2.2 Size Exclusion Chromatography (SEC)

The Size Exclusion Chromatography (SEC) is also known as Gel Permeation Chromatography (GPC). It is an analysis process that allows the separation of substances with different molecular weights. The stationary phase is composed of molecular gel sieves that have pores of different sizes: in this way the mobile phase, in which the analysed material is solubilized by a solvent, must pass through the pores of the stationary phase. Considering the analysis of a polymer, smaller chains take a long time to exit the stationary column

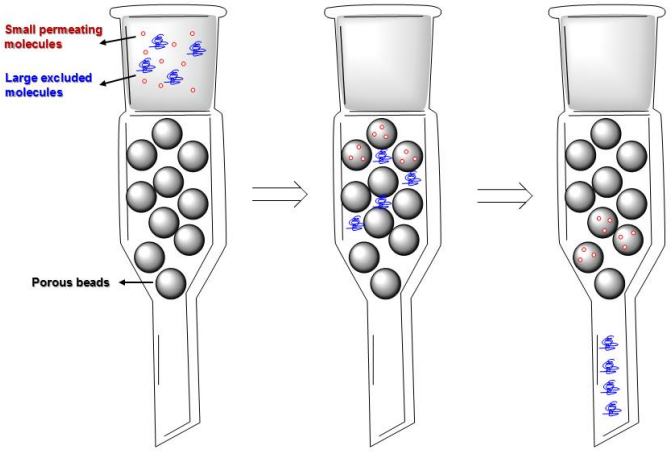

Figure 29 SEC mechanism

because traverse pores of every dimension and their path becomes tortuous, while bigger chains tend to take less time as they pass only in the bigger pores and therefore their path is more linear (Figure 29). It is important to specify that no chemical interactions occur between the stationary phase and the tested material. The elution time is the time with which the different chains leave the station column.

The tested sample is dissolved and pumped into the stationary column at a continuous flow rate. At the exit, chains are arranged according to the size, where the first to go out are

also the biggest and they are evaluated by a Refractive Index Detector (RID) which is composed of an analysis cell and a reference cell. In the analysis cell the solution that comes out from the stationary column flows and this is compared with the reference cell, in order to obtain the formation of peaks in the graph that reports the RID signal as a function of elution time. In order to be able to quantify different molecular weights from the RID signal, it is necessary to have a calibration curve (which it is usually a straight line) obtained by the analysis of standard materials with known molecular weights. Hence, starting from the elution time data to which a peak occurs in the analysed sample it is possible to know to which molecular weight it refers to.

In this thesis work an Agilent Technologies 1200 Series (CA, USA) instrument equipped with a Refractive Index Detector (RID) was used to estimate the molecular weight of the synthesized materials. The solvent used as mobile phase (0.5 mL/min flow rate) was N,N-dimethyl formaldehyde (DMF) added with lithium bromide (LiBr) at 0,1% w/v concentration to avoid longer chain interaction with the stationary phase of the columns. Samples were prepared by dissolving the polymers in DMF+LiBr to obtain a concentration of 2 mg/mL, followed by filtration through a filter with a poly(tetrafluoroethylene) (PTFE) membrane and pores of 0.45 μm. The stationary phase instead was composed of two columns in series (Waters Styragel HR1 and HR4) that allow to distinguish molecular weights from 1000 to 100000 Da. Both the columns and the RIS were maintained at 55 °C during the analyses. Weight average molecular weight, number average molecular weight and polydispersity index were estimated starting from a calibration curve based on 10 poly(ethylene oxide) standards with molecular weights ranging between 982 Da and 205500 Da.

4.2.3 UV-Visible spectroscopy – Ninhydrin Assay (Kaiser Test): quantification of amino groups on SHP407 and SHF68

Ultraviolet-Visible spectroscopy (UV-vis) is used for the determination of chemical compounds and their functional groups. The sample is subjected to an energy that comes from a light source and then the absorption is calculated by means of a detector (Figure 30). The wavelengths used in this specific analysis are between 400 nm and 700 nm for the visible field and between 200 nm and 400 nm for the ultraviolet field.

UV-vis spectrophotometers are composed of several components:

- A Light source which allows to obtain the radiant beam to excite the sample;
- The Monochromator that isolates a range of wavelengths of interest;
- The Cuvette, where the test sample solution is placed;
- The Detector.

Once the measurement of absorbance has been obtained, the concentration of the tested species can be calculated by the Lambert-Beer law.

UV-vis spectroscopy is required to perform colorimetric assays, such as the Kaiser test, which allows to estimate the amount of amines present in an analysed sample, thanks to the use of ninhydrin which selectively binds to these specific groups. When the reaction between ninhydrin and amino groups occurs, the colour of the solution in which the sample is dissolved becomes purple-blue, while, if the sample does not have free amino groups, the solution maintains a yellow colour. To quantify the amount of free amino groups present in the sample it is necessary to measure the absorbance at 565 nm (to which the coloured products resulting from ninhydrin coupling to free amines absorb), and then use this value to calculate the concentration through Lambert Beer law and thus the moles of groups per gram. To make this calculation it is important to remember that each molecule of ninhydrin reacts with two amino groups.

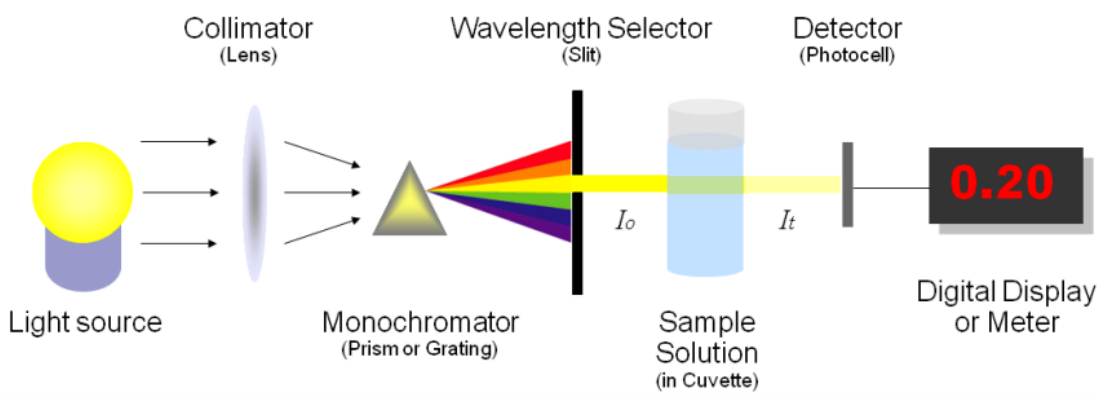

Figure 30 Block Diagram of UV-vis Spectrometer

In this thesis work, Kaiser test was performed on SHP407 and SHF68 polyurethanes which were compared with the respective polyurethanes NHP407 and NHF68 used as control. For sample preparation, 20 mg of polymer (NHP407 and SHP407, NHF68 and SHF68) were precisely weighed and dissolved using the Kaiser test reagents (Sigma Aldrich, Italy) according to supplier's instructions. First, 200 µL of a solution of pyridine, water and KCN (potassium cyanide) was added to the synthetic polymer. Then 150 µL of phenol solution (80% in ethanol) and finally 150 µL of ninhydrin solution (6% in ethanol) were added. The resulting samples were incubated at 120 °C for 10 minutes. In parallel, a solution with 60% ethanol and 40% bi-distilled water was prepared to dilute the obtained samples. The absorbance of the samples at 565 nm was measured using a UV-vis spectrophotometer (Perkin Elmer Lambda 365 UV/VIS Spectrometer) and finally the amount of amino groups per gram of polyurethane was determined by exploiting Lamber Beer law.

4.3 Characterization of not-gelling polyurethane solutions

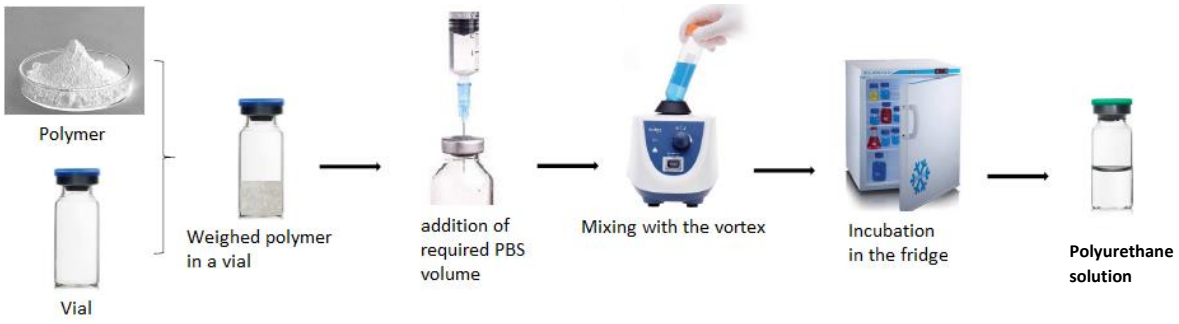

Figure 31 Process of preparation of a Polyurethane solution

4.3.1 Preparation of polyurethane solutions

Polyurethanes obtained through the synthesis process (NHP407, SHP407, NHF68, SHF68, CHP407) were used for the preparation of aqueous solutions for Dynamic Light Scattering analysis and the evaluation of the antibacterial properties of the developed materials. In detail, the polymers were solubilised at the required concentration (%w/v) in phosphate buffered saline (PBS, pH=7,4) and samples were mixed with a Vortex. Due to the thermos-sensitivity of these systems, the solubilization occurred at the temperature of 5 °C in order to avoid the formation of micelles and undesired gelation (Figure 31).

4.3.2 Dynamic Light Scattering (DLS) analysis

The Dynamic Light Scattering is an analysis technique that allows to evaluate the distribution profile of the size of suspended nanoparticles or polymeric aggregates in

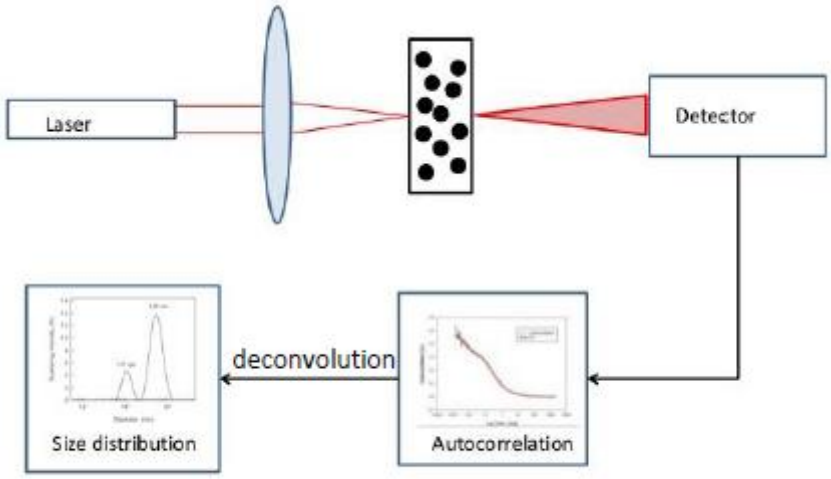

Figure 32 Block Diagram of DLS analyser

solution.

During these measurements, the sample is illuminated by a laser beam and changes in the intensity of diffuse light are measured in the time domain. Thus, maintaining constant temperature and viscosity of the solution, smaller particles move faster and cause faster intensity variations, while larger particles have slower movements and therefore give slower intensity variations. Thanks to a detector, the fluctuation of light scattering is recorded, the diffusion coefficient is calculated with an autocorrelation function and then the hydrodynamic particle size is obtained through the deconvolution of the signal and the use of the Stokes-Einstein formula (Figure 32).

To characterize the size of the complexes formed in solutions by the synthesized polyurethanes, a Zetasizer Nano S90 (Malvern Instruments, Worcestershire, UK) was used. In detail, different polymeric solutions (CHP407 at 1%w/v, SHF68 at 1%w/v, SHP407 at 1%w/v and a blend of CHP407 and SHF68 at 0.8% w/v and 0.2% w/v, respectively, all in PBS) were characterized at 25 °C and 37 °C. The size of the micelles and their aggregates

were obtained as mean of three measurements and with an equilibration phase of 600 seconds.

4.3.3 Evaluation of Antibacterial Activity of Polyurethanes Solution

The tests to assess the antibacterial properties of materials were conducted by the Laboratory of Microbiology, Department of Pharmacological Science, University of Eastern Piedmont.

Solutions of polyurethanes (NHP407, SHP407, NHF68 and SHF68) at 5% w/v in bi-distillate water were prepared and then tested in terms of antibacterial properties on four different types of bacteria: Escherichia coli (ATCC 25922), Pseudomonas aeruginosa (ATCC 10145), Staphylococcus aureus (ATCC 25923) and Candida albicans (ATCC 10231).

For what concerns the antibacterial properties of the materials on Escherichia coli, Pseudomonas aeruginosa and Staphylococcus aureus, the agar diffusion method (Eucast Method) was used. These bacterial strains were thawed on an MHA culture medium and incubated at 37 °C for 16-20 hours. Then, for each bacterial strain, an inoculum was prepared with OD_{600} 0,132 in physiological solution (equivalent to $1\text{-}2\times10^8$ CFU/mL of cellular concentration). Petri dishes containing 25 ml of MHA medium were inoculated using a sterile cotton swab soaked in bacterial suspension. 10 µL of the tested solution (50 µg/mL) were deposited on the surface of the MHA medium. Bi-distilled water was used as negative control and a solution of Pennicilin-Streptomicin (Pen-Strep) at 20% v/v in bi-distilled water was used as positive control. Petri dishes were then incubated for 24 hours at 37 °C and then the area of the inhibition halo (index of antimicrobial activity) was measured with the statistic software R , 3.1.2 (R Development Core Team, http://www.R-project.org).

For the assessment of the antibacterial properties of the three above mentioned bacteria (Escherichia coli, Pseudomonas aeruginosa and Staphylococcus aureus), micro-dilution in broth with microplate (Wiegand et al. 2008) was also used. Also in this case, the bacteria were thawed on MHA culture medium and incubated at 37 °C for 16-20 hours but a pre-inoculum of OD_{600} 0.257 was prepared for each strain in MHB 2x medium. The resulting suspension was diluted 1:300 v/v to MHB 2x to obtain an inoculum with a cell density of $1x10^6$ CFU/mL. 96-well plates were then prepared in order that for each tested compound there were:

- Three replicates for concentration 0 (positive growth control), containing 100 µL inoculum and 100 µL sterile bi-distillate water;
- Three replicates for each tested sample concentration, containing 100 µL of inoculum and 100 µL of its solution 2x;
- Three replicates for the negative control, containing 100 µL MHB 2x medium and 100 µL sterile bi-distillate water.

The plates were incubated at 37 °C for 24 hours and the absorbance values and inhibition percentages were calculated by spectrophotometric reading.

The microdilution method in brode in microplate (EUCAST method) was also used to understand the antibacterial properties of polymeric solutions on Candida albicans. In this case, the strain of fungus was thawed on SDA culture medium and incubated at 37 °C for 16-20 hours. A pre-inoculum was prepared, with OD_{530} between 0.12 and 0.15, in the medium RPMI 1640 2x + 2% glucose. The resulting suspension was diluted 1:10 v/v into the medium to obtain an inoculum with cell density of 1-5 $x10^6$ CFU/ml. 96-well plates were then prepared in order that for each tested compound there were:

- Three replicates for concentration 0 (positive growth control), containing 100 µL inoculum and 100 µL sterile bi-distillate water;
- Three replicates for each tested concentration, containing 100 µL of inoculum and 100 µL of its solution 2x;
- Three replicates for the negative control, containing 100 µL RPMI 1640 2x + 2% glucose medium and 100 µL sterile bi-distillate water.

The plates were incubated at 37 °C for 24 hours and the absorbance values and inhibition percentages were calculated by spectrophotometric reading.

The concentrations of polymeric solutions which were tested by the micro-dilution in broth with microplate were 25 mg/mL, 12.5 mg/mL, 6.25 mg/mL, 3.12 mg/mL, 1.56 mg/mL and 0.78 mg/mL.

4.4 Supramolecular Hydrogels Preparation

For the preparation of supramolecular hydrogels formed by polyurethane and α-cyclodextrins (αCDs, TCI, M_w=972,85, purity>98%), as a first step, the polyurethane was weighed and dissolved in PBS, in the required amount the reach the desired concentration in the final hydrogels. To achieve optimal solubilisation, the polyurethane and PBS solution was maintained at 5 °C overnight. α-cyclodextrins were then weighed and PBS was added in order to reach a concentration of 14% w/v. To enhance solubilization, the solution was stirred and heated by an external bath (40-50 °C) for about 15 minutes, until a clear solution was obtained without dispersed crystals. Once good solubilisation was achieved, the α-cyclodextrin solution was added to the solubilised polyurethane to finally obtain the desired polyurethane and αCD content within the hydrogels. The obtained samples were vortexed and left to assemble for 48 hours at 25°C.

4.5 ATR-FTIR analysis of supramolecular complexes formed by Polyurethanes and α-Cyclodextrins

ATR-FTIR analysis was also used to evaluate the formation of polyurethane and cyclodextrin complexes. The tested polyurethanes (CHP407, SHP407 and SHF68) were dissolved in bi-distillate water at 3 °C overnight. α-cyclodextrins solution (14%w/v) was obtained by dissolving oligosaccharides in bi-distilled water under stirring for 15 minutes with the help of an external bath at 40 °C - 50 °C. The polymeric and α-cyclodextrin solutions were then combined and vortexed to obtain a final 1%w/v and 10%w/v concentration of polyurethane and α-cyclodextrins, respectively. After 4 hours, the samples were centrifuged at 4500 rpm and 10 °C for 15 minutes to collect the formed poly(pseudo)rotaxanes in the form of pellets.

Samples were frozen instantly using liquid nitrogen and then freeze-dried (Martin Christ ALPHA 2-4 LSC, Germany) for 24 hours.

4.6 Gelation time and phase separation of Supramolecular hydrogels

For the preparation of the final supramolecular hydrogels which were then further characterised, different combinations of Pluronic or polyurethanes and α-cyclodextrin were tested to assess the kinetics of transition from solution to gel. Synthetic polymer component (i.e., F68, P407, NHP407, SHP407, NHF68, SHF68, CHP407) were tested at concentrations ranging between 1 and 9 %w/v, meanwhile α-cyclodextrin was varied between 9 and 11 %w/v. Hereafter, the designed formulations will be referred to with an acronym in the form X-Y-ZCD, where X and Y identify the synthetic polymer composing the supramolecular formulation and its concentration, respectively, while Z defines the concentration of αCD.

The evaluation of gelation kinetics was carried out by observing every 15 minutes the turbidity and viscosity of the supramolecular hydrogels until gelation (i.e., absence of flow).

4.7 Swelling and Stability of Supramolecular Hydrogels

Based on previous optimization of hydrogel formulation, swelling and stability tests were performed only on a selection of samples able to undergo gelation and with proper composition to allow comparisons among them. Briefly, the analysed samples contained 1% w/v, 3% w/v or 5%w/v concentrated polyurethane (CHP407, SHP407) and 10% w/v concentrated α-cyclodextrins. Regarding the blend formulations, they contained CHP407 and SHF68 at different concentrations: 0.8% and 0.2% w/v concentration (total 1% w/v synthetic polymer concentration), 2.4% w/v and 0.6% w/v (total 3% w/v synthetic polymer concentration), 4% w/v and 1% w/v (total 5% w/v synthetic polymer concentration). For each blend formulation α-cyclodextrins concentration was kept constant at 10% w/v. These

samples were prepared in bijou sample containers (17 mm diameter, polystyrene, Carlo Erba labware, Italy) and allowed to undergo the transition from solution to hydrogel at 25 °C for 48 h. Four different time steps were defined (6 hours, 24 hours, 3 days and 5 days) and five samples were prepared for each time step. The prepared supramolecular hydrogels were thus weighed (w_{gel_i}) and then placed in the incubator at 37 °C for 15 minutes to equilibrate temperature. Then, 1 mL of PBS or PBS with Amphotericin B solution (Sigma-Aldrich, M_w=924.,08 g/mol) was gently added to each sample and, for longer time points, the eluate was refreshed at the second day of incubation. Analyses were conducted using PBS or PBS added with Amphotericin B solution as medium surrounding the gel with the aim with the aim of blocking the formation of mould in the samples and understanding whether the addition of a molecule in the eluate changed the stability and swelling profiles.

At each step, the samples were taken and weighed (w_{gel_f}) upon residual PBS (or PBS with antifungal) removal. Each sample was then freeze dried for 2 days (Martin Christ ALPHA 2-4 LSC, USA) and subsequently weighed ($w_{freeze\ dried\ gel\_f}$). Control samples were also prepared with the same compositions as those tested, freeze-dried without being incubated with eluates (PBS or PBS with Amphotericin C) and finally weighed to obtain the initial dried weight of the hydrogels ($w_{freeze\ dried\ gel\_i}$). The following formulae were used for the calculation of PBS absorption (Equation 2) and dissolution of samples (Equation 3):

$$PBS\ absorption\ \% = \frac{(w_{gel_f} - w_{gel_i}) \cdot 100}{w_{gel_f}} \qquad \text{(Equation 2)}$$

$$Hydrogel\ Dissolution\ \% = \frac{\left(w_{freeze\ dried\ gel_i} - w_{freeze\ dried\ gel_f}\right) \cdot 100}{w_{freeze\ dried\ gel_i}} \qquad \text{(Equation 3)}$$

Data are reported as mean ± standard deviation.

4.8 Thermo-sensitive Supramolecular Hydrogel Characterization

4.8.1 Rheological Characterization

Rheology is a science that studies the characteristics of fluids and semi-fluids that are deformed by external forces in reference to their characteristics (such as density, viscosity, etc.) and their relationships with the external environment (contact with container, etc.).

The real utility of rheological characterization is that of being able to evaluate the characteristics of viscoelastic bodies, which do not have their own constitutive equation. In fact, the two ideal cases of an elastic solid of modulus G and a viscous liquid of modulus η are described by the law of Hooke (Equation 4) and Newton (Equation 5) respectively which relate strain ($\sigma(t)$) to sinusoidal deformation ($\gamma(t) = \gamma_0 sen(\omega t)$) as a function of time.

$$\sigma(t) = G\gamma_0 sen(\omega t) = \sigma_0 sen(\omega t) \qquad \text{(Equation 4)}$$

$$\sigma(t) = \eta\gamma_0\omega\cos(\omega t) = \sigma_0\cos(\omega t) \qquad \text{(Equation 5)}$$

Instead, the viscoelastic body has an effort that does not evolve neither in phase nor in phase square with the deformation and the stress is described considering both its maximum width (σ_0) and the phase shift (δ) (Equation 6).

$$\sigma(t) = \sigma_0 sen(\omega t + \delta) \qquad \text{(Equation 6)}$$

In this case, it is possible to describe the storage module and the loss module as shown in Equation 7 and 8.

$$G' = \frac{\sigma_0}{\gamma_0} cos(\delta) \qquad \text{(Equation 7)}$$

$$G'' = \frac{\sigma_0}{\gamma_0} sen(\delta) \qquad \text{(Equation 8)}$$

and therefore, the Equation 5 is rewritten going to replace the Storage Modulus and the Loss Modulus, in such a way as to estimate the elastic (G') and viscous (G'') contribution in the response of the material (Equation 9) [45].

$$\sigma(t) = \gamma_0[G' sen(\omega t) + G'' cos(\omega t)] \qquad \text{(Equation 9)}$$

Using the rheometer, it is possible to understand the behaviour of viscoelastic materials that are not calculable with formulas. As regards application to hydrogels, it allows to evaluate the sol-gel transition temperature and kinetics of the hydrogel. Moreover, through rheological characterization it is also possible to study the mechanical properties of the formulated gels. In the case of fused polymers or polymeric solutions, the rheometer with parallel plates is used and the sample is placed in contact with these two in such a way as to deform it correctly (Figure 33).

Depending on how the plates move and how the temperature is maintained (constant or variable), tests that characterize different properties of the material can be conducted.

The strain sweep test is one method for studying the mechanical properties of the hydrogel. The applicated frequency for the deformation and the temperature are kept constant while

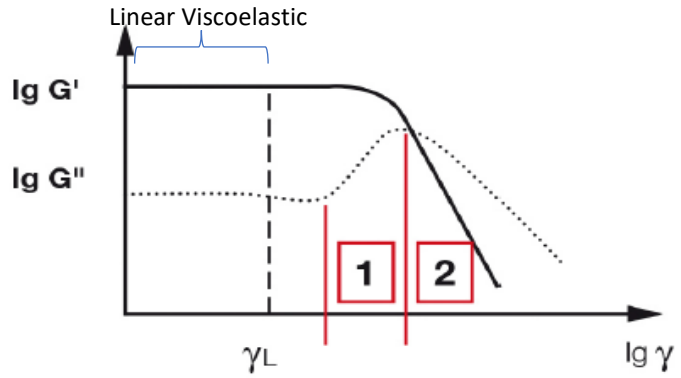

Figure 34 Strain Sweep Test

the strain varies within a predefined range. The material is placed on the lower plate at a specific temperature. Then the upper plate comes into contact with the material, the system heats up to the required temperature and then the test phase begins: the upper

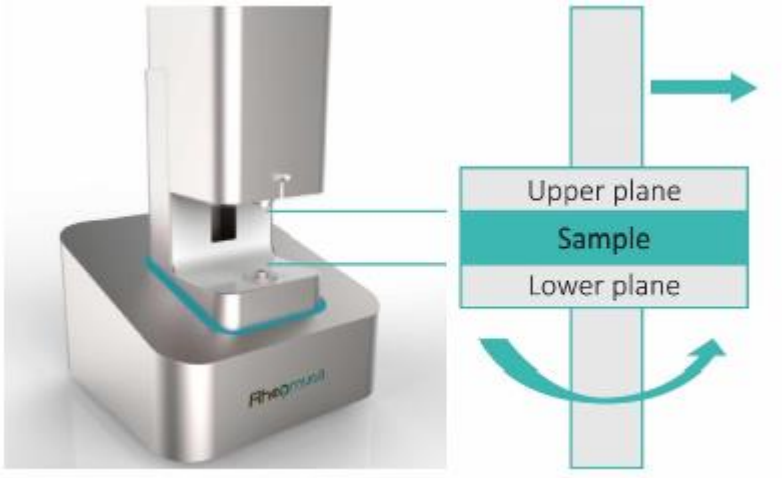

Figure 33 Rheometer configuration

plate rotates at the selected frequency and applies increasing deformation until the maximum set is reached. Concluded the analysis, a graph is obtained that in ordinate reports the variations of loss and storage moduli (in logarithmic axis) and in abscissa has the variation of the applied strain (in logarithmic axis) (Figure 34).

Both functions are characterized by an initial plateau that matches the linear viscoelastic region (LVE region): only if the test is conducted within this range the sample can be tested without being destroyed. Considering the LVE region, the storage modulus (G') may be higher than the loss modulus (G'') and in this case the sample is in its gel form or solid structure. While if the loss modulus (G'') is greater than the storage modulus (G') then the sample is at its fluid state. As regards the Figure 36, it is possible to note that initially the sample is in its solid state (G'>G'') and therefore it has a compact network; increasing the strain at which it is deformed, an increase of G'' is observed up to a point where it reaches a maximum and has the same value of G' (which in the meantime has begun to decrease): in this area of the graph (zone 1) there are micro cracks that are still contrasted by the elasticity of the material; from the moment when the maximum of G'' is exceeded (zone 2, which corresponds to the point where G'=G''), cracks become macroscopic, the sample no longer has a consistent network and therefore the viscous behaviour characterizing a material in the fluid state prevails.

For the evaluation of the self-healing (SH) capacity of the material two strain sweep tests are conducted on the same sample in series. In this way it is possible to compare the two graphs and to evaluate if the characteristic pattern of G' and G'' is maintained even after an already applied increasing deformation.

Another method for the evaluation of self-healing property is the strain test: the sample is first deformed by a weak strain (within the LVE region) for a defined time interval; subsequently a higher strain (higher that the LVE limit) is applied inducing the system rupture for a limited time frame and then the previous procedure is repeated cyclically. By means of this test it is possible to observe how the sample recovers its mechanical qualities even if it is drastically deformed.

Another test that can be conducted on hydrogels using the rheometer is the frequency sweep test. This analysis is carried out keeping constant temperature and strain (always within the limits of the LVE region) and varying the frequency within a predefined range. For thermosensitive hydrogels it is necessary to carry out this test at different temperatures, in order to evaluate the state of the system (i.e., sol, gel, semi-gel state) at different temperatures. Once the characterization is complete, a graph is obtained which shows the loss and storage moduli as a function of applied frequency (Figure 35). The parameters obtained with this test are the crossover frequency that identifies the sol-gel transition frequency and the longest relaxation time (t_{max}) of the sample. The latter is calculated with the inverse of the crossover frequency and emphasizes how long the polymeric chains take to untangle in the solution.

With regard to rheological characterization of the supramolecular hydrogels developed in this thesis work, a stress-controlled rheometer was used (MCR302, Anton Paar GmbH, Graz, Austria) equipped with 25 mm parallel plates. A Peltier system connected to the rheometer was used for temperature control during the tests. For each carried out test a gap of 0.6 mm was set between the plates.

Frequency sweep tests were conducted at constant temperatures of 25 °C, 30 °C and 37 °C, with a constant strain of 0.1% and an increasing angular frequency from 0.1 rad/s to 100 rad/s.

Strain sweep test were conducted for each sample at a temperature of 37 °C, a constant frequency of 1 rad/s and a strain in the range between 0.01% and 500%. This test was

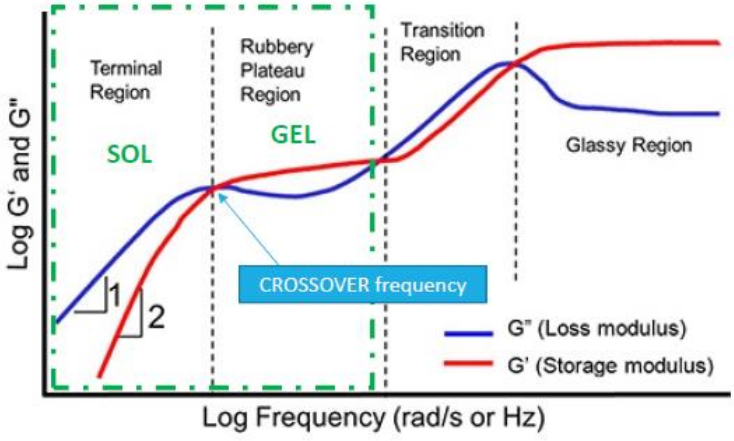

Figure 35 Frequency Sweep Test Graph

repeated on the same sample already tested after 15 minutes re-equilibration at 37 °C to

assess gel self-healing ability. With the same aim, strain tests were also conducted at 37 °C at a constant frequency of 1 Hz and applied strain kept constant for predefined time intervals and changed cyclically. In detail, strain was initially set at 0.1% for 2 minutes and then increased at 100% for 1 min. These two intervals were repeated cyclically three times and the test was concluded with an additional interval at 0.1% strain (Table 2).

Table 2 Strain Test, Application Interval

	I1	I2	I3	I4	I5	I6	I7
Strain	0,1%	100%	0,1%	100%	0,1%	100%	0,1%
Temperature	37°C	37°C	37°C	37°C	37°C	37°C	37°C
Frequency	1 Hz	1 Hz	1 Hz	1 Hz	1 Hz	1 Hz	1 Hz
Time	120 sec	60 sec	120 sec	60 sec	120 sec	60 sec	120 sec

4.9 Cytotoxicity evaluation

The cytotoxicity of hydrogels was assessed indirectly on mouse fibroblasts (NIH3T3, Atcc, USA). Cyclodextrins were added to the polyurethanes dissolved in PBS and, before complete gelation, the samples were injected in bijou sample containers in such a way as to have approximately 250 mg of solution for each vial. Then, the samples were sterilized by UV for 30 minutes and then left to gel for 48 hours. Dulbecco's Modified Eagle Medium (DMEM) (supplemented with 10% fetal bovine serum, 290 µg/mL glutamine, 100 U/mL penicillin and 100 µg/mL streptomycin) and the obtained samples were equilibrated for 15 minutes at 37 °C. Then, DMEM was added to the hydrogels (1 ml of medium was added per 100 mg of hydrogel) and the samples were incubated for 24 hours at 37 °C. In parallel, 3T3 cells were seeded (20’000 cells/well) into a 96-well plate (LLG Labware, Germany) coated with gelatin (Sigma Aldrich, Milan, Italy) and incubated for 24 hours (37° C, 5% CO_2). After this period, the DMEM eluate containing also sample extracts was collected, sterilised through a 0.22 µm syringe filter (LLG Labware, Germany) and incubated in contact with the

previously cultured cells for 24 h at 37 °C (100 µL/well). Then, the eluates were removed from each well and the media was totally refreshed with new one (100 µL/well) containing Resazurine (0.1 mg/mL, Sigma Aldrich, Milan, Italy) to perform alamarBlue assay. This test allowed to evaluate cell viability since the dye becomes fluorescent only if it has been reduced at mitochondrial level by viable cells. The reduced product is sensitive to light at 530 nm and is able to emit radiation at 595 nm. Upon incubation of cells in the presence of Resazurine for 1 h at 37 °C, fluorescence was measured through a plate reader (Perkin Elmer Victor X3). Positive control samples were also prepared with pure DMEM. Data are reported as average ± standard deviation.

4.10 Evaluation of curcumin degradation in different solvents

Different solvents were used to evaluate the characteristic curcumin peak and the possible presence of degradation products by UV-visible spectroscopy. To this aim, curcumin was dissolved in ethanol (1 mg/mL) and then diluted in bi-distilled water (ddH2O) and PBS to obtain a final concentration of 10 µg/mL. Other two solutions were obtained by using an α-cyclodextrins (14% w/v) solution previously prepared in bi-distilled water or PBS as solvent for curcumin. In detail, α-cyclodextrins aqueous solutions were added to curcumin in order to obtain solutions with curcumin concentration of 0.1 mg/ml and then they were properly diluted to obtain solutions at 10 µg/mL curcumin concentration. These four solutions (curcumin_ddH2O, curcumin_PBS, curcumin_ddH2O_αCD and curcumin_PBS_αCD) were analysed with an UV-visible spectrophotometer (Perkin Elmer Lambda 365 UV/VIS Spectrometer, range 300-700 nm, resolution 1 nm, room temperature) in order to evaluate the peak at 430 nm which is characteristic of curcumin and any variation of the entire curcumin spectrum.

4.11 Preparation of Supramolecular Hydrogels loaded with curcumin

In order to prepare supramolecular hydrogels containing curcumin, CHP407, SHP407 and blend composed of CHP407 and SHF68 were first dissolved in PBS for 24 h at 5 °C. Then, half the amount of α-cyclodextrins required for supramolecular hydrogels preparation (final αCD content in the hydrogels 10% w/v) was dissolved in PBS (14% w/v concentration) for 15 min with the help of an external water bath at 40-50 °C. The other half was dissolved

in ddH2O, using the same process as described above. This solution was used as a solvent for curcumin (Sigma-Aldrich, M_w=368.38 g/mol, purity>65%) and the resulting solution containing α-cyclodextrins and curcumin at 14% w/v and 100 μg/mL concentration, respectively, was stirred overnight and then sonicated for 3 minutes (30% total power (130W), Vibracell VCX130, Sonics, USA) in a water-ice bath. Finally, the solutions containing only α-cyclodextrins in PBS and that containing α-cyclodextrins and curcumin in bi-distilled water were added to the previously prepared polyurethane solution in order to obtain the desired concentration of drug (35 μg/mL), α-cyclodextrins (10% w/v) and synthetic polymer (CHP407 and SHP407 final concentrations of 1% w/v, 3% w/v, and CHP407 and SHF68 blend final concentration of 0.8%w/v and 0.2%w/v -final synthetic polymer content of 1% w/v- or 2.4%w/v and 0.6%w/v -final synthetic polymer content of 3% w/v-) within the hydrogel. To make the hydrogel solution homogeneous, the samples were vortexed and allowed to assemble for 72 hours.

4.12 Study of Curcumin Release from Supramolecular Hydrogels

Supramolecular hydrogels containing curcumin were prepared by the previously explained method, equilibrated at 37 °C for 15 minutes and then added with 1 mL releasing medium (PBS) at 37°C. At different time steps (2, 4, 6, 24, 30, 48, 72 and 96 hours) PBS was completely renewed and the collected eluates were collected and analysed through a plate reader (Perkin Elmer Victor X3) at a wavelength of 450 nm. For the quantification of curcumin in solution, a calibration curve was obtained through the preparation of specific standard samples at different concentrations ranging between 0 μg/mL and 10 μg/mL.

4.13 Statistical Analysis

The results obtained were analysed through the program OriginPro 8 for Windows 10 HOME. The comparison between the different results was carried out using the One-way ANOVA analysis and statistical significance of each comparison has defined as summarized in Table 3.

Table 3 Statistical Significance

P	Statistical Significance	Summary
<0,0001	Extremely significant	****
0,0001 to 0,001	Extremely significant	***
0,001 to 0,01	Very significant	**
0,01 to 0,05	Significant	*
>0,05	Not significant	-

5. Results and Discussion

5.1 Synthesized Polyurethanes and Composition

As described in section 2.1, the synthesis of polyurethanes was conducted according to the same protocol, but using different reagents. These variations in composition allowed to obtain materials with extremely different behaviour and, in this regard, this thesis work aimed at comparing the characteristics and possible uses of these different polymers. Table 2 summarizes the composition and acronyms of the synthesized materials.

Table 4 Synthesized Polyurethanes and their composition

	MACRODIOL	CHAIN EXTENDER	DIISOCYANATE	DEPROTECTED FORM
CHP407	Poloxamer 407	1,4-cyclohexane dimethanol	1,6-Hexamethylene diisocyanate	-
NHP407	Poloxamer 407	N-Boc serinol	1,6-Hexamethylene diisocyanate	**SHP407**
NHF68	Poloxamer F68	N-Boc serinol	1,6-Hexamethylene diisocyanate	**SHF68**

5.2 Chemical Characterization of Polyurethanes

5.2.1 Attenuated Total Reflectance Fourier Transformed Infrared (ATR-FTIR) Spectroscopy

ATR-FTIR analysis allowed to verify if the synthesis of polyurethane was performed correctly. In fact, by comparing the transmittance (or the absorbance) spectra of the macrodiol and the synthesized polyurethane, the appaerance of the characteristic peaks of the urethane bond allowed to prove the success of the synthesis process.

Figure 36 reports the ATR-FTIR spectra of P407 and the two P407-based polyurethanes, NHP407 and CHP407. The urethane bonds present in the polyurethanes were characterized by the peaks at 3348 cm^{-1}, 1720 cm^{-1} and 1530 cm^{-1} which identify the stretching of the N-H bonds, the stretching of the C=O groups and the concurrent bending of N-H and stretching of C-N bonds, respectively. These listed peaks were not present in the macrodiol spectrum and they were present in NHP407 and CHP407 ATR-FTIR spectra, thus suggesting that the urethane domains were successfully obtained. Additionally, all the characteristic peaks of the macrodiol were also present in CHP407 and NHP407. In addition, no peaks were identified at 2200 cm^{-1}, suggesting that the diisocyanate used during the synthesis reacted completely without leaving any isocyanates residue.

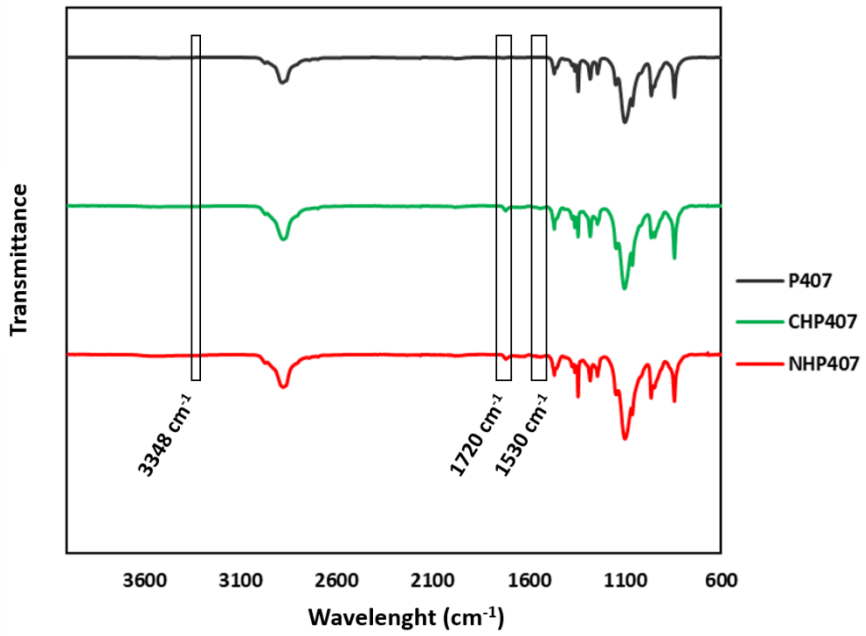

Figure 36 ATR-FTIR spectra of P407, NHP407, CHP407

Figure 37 compares the ATR-FTIR spectra of the polyurethane in its original state (NHP407) and the one obtained after the deprotection of the Boc-protected amino groups (SHP407). Substantial differences in the characteristic peaks of polyurethane were not noticeable, suggesting that the material was not significantly degraded during the deprotection process.

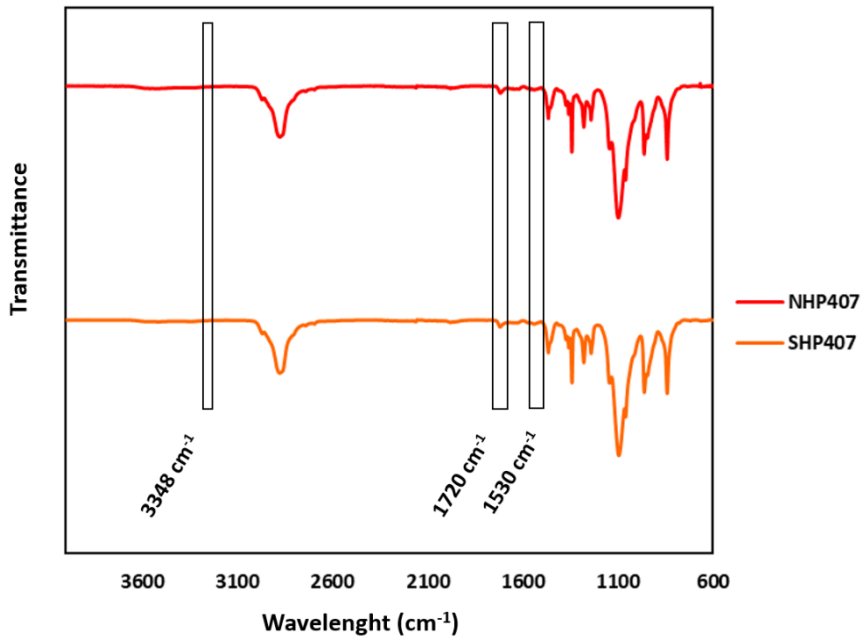

Figure 37 ATR-FTIR spectra of NHP407 and SHP407

Similar considerations were made for NHF68 polyurethane compared to its macrodiol F68 (Figure 38), suggesting that changing the macrodiol did not affect the successful synthesis of the polyurethane and the complete conversion of isocyanate groups.

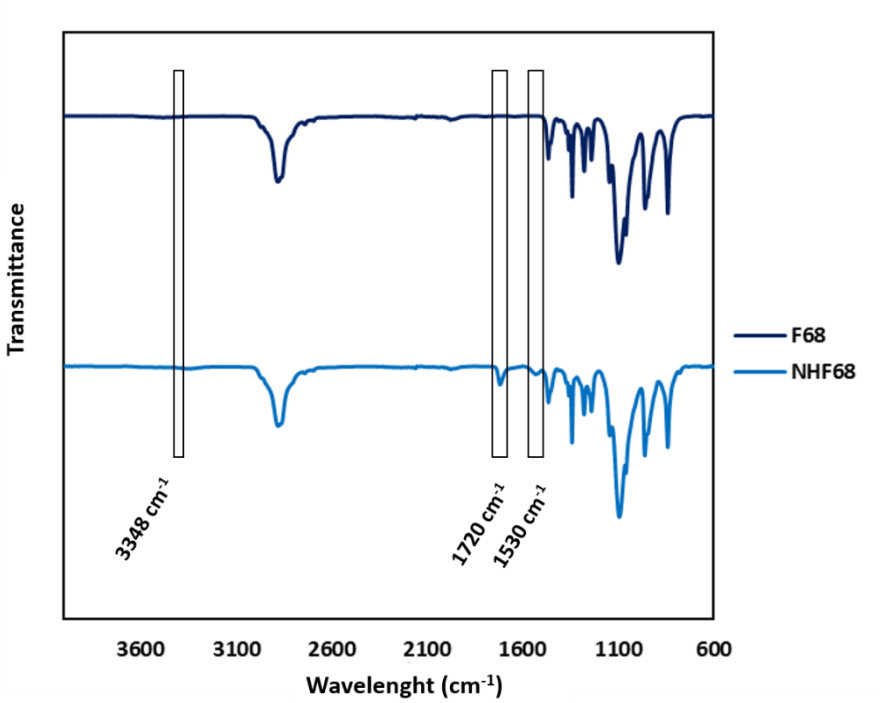

Figure 38 ATR-FTIR spectra of F68 and NHF68

Similarly, the deprotection reaction did not induced any significant degradation of F68-based polyurethane, as shown in Figure 39 that compares NHF68 and SHF68 ATR-FTIR spectra.

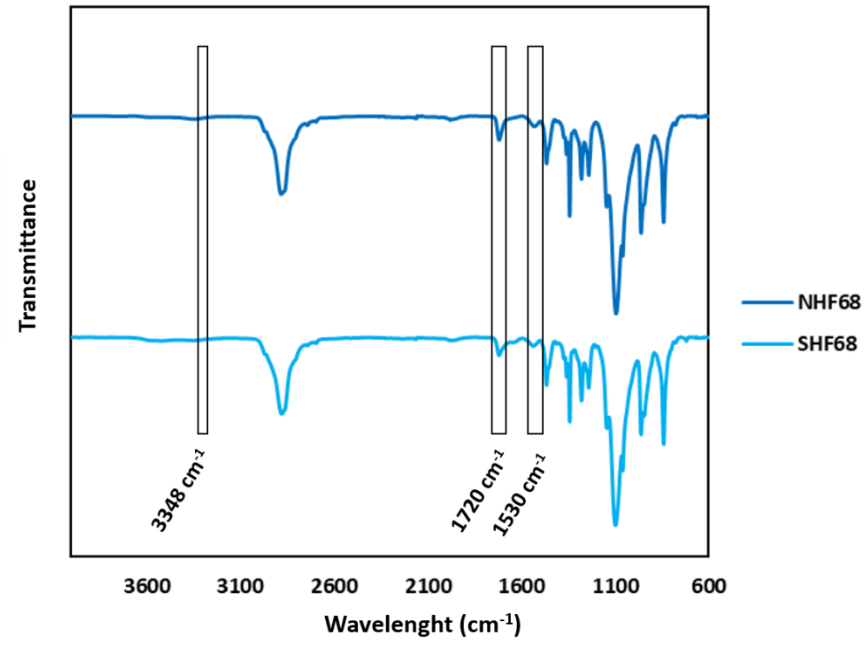

Figure 39 ATR-FTIR spectra of NHF68 and SHF68

5.2.2 Size Exclusion Chromatography (SEC)

Size Exclusion Chromatography measurements allows to estimate the molecular weight of polymers. In the present work, SEC analyses allowed to first assess the success of the synthesis reaction and then to verify the absence of degradation phenomena induced by the deprotection process performed on NHP407 and NHF68.

Figure 40 compares the trends of normalized RID signal *vs* elution time for Poloxamer 407, NHP407 and SHP407. As it was seen from the graph, the macrodiol had a much lower molecular weight (corresponding to a longer elution time) than the polyurethanes, while the signals of NHP407 and SHP407 were comparable, suggesting that the deprotection reaction did not induce any degradation of the polyurethane backbone. The two polyurethanes NHP407 and SHP407 were found to have a similar number average molecular weight (M_n) in the neighbourhood of 27000 Da with a polydispersity index of about 1.75, while P407 showed M_n of 8000 Da with a polydispersity index of 1.2.

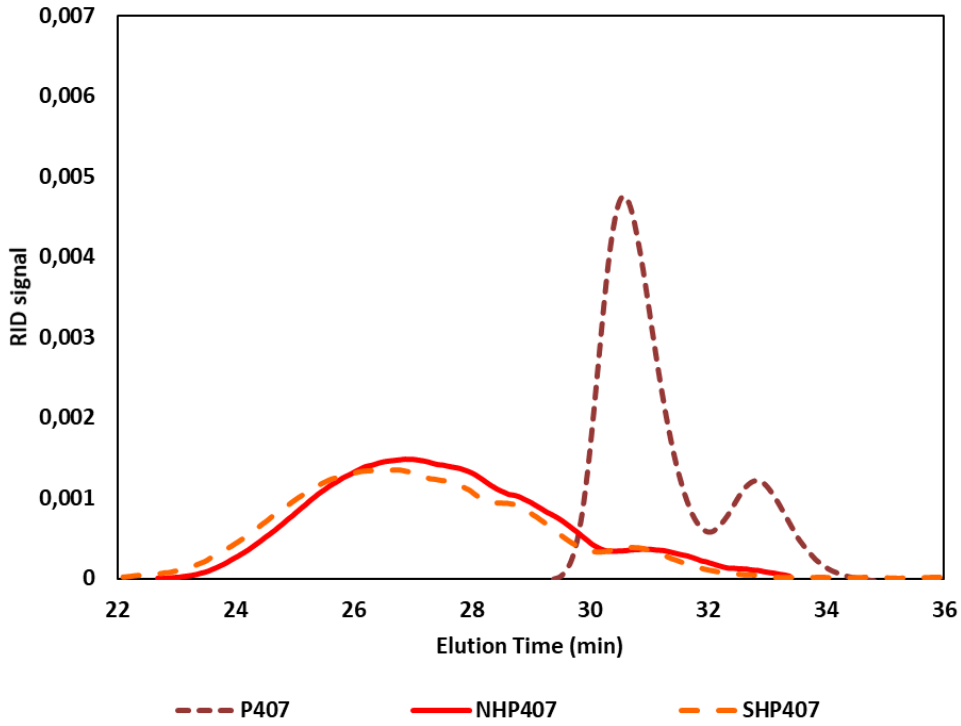

Figure 40 Trends of normalized RID signal as a function of elution time for P407 (dotted line), NHP407 (continuous line) and SHP407 (dashed line)

Figure 41 reports the comparison of the trends of normalized RID signal *vs* elution time for P407 and CHP407. Also, in this case the macrodiol alone had a lower M_n than the polyurethane, which showed M_n of 31000 Da with a polydispersity index of 1.7. Hence, being diisocyanate and macrodiol the chain, changing the chain extender (CDM instead of N-Boc serinol) did not significantly affect the molecular weight of the resulting polyurethane, being the difference in M_n of NHP407 and CHP407 within instrument error.

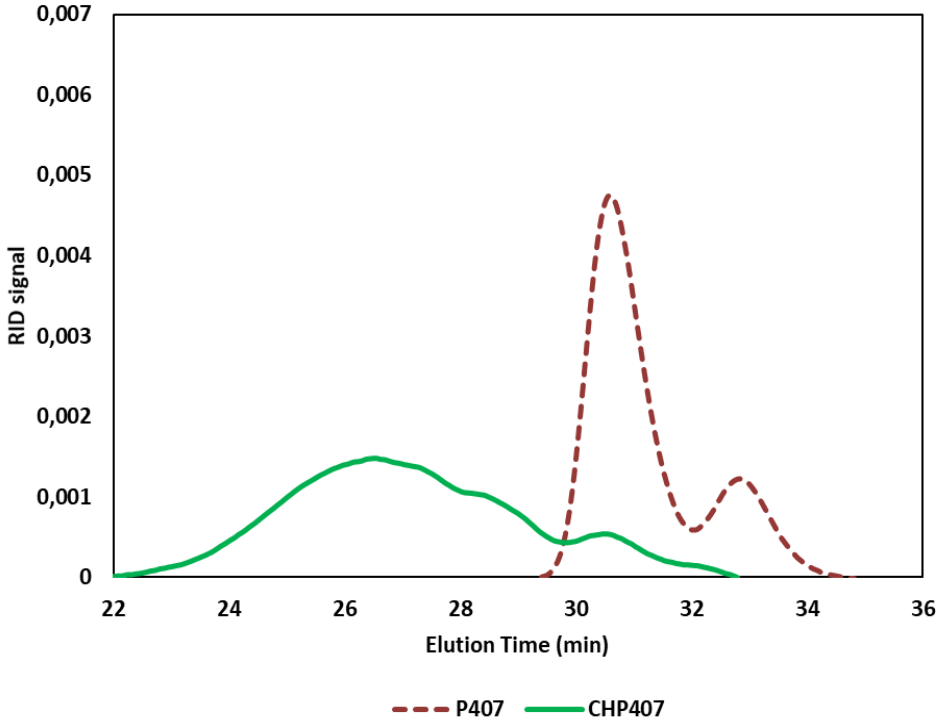

Figure 41 Trends of normalized RID signal as a function of elution time for P407 (dotted line), CHP407 (continuous line)

With regard to polyurethane NHF68 and its deprotected form SHF68, the trends of normalized RID signal as a function of elution time are reported in Figure 42, comparing them with their constituent Poloxamer F68. Also, in this case F68 turned out to have a molecular weight M_n much lower than polyurethanes: 6300 Da with a polydispersity index of about 1.1 compared to 22000 Da and 25000 Da for NHF68 and SHF68 (polydispersity index of 1.8 and 1.6), respectively. As for the deprotection process, the molecular weight of the protected polyurethane was not too different from that of the deprotected polyurethane and therefore there was no degradation of the polymer (the observed differences are within instrument error). However, the peak at around 31 minutes elution time present in NHF68 signal turned out to be attenuated in SHF68, probably as a

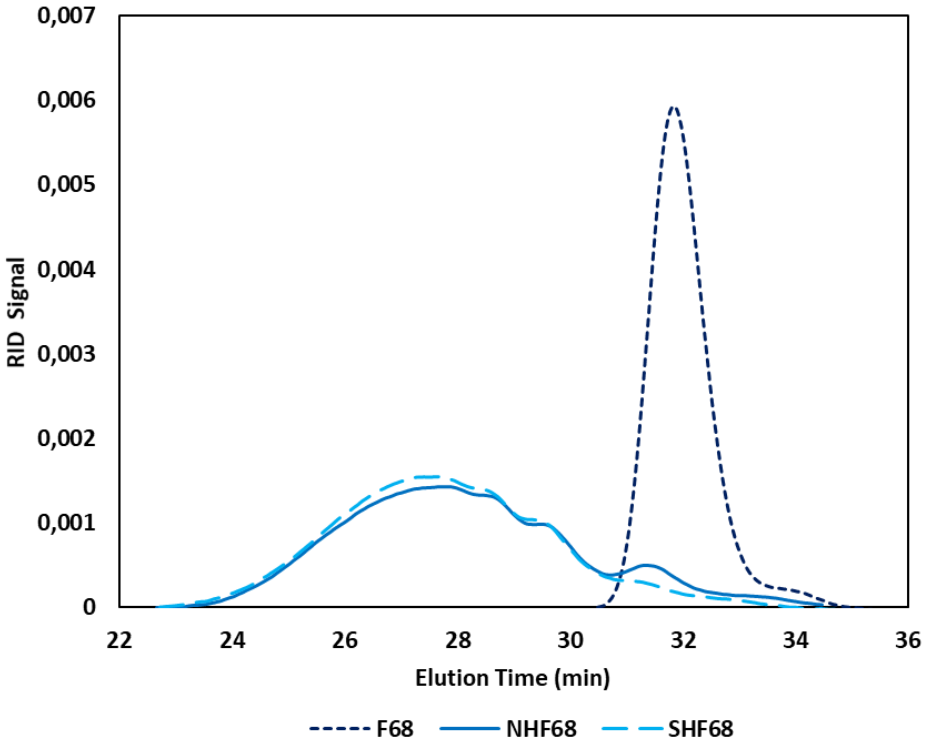

Figure 42 Trends of normalized RID signal as a function of elution time for F68 (dotted line), NHF687 (continuous line) and SHF68 (dashed line)

consequence of the dialysis step which allowed to remove those species with a molecular weight of approx. 10000 Da.

To understand which chemical species were involved, a differential chromatography in which the different species going out of the SEC instrument can be divided and separately analysed by ATR-FTIR and ^{1}H-NMR characterizations would be necessary.

Table 5 summarizes the number average molecular weights and the polydispersity indexes calculated for each material analysed.

Table 5 Number average Molecular weight and polydispersity indexes of Synthetized Polyurethanes and Poloxamers

	Number average Molecular Weight (Da)	**Polidispersity index**
P407	8000	1.2
CHP407	31000	1.2
NHP407	27000	1.75
SHP407	27000	1.75
F68	6300	1.1
NHF68	22000	1.8

SHF68	25000	1.6

5.2.3 UV-Visible spectroscopy – Ninhydrin Assay (Kaiser Test): quantification of amino groups exposed on SHP407 and SHF68

The Ninhydrin Assay is a method for the evaluation and quantification of the free amino groups present in a given material. Hence, in this thesis work, it was exploited to quantify the number of free amino groups present in the polyurethanes that had undergone the process of cleavage of Boc-protected amino groups. Then, the collected data for polyurethanes with the Boc-protected amines and for those exposing free amino groups were compared. The colour of the material solution obtained as a result of the Kaiser test was indicative of the quantity of free amino groups exposed: if the colour was predominantly yellow there were no free amino groups, while the more the blue colour intensified the higher was the amount of free NH_2 groups. The number of units of free amino groups per gram were calculated by evaluating the ninhydrin peak of absorbance at 570 nm obtained through UV-visible spectroscopy.

Regarding the NHP407 polyurethane and the comparison with its deprotected species (SHP407), it was possible to notice from the material solutions that the first turned out to be yellow while the SHP407 had a light blue/purple colour (Figure 43).

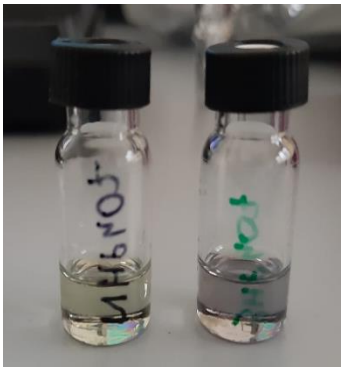

Figure 43 Solution of NHP407 (left) and SHP407 (right) resulting from the Ninhydrin Assay

By analysing the two solutions with the UV-visible spectrophotometer, it was possible to note that the absorbance peak at 570 nm was higher in the case of the deprotected polyurethane compared to native NHP407 (Figure 44). In fact, by analysing the data and subtracting the contribution of NHP407 absorbance at 570 nm to that of SHP407, the

effective number of free amino groups exposed in SHP407 turned out to be $0.07 * 10^{18}$ units/gram.

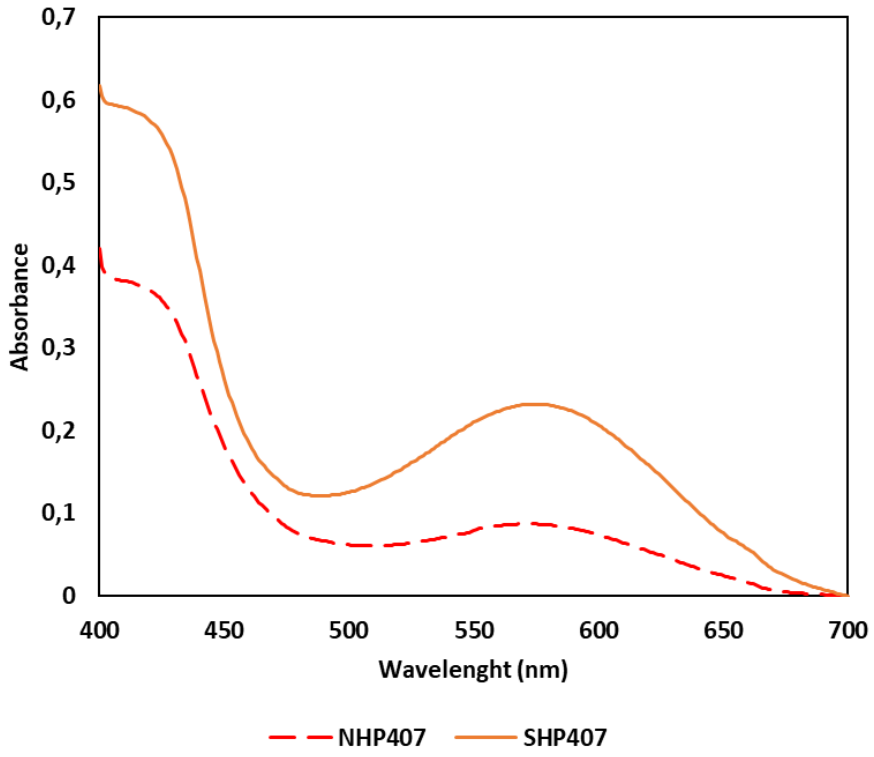

Figure 44 Trend of absorbance vs wavelength within the spectra range between 400 and 700 nm for NHP407 (dashed line) and SHP407 (continuous line) samples resulting from Kaiser test

Similarly, also NHF68 and its deprotected form SHF68 was analysed through Kaiser test, showing a similar behaviour to NHP407 and SHP407. In fact, NHF68 and SHF68 solutions resulting from Kaiser test turned out to be yellow and deep blue/purple, respectively (Figure 45).

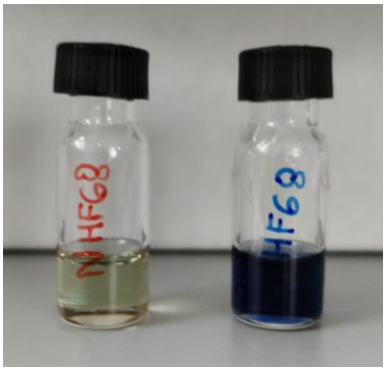

Figure 45 Solution of NHF68 (left) and SHF68 (right) obtained with the Ninhydrin Assay

By analysing the solutions with the UV-visible spectrophotometer (Figure 46) and subtracting the contribution of NHF68 absorbance at 570 nm to that of SHF68, the effective number of free amino groups exposed in SHF68 turned out to be $1.6 * 10^{18}$ units/gram.

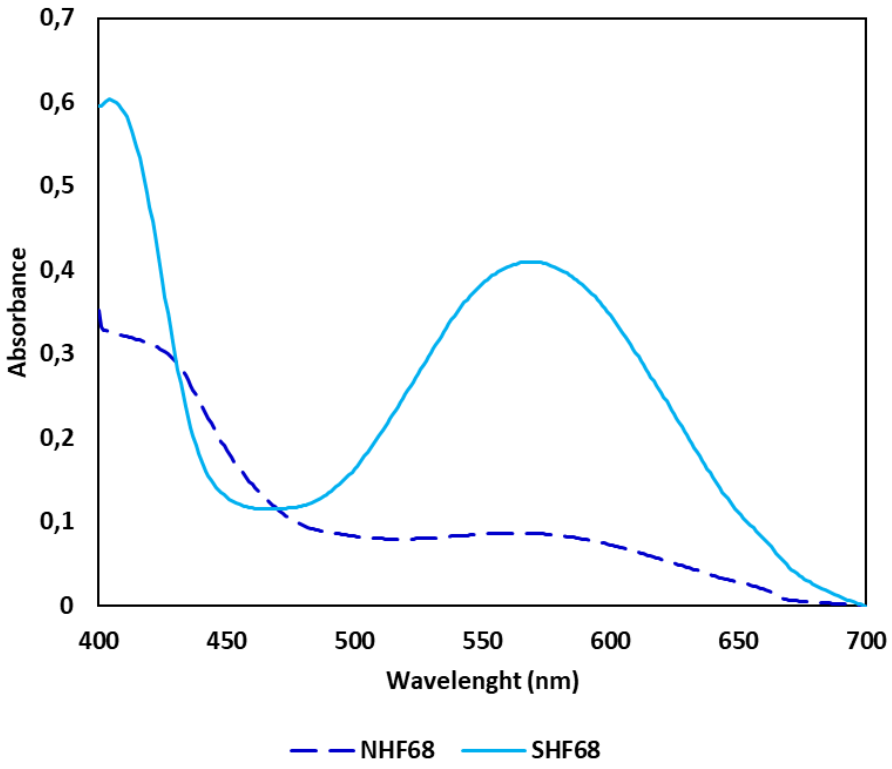

Figure 46 Trend of absorbance vs wavelength within the spectra range between 400 and 700 nm for NHF68 (dashed line) and SHF68 (continuous line) samples resulting from Kaiser test

As inferred from the comparison of the graphs and the calculated amount of free amino groups exposed per each gram of polyurethane, the SHF68 exhibited a higher amount of free amines than SHP407. Another confirmation of this was found in the colour of the solutions obtained by the ninhydrin test: in fact, as shown in the Figure 43 and in the Figure 45, the solution of SHF68 had a much darker blue than that of the SHP407, because ninhydrin reacted with a higher amount of amino groups.

This result can be explained hypothesizing a higher degree of polymerisation for NHF68 than for NHP407. In fact, with increasing the degree of polymerisation, which can also be theoretically calculated by the molecular weights of the macrodiol and the obtained polyurethane, also the number of amines present in the chain increased.

Hence, SHF68 showed a higher number of available functionalities for the potential functionalization of the material with carbodiimide chemistry or its chemical crosslinking. On the other hand, this higher number of exposed amines is expected to provide the material with a stronger antibacterial power.

Table 6 summarizes the obtained results with Ninhydrin Assay.

Table 6 Amount of free amino groups exposed along SHP407 and SHF68 polymer chains

	exposed amines (units/$g_{polymer}$)
SHP407	$0.07 * 10^{18}$
SHF68	$1.6 * 10^{18}$

5.3 Characterization of not-gelling polyurethane solutions

5.3.1 Dynamic Light Scattering (DLS)

Not-gelling polyurethane solutions were analysed by Dynamic Light Scattering to evaluate the formation of micelles and micelle aggregates and their hydrodynamic diameter at different temperatures. The characterized materials were CHP407, SHP407, SHF68 and a blend composed of CHP407 and SHF68, all kept at a total concentration of 1% w/v (for the blend, the composition was 80:20 w/w CHP407/SHF68), dissolved in PBS and tested at 25 °C and 37 °C. With regard to CHP407, the graphs in Figure 47 reports the formation of stable micelles at both 25 °C and 37 °C with an average diameter of 30 nm ($\pm$5.69 nm) and 34 nm ($\pm$4.38 nm), respectively. This result can be correlated to the fact that CHP407

polyurethane had very strong hydrophobic domains, which allowed to obtain very stable micelles even at 25°C.

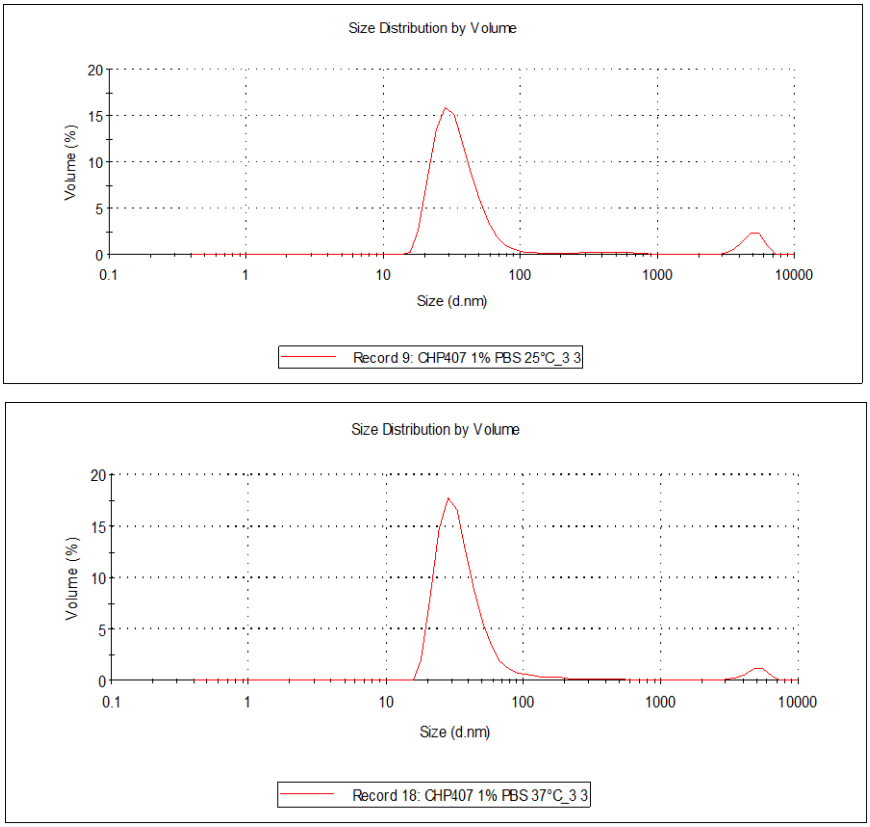

Figure 47 Size distribution by volume for CHP407 solutions (1% w/v) at 25°C (top) and 37°C (bottom)

As shown in the diagrams in Figure 48, SHP407 solution instead had a different behavior: at 25 °C it did not form stable micelles, as evidenced by the three curves reported in the figure which were recorded on three different samples. By increasing the temperature to 37°C, micelles stabilized, reaching a size of approximately 35 nm ($\pm$1.7 nm), in accordance with data obtained for CHP407.

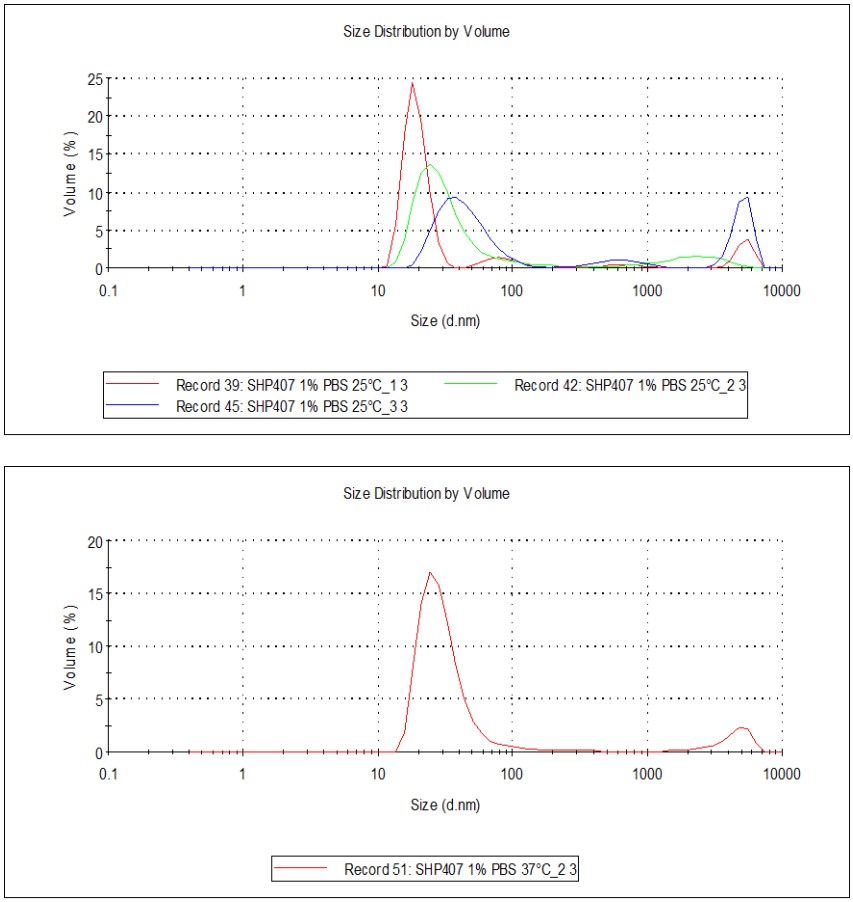

Figure 48 Size distribution by volume for SHP407 solutions (1% w/v) at 25°C (top) and 37°C (bottom)

Observing the behaviour of the solution of SHF68 polyurethane, this sample did not show stable micelles neither at 25 °C nor at 37 °C as a consequence of its high hydrophilicity (Figure 49). Since this high hydrophilicity could impair polymer capability to undergo micellization also at high concentrations, with detrimental consequences on the possibility of formulations with proper composition to undergo sol-gel transition resulting in the formation of supramolecular hydrogels, SHF68 was blended with CHP407. The rationale underpinning this choice lies on the possibility to combine a polymer with high functionalization, crosslinking and antibacterial potential with a polymer which in previous works showed excellent mechanical characteristics, stability in aqueous environment and fast gelation kinetics [46][47 in preparation].

Hence, DLS analyses were performed on a blend composed of 80% w/w of CHP407 and 20% w/w of SHF68 (total polymer concentration of 1% w/v). At 25 °C there were no stable micelles, while at 37 °C the three analyzed samples appeared to have a greater stability of

the formed micelles, with an average hydrodynamic diameters of 32 nm (±7.32 nm) (Figure 50).

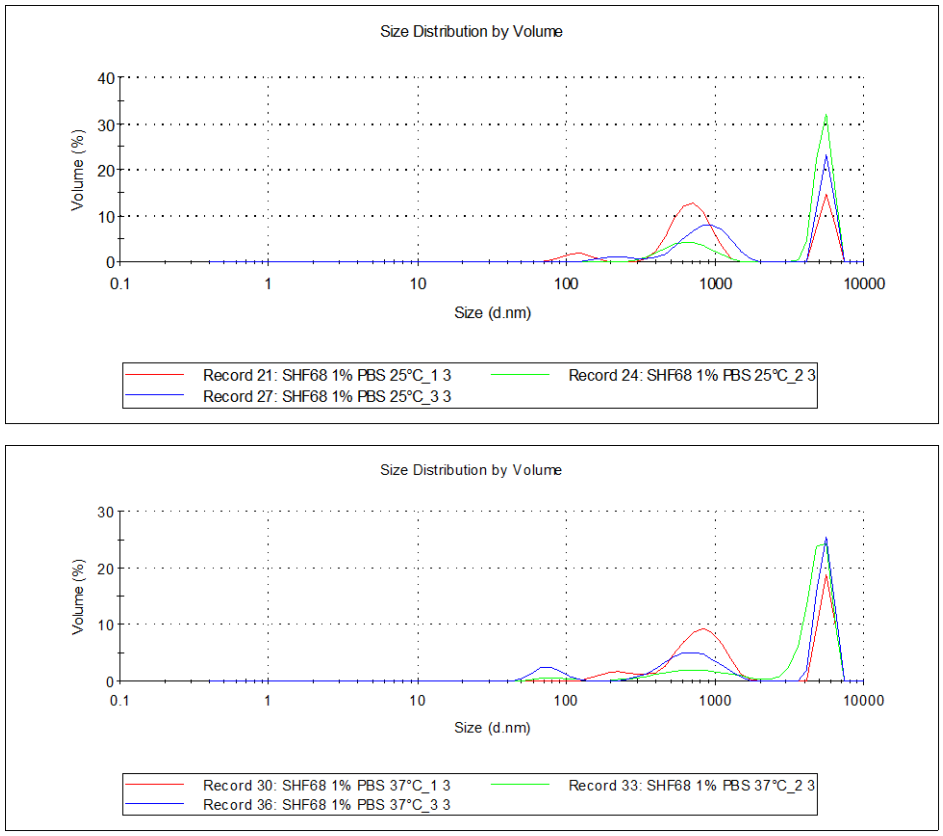

Figure 49 Size distribution by volume for CHP407 solutions (1% w/v) at 25°C (top) and 37°C (bottom)

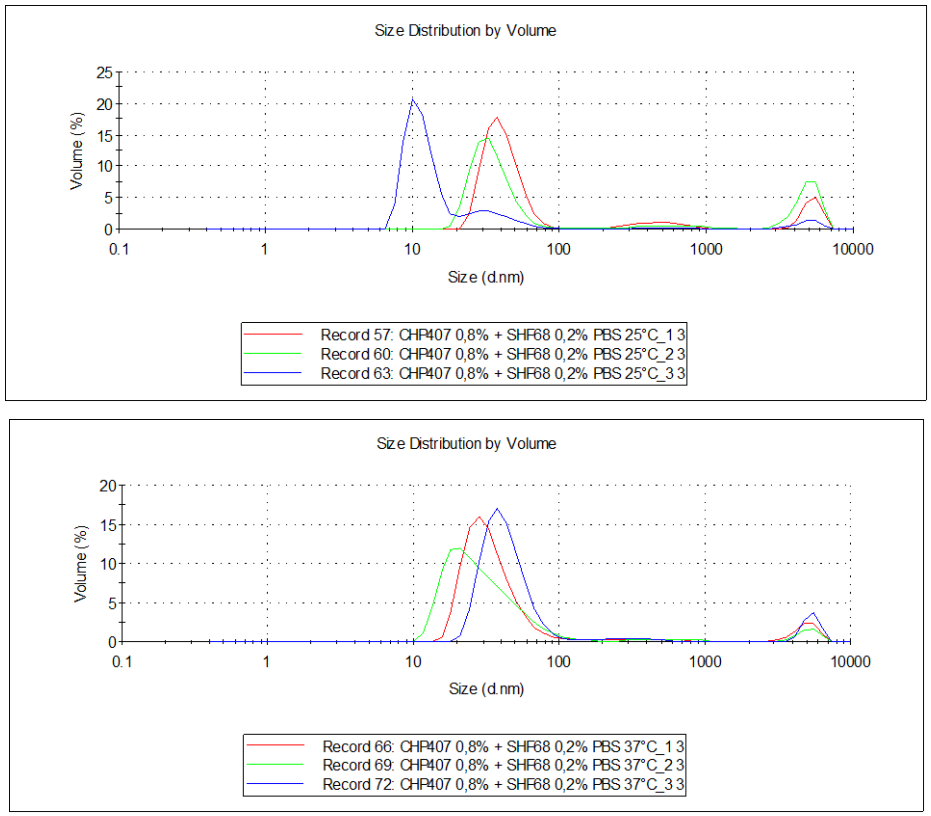

Figure 50 Size distribution by volume for CHP407 solutions (1% w/v) at 25°C (top) and 37°C (bottom)

5.3.2 Evaluation of Antibacterial Activity of Polyurethanes Solution

Antibacterial tests were conducted on 5%w/v concentrated NHP407, SHP407, NHF68 and SHF68 aqueous solutions and their behaviour in contact with different bacteria was evaluated.

Using the agar diffusion method, NHP407, SHP407, NHF68 and SHF68 solutions were evaluated in contact with *Escherichia coli*, *Pseudomonas aeruginosa* and *Staphylococcus aureus*. For what concerns NHP407 and SHP407 solutions, they exhibited partial bacterial inhibition for all the three tested strains. On the other hand, NHF68 and SHF68 solutions did not show any antibacterial activity against *Escherichia coli* and *Pseudomonas aeruginosa* but expressed a slight growth inhibition against *Staphylococcus aureus* (Figure 51, Figure 52, Figure 53).

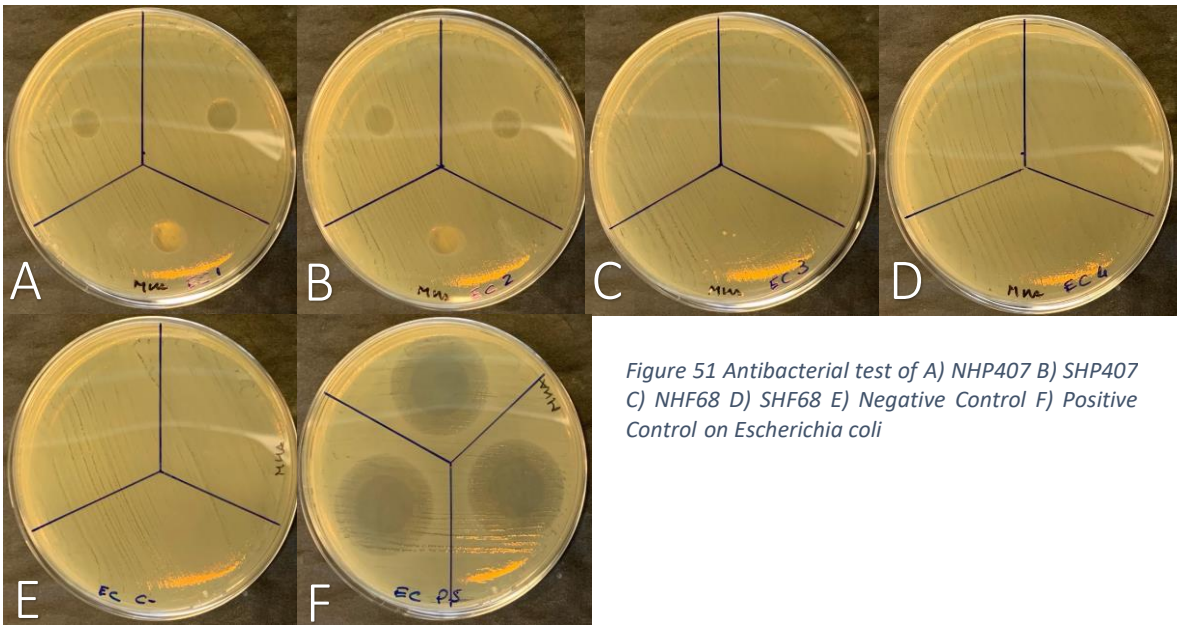

Figure 51 Antibacterial test of A) NHP407 B) SHP407 C) NHF68 D) SHF68 E) Negative Control F) Positive Control on Escherichia coli

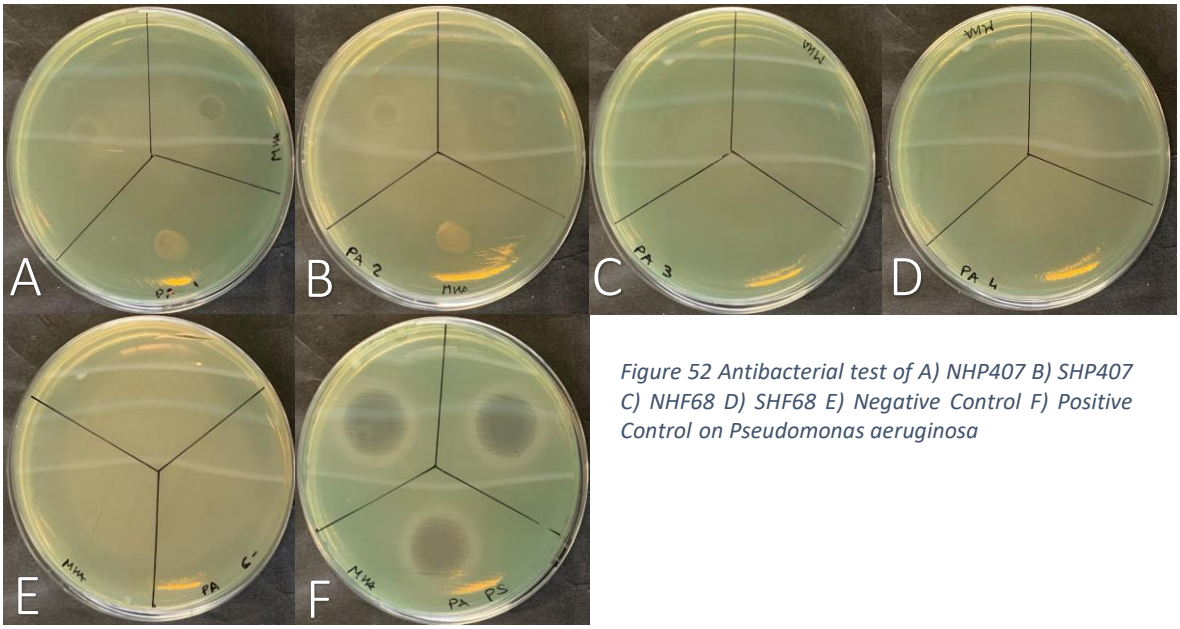

Figure 52 Antibacterial test of A) NHP407 B) SHP407 C) NHF68 D) SHF68 E) Negative Control F) Positive Control on Pseudomonas aeruginosa

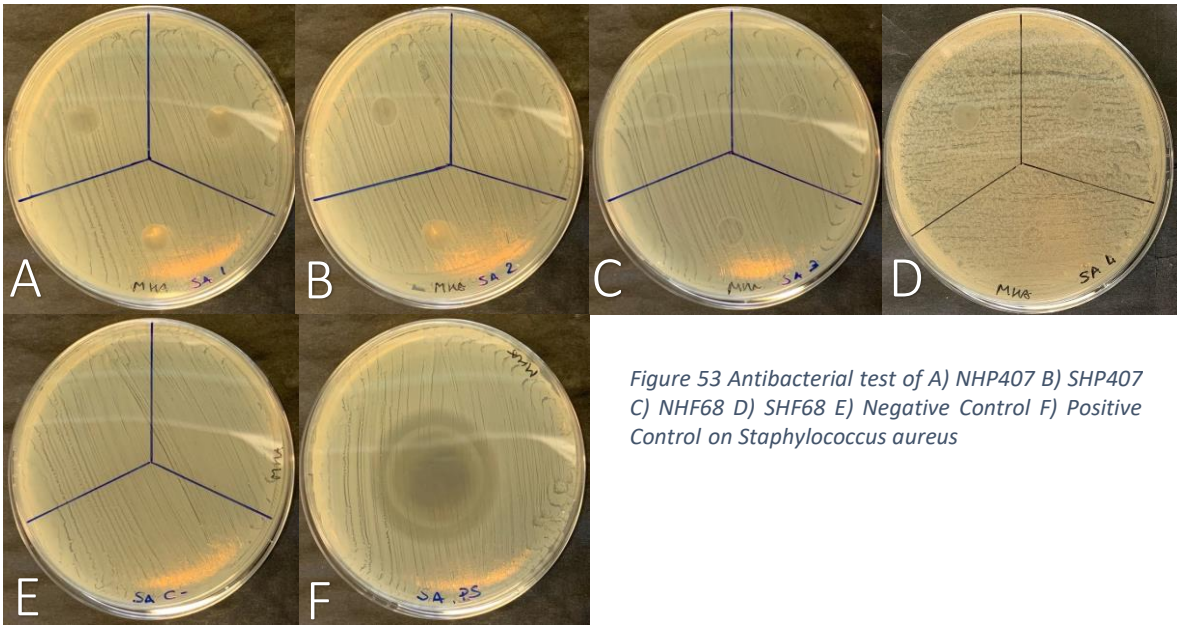

Figure 53 Antibacterial test of A) NHP407 B) SHP407 C) NHF68 D) SHF68 E) Negative Control F) Positive Control on Staphylococcus aureus

Polyurethane antibacterial activities on *Escherichia coli*, *Pseudomonas aeruginosa*, *Staphylococcus aureus* and *Candida albicans* were also evaluated using solutions of polyurethanes (NHP407, SHP407, NHF68 and SHF68) at different concentrations (25 mg/mL, 12.5 mg/mL, 6.25 mg/mL, 3.12 mg/mL, 1.56 mg/mL and 0.78 mg/mL) with the micro-dilution in broth with microplate method.

Tables 7, 8, 9 and 10 report the percentage of inhibition induced by each polyurethane on each investigated strain as a function of polyurethane concentration. No polyurethane had an evident antibacterial action on *Pseudomonas aeruginosa* and *Candida albicans* while an intermediate inhibitory force was displayed against *Escherichia coli*. In the latter case NHP407 and NHF68 shown greater inhibitory power at each tested concentration compared to SHF68 and SHP407. For what concerns *Staphylococcus aureus*, all the solutions exhibited a good antibacterial activity, in particular NHF68 and SHF68 at 25 mg/mL.

These data suggest that the exposed amino groups did not increase the antibacterial potential of the material. Probably, the most important role on the antibacterial behaviour was related to the amphiphilic nature of the materials rather than to the exposure of free amino groups. In fact, the amphiphilic nature of these materials induces a better inhibition of bacteria growth due to an enhanced interaction and damage of their cell membrane [48].

Table 7 Percentage of inhibition induced by each polyurethane on Escherichia coli as a function of polyurethane concentration

	0 mg/mL	**0.78 mg/mL**	**1.56 mg/mL**	**3.12 mg/mL**	**6.25 mg/mL**	**12.5 mg/mL**	**25 mg/mL**
NHP407		50%	50%	51%	62%	68%	74%
SHP407		22%	33%	33%	34%	35%	45%
NHF68		32%	32%	43%	56%	63%	75%
SHF68		29%	32%	34%	37%	29%	59%

Table 8 Percentage of inhibition induced by each polyurethane on Pseudomonas aeruginosa as a function of polyurethane concentration

	0 mg/mL	**0.78 mg/mL**	**1.56 mg/mL**	**3.12 mg/mL**	**6.25 mg/mL**	**12.5 mg/mL**	**25 mg/mL**
NHP407		2%	-	-	1%	-	6%
SHP407		1%	2%	-	1%	-	2%
NHF68		4%	5%	8%	3%	4%	6%
SHF68		5%	5%	9%	5%	5%	6%

Table 9 Percentage of inhibition induced by each polyurethane on Staphylococcus aureus as a function of polyurethane concentration

	0 mg/mL	**0.78 mg/mL**	**1.56 mg/mL**	**3.12 mg/mL**	**6.25 mg/mL**	**12.5 mg/mL**	**25 mg/mL**
NHP407		46%	47%	51%	52%	58%	70%
SHP407		42%	47%	54%	60%	63%	64%
NHF68		55%	55%	57%	58%	62%	84%
SHF68		50%	52%	54%	56%	56%	82%

Table 10 Percentage of inhibition induced by each polyurethane on Candida albicans as a function of polyurethane concentration

	0 mg/mL	**0.78 mg/mL**	**1.56 mg/mL**	**3.12 mg/mL**	**6.25 mg/mL**	**12.5 mg/mL**	**25 mg/mL**
NHP407		1%	3%	6%	6%	5%	9%
SHP407		-	8%	2%	4%	4%	4%
NHF68		3%	-	2%	-	1%	-
SHF68		3%	5%	1%	-	-	3%

5.4 Supramolecular Hydrogels Preparation and Gelation Kinetics

After the physico-chemical and thermal characterization of the synthesized polyurethanes and their aqueous solutions, in this work of thesis supramolecular hydrogels were then designed by combining these custom-made materials with α-cyclodextrins. As in the literature [35], by mixing cyclodextrins and specific linear polymers it is possible to obtain gels with physical crosslinks. In these systems, a small amount of synthetic component combined with αCD could be enough to observe a sol-to-gel transition, with no need of further agents which could damage the cells the material will interact with (e.g., chemical crosslinkers, etc.). Whereas the solubility threshold of α-cyclodextrins in PBS is 14% w/v [49] [50], the kinetics and gelation capacities of different supramolecular hydrogels containing high cyclodextrin concentrations within the range 9-11% w/v (i.e., 9% w/v, 10% w/v and 11% w/v) and low synthetic polymer content (i.e., 1% w/v, 3% w/v, 5% w/v and 9% w/v) were tested.

Firstly, the gelation kinetics of supramolecular hydrogels based on the two Poloxamers as such (F68 and P407) were evaluated (Table 11).

Table 11 Gelation time and appearance of supramolecular hydrogels based on F68 and P407 (observation time up to 72h)

Formulation code	**Appearance and Gelation Time**
F68-1-9CD	gel (3 h)
F68-1-10CD	gel (3 h)
F68-1-11CD	gel (3 h)
F68-5-9CD	gel (3 h)
F68-5-10CD	gel (3 h)
F68-5-11CD	gel (1 h 30 min)

As it is possible to observe from the data shown in the table 11, F68, even at low concentrations, had a fast transition kinetics from solution to gel and it was easy to solubilize even at higher concentrations, thanks to its more hydrophilic character. Instead, with regard to Poloxamer 407, in a previous work [41]phase separation phenomena have been observed within this polymer concentration range, which can limit the use P407 as

synthetic constituent of supramolecular hydrogels. In fact, in literature [42] P407 has been used in supramolecular systems at remarkably higher concentrations (ranging between 6,5% w/v and 20% w/v) in order to guarantee the formation of stable hydrogel systems.

Similar analyses were conducted on supramolecular formulations prepared starting from the polyurethanes synthesized in the present work. Table 12 reports gelation time and appearance of supramolecular hydrogels based on NHP407 and NHF68 up to 72 hour observation.

Table 12 Gelation time and appearance of supramolecular hydrogels based on NHF68 and NHP407 (observation time up to 72h)

Formulation code	**Appearance and Gelation Time**
NHP407-1-9CD	gel (overnight)
NHP407-1-10CD	gel (overnight)
NHP407-1-11CD	gel (overnight)
NHP407-5-9CD	gel (overnight)
NHP407-5-10CD	gel (2 h 30 min)
NHP407-5-11CD	gel (1 h)
NHP407-9-9CD	gel (1h 30 min)
NHP407-9-10CD	*
NHF68-1-9CD	sol
NHF68-1-10CD	sol
NHF68-1-11CD	sol
NHF68-5-9CD	gel (72 h)
NHF68-5-10CD	gel (72h)
NHF68-5-11CD	gel (overnight)
NHF68-9-9CD	gel (72 h)
NHF68-9-10CD	gel (overnight)

* polyurethane difficult to solubilize at the required concentration to finally achieve a polymer and αCD of 9 and 10 % w/v

The highest investigated concentration of α-cyclodextrins (i.e., 11% w/v) required the polyurethanes to be initially solubilized at very high concentration (around 5% w/v), thus making not possible the production of samples containing a final polyurethane

concentration of 9% w/v. NHF68-based formulation at low concentrations (1% w/v) did not reach gelation even with high amounts of cyclodextrins. With regard to the other compositions having NHF68 as a synthetic part, also in these cases gelation occurred in much longer time than NHP407-based samples with the same composition. Probably, this was caused by the higher amount of BOC pendant groups exposed by SHF68 compared to NHP407 which acted as a steric hindrance to the entry of the chains inside the α-cyclodextrins cavity. Moreover, in a previous work [37] it has been supposed that the hydrophobic domains could play a fundamental role in the stabilisation of the polymer network during the process of self-assembly of hydrogels. As NHF68 was based on a macrodiol containing smaller hydrophobic regions of PPO, probably the observed slower gelation kinetics can be related to a less stable polymer network in solution. On the other hand, NHP407 polyurethane was not as easily to solubilize as NHF68 because P407-based polymers have a more hydrophobic character.

Gelation kinetics was also studied for supramolecular hydrogels based on SHF68 and SHP407 (Table 13).

Table 13 Gelation time and appearance of supramolecular hydrogels based on SHF68 and SHP407 (observation time up to 72h)

Formulation code	**Appearance**
SHP407-1-10CD	gel (overnight)
SHP407-5-10CD	gel (2 h)
SHF68-1-9CD	sol
SHF68-1-10CD	gel (overnight)
SHF68-1-11CD	gel (overnight)
SHF68-5-9CD	gel (overnight)
SHF68-5-10CD	gel (5 h 30 min)
SHF68-5-11CD	gel (5 h)

As expected from the previous results on NHP407, SHP407-based supramolecular hydrogels showed fast gelation kinetics and a set of promising hydrogels was selected in the concentration range of polyurethane between 1% and 5% w/v with α-cyclodextrins at 10% w/v. In case of SHF68-based hydrogels, the transition from solution to gel was also

achieved for those hydrogels composed of SHF68 at 1% w/v concentration and α-cyclodextrins at 10% w/v and 11% w/v, thus confirming the previous hypothesis on the steric hindrance of the pendant Boc groups of NHF68 in hindering the formation of poly(pseudo)rotaxanes and slowing down hydrogel gelation kinetics. In addition, both SHP407- and SHF68-based hydrogels showed faster gelation kinetics because the ions present in the solvent (PBS) interacted with the exposed amino groups, forming electrostatic interactions that enhanced the transition. In order to overcome the slow gelation kinetics of SHF68-based hydrogels, while maintaining the high potential of this material deriving from the huge amount of available pendant amines, a new class of supramolecular hydrogels was developed by blending it with CHP407, which in previous work [] has shown high potential as synthetic component of supramolecular gels. In detail, these new formulations were designed by blending CHP407 and SHF68 at different ratios so at to achieve an overall polyurethane concentration of 1% w/v, 2% w/v, 3% w/v and 5% w/v, while keeping α-cyclodextrins content constant (10% w/v concentration). Table 14 reports gelation time and appearance of supramolecular hydrogels based on CHP407 and CHP407/SHF68 blends up to an observation time of 72 hours.

Table 14 Gelation time and appearance of supramolecular hydrogels based on CHP407 and CHP407/SHF68 (observation time up to 72h)

Formulation code	**Appearance**
CHP407-1-10CD	gel (overnight)
CHP407-2-10CD	gel (3 h)
CHP407-3-10CD	gel (3 h)
CHP407-5-10CD	gel (1 h 30 min)
BLEND-0,5-0,5-10CD	gel (overnight)
BLEND-0,8-0,2-10CD	gel (overnight)
BLEND-1-1-10CD	gel (overnight)
BLEND-1,6-0,4-10CD	gel (2 h 45 min)
BLEND-2,4-0,6-10CD	gel (3 h)
BLEND-4-1-10CD	gel (1 h)

Although SHF68 was added to the formulations, hydrogel gelation was still obtained. Additionally, in some cases the blend showed a faster gelation kinetics than the respective sample containing only CHP407 (Figure 54).

This behaviour could be related to different reasons. One of the most probable was the interconnection between CHP407-based aggregates given by SHF68 chains, acting similarly to mild physical crosslinkers that interact with both hydrophilic and hydrophobic domains of micelles. Moreover, the addition of a smaller polyurethane could enhance the formation of entanglements thus stabilising the entire polymeric network.

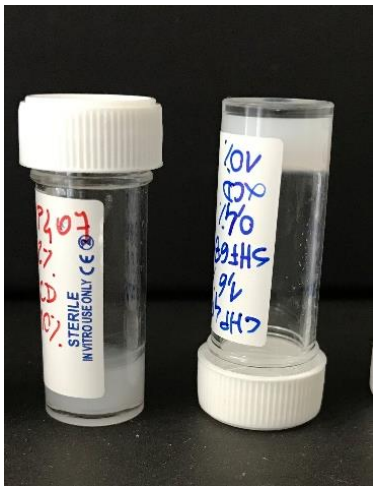

Figure 54 a viscous solution of CHP407-2-10CD (right) and a gel of BLEND-1,6-0,4-10CD (left) in a tube inverting test to qualitatively investigate gelation kinetics

To summarize, α-cyclodextrins allowed to obtain gels also using a relatively low amount of polyurethane. The analysed materials showed different characteristics once used in the formation of supramolecular hydrogels, thus making the designed platform of hydrogels versatile. CHP407-based hydrogels generally had a fast gelation kinetics, they were stable, but difficult to solubilize at high concentrations. SHP407-based systems had good physical stability over time and good gelation kinetics, but they were not easy to solubilize. Finally, SHF68-based hydrogels were very easy to solubilize, they had a great number of free amino groups, but they were very weak gels. Then, hydrogels based on blends were designed to bring together the positive features of both CHP407 and SHF68, in order to obtain stable and highly soluble hydrogels, with fast gelation kinetics and having a great number of free amino groups for potential antibacterial purposes or functionalization. Based on this considerations, hereafter the following compositions have been further characterized in the present work: CHP407-1-10CDs, CHP407-3-10CDs, CHP407-5-10CDs, BLEND-0.8-0.2-

10CDs, BLEND-2.4-0.6-10CDs, BLEND-4-1-10CDs, SHP407-1-10CDs, SHP407-3-10CDs and SHP407-5-10CDs.

5.5 ATR-FTIR analysis of supramolecular complexes between Polyurethanes and α-Cyclodextrins

ATR-FTIR spectra of the PPRs pellets collected through centrifugation exhibited the characteristic peaks of urethane bonds (1720 cm^{-1}) and cyclodextrin's hydroxyl groups (3700 cm^{-1}) (Figure 55, 56 and 57), thus proving the occurrence of a self-assembly process between polyurethane and cyclodextrins.

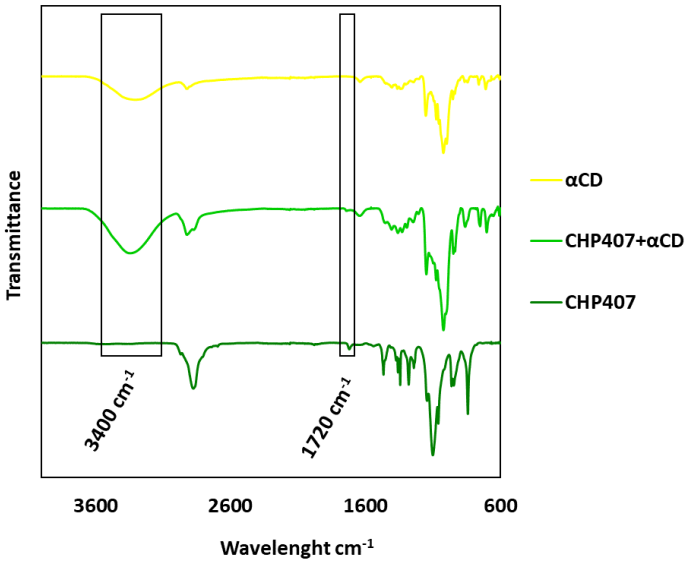

Figure 55 ATR-FTIR spectra of αCDs, CHP407 added with αCDs and CHP407

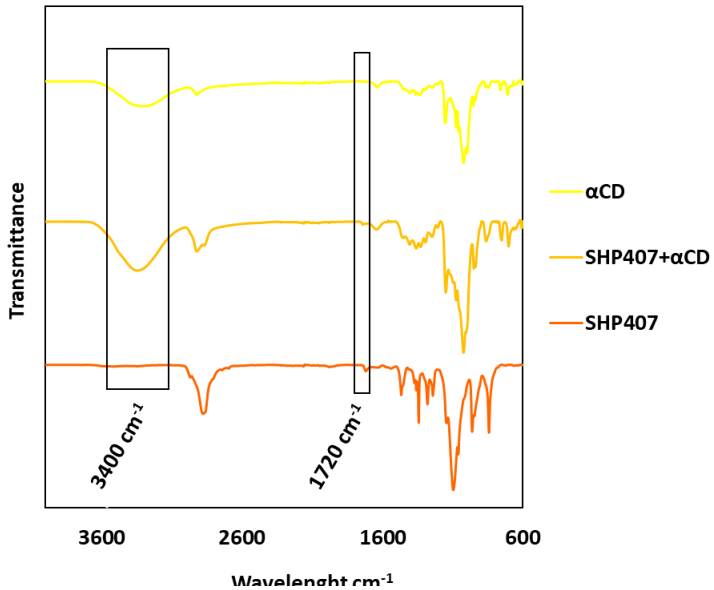

Figure 56 ATR-FTIR spectra of αCDs, SHP407 added with αCDs and SHP407

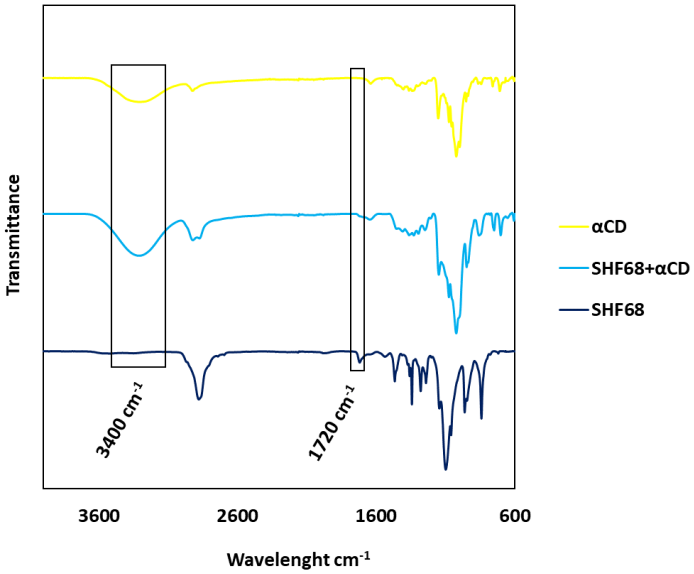

Figure 57 ATR-FTIR spectra of αCDs, SHF68 added with αCDs and SHF68

5.6 Swelling and Stability of Supramolecular Hydrogels

Swelling and stability tests are essential to understand the behaviour of designed supramolecular hydrogels in close contact with an aqueous solution, which simulates the physiological environment in a simplistic way. The contact with the eluate reflects the continuous exchange that would occur if the supramolecular systems are inserted inside the body and therefore it is necessary to evaluate how the hydrogels maintain their weight in the wet and dry state. In addition, considering the high concentration of cyclodextrins inside the hydrogels and the not-sterile conditions of working, an issue exists regarding to potential appearance of moulds inside the gels. For this reason, PBS (which, with its components, simulates a body solution better than water) containing the antifungal Amphotericin B was used as eluate in contact with the hydrogels. First, qualitative stability and swelling tests were performed in duplicate on supramolecular hydrogels with composition CHP407-1-10CD to assess if the addition of an antifungal molecule to PBS could affect the stability of the systems. In detail, gel swelling and dissolution were evaluate

after five days (with a refresh at the second day) incubation in contact with PBS as such or PBS added with Amphotericin B (Figure 58 and Figure 59).

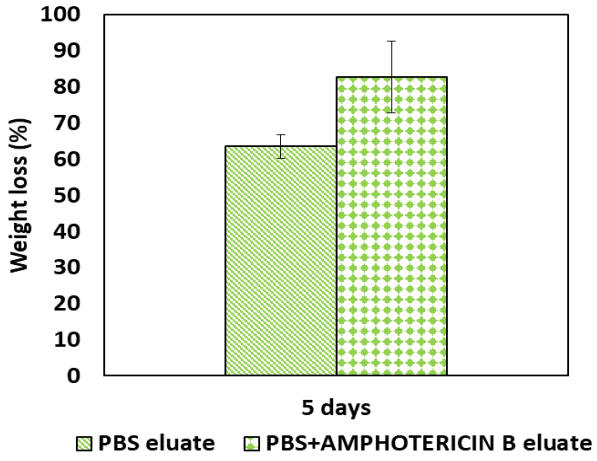

Figure 58 Weight Loss (%) as a function of time for CHP407-1-10CD in contact with PBS or PBS+AMPHOTERICIN B

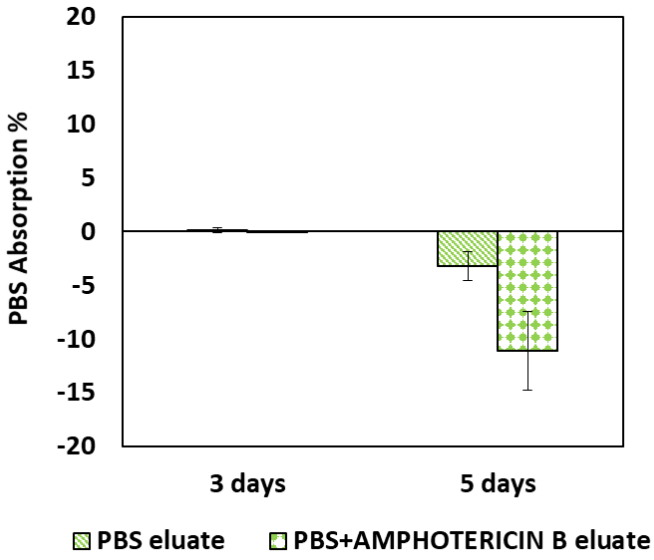

Figure 59 PBS and PBS+AMPHOTERICIN B absorption (%) as a function of time for CHP407-1-10CD

As shown in the graphs, the use of an eluate containing Amphotericin B instead of pure PBS caused an increased deswelling and a consequent enhanced weight loss on the fifth day of incubation at 37 °C. The antifungal used was a very amphiphilic molecule that could interact with both the polyurethane micelles and the cyclodextrins present in the hydrogel. Hence, it probably interfered with the structure of the supramolecular systems by decreasing the stability on the long periods (5 days). On the other hand, the different response of the

hydrogels caused by the absorption of an external molecule could be an indication of a chemo-receptive potential of the developed systems.

Nevertheless, the use of an antifungal was mandatory to avoid mould formation. Hence, the definitive swelling and stability tests were conducted using PBS added with amphotericin B as eluate. The swelling and stability behaviour of the supramolecular hydrogels formed by the different polyurethanes (CHP407-1-10CDs, CHP407-3-10CDs, CHP407-5-10CDs, SHP407-1-10CDs, SHP407-3-10CDs, SHP407-5-10CDs BLEND-0.8-0.2-10CDs, BLEND-2.4-0.6-10CDs, BLEND-4-1-10CDs) were thus compared and results are summarized in Figure 60, Figure 61, Figure 62, Figure 63, Figure 64 and Figure 65.

With regard to weight loss trend, all three graphs (Figure 60, Figure 61, Figure 62) showed a similar trend, characterized by an increasing weight loss overtime that was more pronounced between 24 hours and three days. Substantial weight loss was due to the presence of weak interactions and physical bonds given by polyurethane chains and cyclodextrins. However, with increasing the amount of synthetic material, it was probably more difficult to break these interactions because they were much more present: therefore, supramolecular hydrogels with a concentration of 3%w/v or 5%w/v of synthetic polymer had a less pronounced weight loss. For what concerns the difference between the polyurethanes used, CHP407-based supramolecular hydrogels had the same behaviour as those based on CHP407/SHF68 blends. This phenomenon could be ascribed to the fact that CHP407 was the main component of the blends. Comparing the behaviour of the gels based on SHP407 with those based on CHP407 as such or CHP407 blended with SHF58, weight loss was more pronounced in the former compared to the latter. Hence, SHP407-based gels showed a faster solubilisation of the supramolecular structures when incubated in contact with aqueous solutions probably as a consequence of the presence of pendant amines.

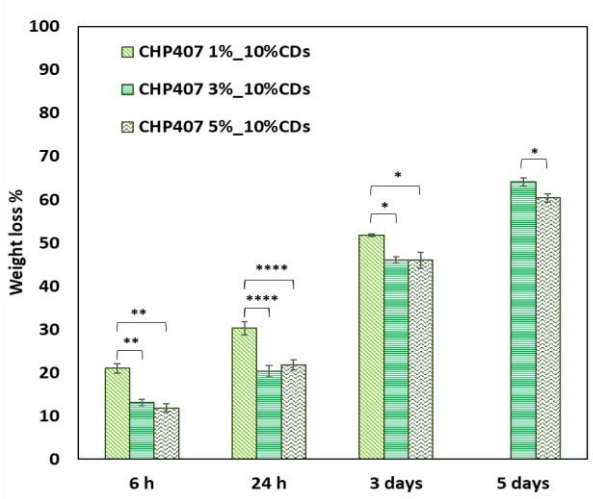

Figure 60 Weight Loss (%) at different time points for CHP407-based supramolecular hydrogels with 1%w/v, 3% w/v and 5% w/v synthetic polymer content and αCDs at 10%w/v concentration

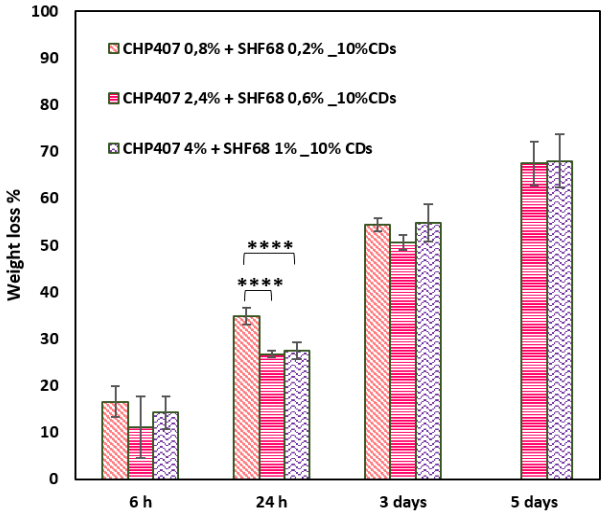

Figure 61 Weight Loss (%) at different time points for BLEND-based supramolecular hydrogels with 1%w/v, 3% w/v and 5% w/v synthetic polymer content and αCDs at 10%w/v concentration

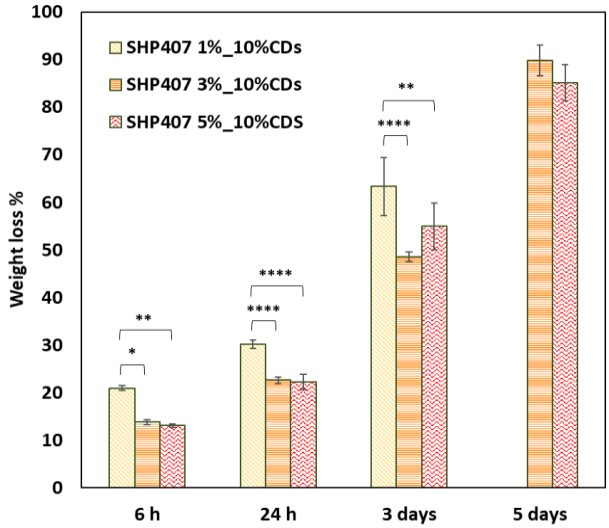

Figure 62 Weight Loss (%) at different time points for SHP407-based supramolecular hydrogels with 1%w/v, 3% w/v and 5% w/v synthetic polymer content and αCDs at 10%w/v concentration

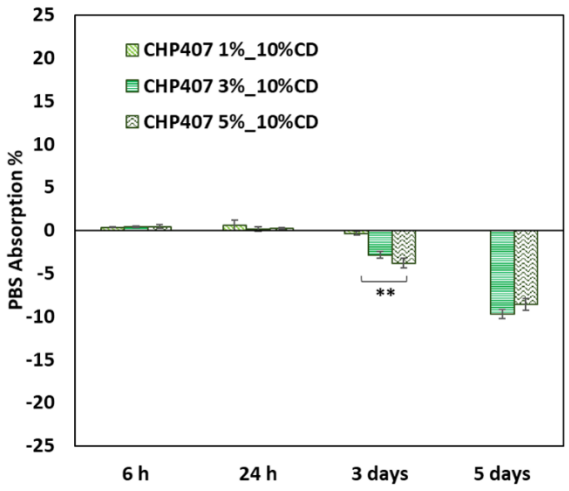

Figure 63 PBS absorption (%) at different time points for CHP407-based supramolecular hydrogels with 1%w/v, 3% w/v and 5% w/v synthetic polymer content and αCDs at 10%w/v concentration

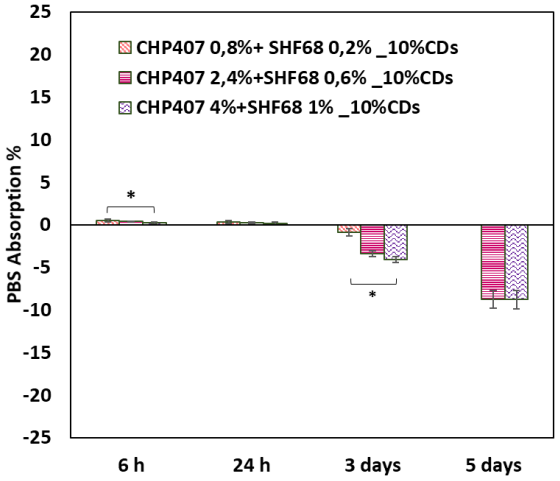

Figure 64 PBS absorption (%) at different time points for BLEND-based supramolecular hydrogels with 1%w/v, 3% w/v and 5% w/v synthetic polymer content and αCDs at 10%w/v concentration

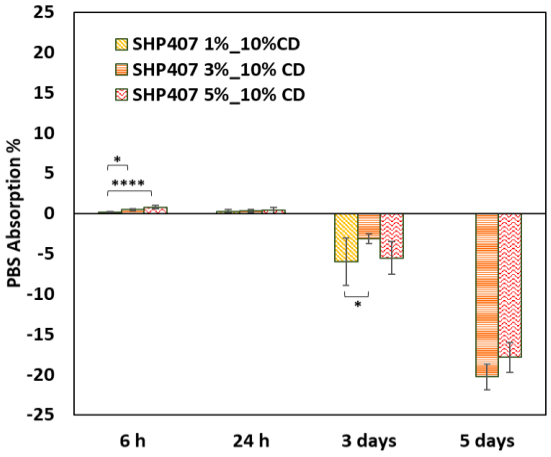

Figure 65 PBS absorption (%) at different time points for SHP407-based supramolecular hydrogels with 1%w/v, 3% w/v and 5% w/v synthetic polymer content and αCDs at 10%w/v concentration

For what concerns swelling percentage, the trend for all three graphs was similar (Figure 63, Figure 64, Figure 65). For the first two time-steps referring to 6 hours and 24 hours, the supramolecular hydrogels maintained a practically zero absorption of eluate while after 3 and 5 days incubation in aqueous media a marked deswelling was observed, as a consequence of wet weight loss. Again, supramolecular hydrogels based on CHP407 as such or its blends with SHF68 had a very similar deswelling behaviour, while they significantly differed from those obtained with SHP407.

Evaluating together the bar diagrams of sample dissolution and PBS absorption, supramolecular hydrogels composed of CHP407 and CHP407/SHF68 at 1%w/v and 3%w/v synthetic polymer concentration showed high weight loss accompanied by a slightly marked de-swelling on day 3 incubation. This data highlight the capability of the developed supramolecular hydrogels to exchange mass (that is polyurethane and/or α-cyclodextrins) with the surrounding environment while maintaining their wet weight, and as a consequence their shape. This behaviour conferred to these hydrogels the suitability for advanced drug delivery applications. In fact, they could be used as carrier of drugs required a sustained and prolonged release within few days.

5.7 Thermo-sensitive Supramolecular Hydrogel Characterization

5.7.1 Rheological Characterization

The rheological characterization of the designed supramolecular hydrogels was necessary to understand the mechanical properties of the gels and the gelation kinetics. Compositions containing a total concentration of synthetic material of 1%w/v and 5%w/v, and α-cyclodextrins at 10%w/v concentration were selected for these characterizations in order to evaluate the different behaviours with increasing the amount of polyurethane.

5.7.1.1 Frequency Sweep Test

CHP407-based supramolecular hydrogels were tested through frequency sweep test at 25 °C, 30 °C and 37 °C. Figure 66 and 67 report the trend of storage (G') and loss (G'') moduli as a function of angular frequency for all the analysed formulations at the analysed

temperatures. At all the tested temperatures, both CHP407- and SHP407-based systems were in the gel state as demonstrated by the higher value assumed by the storage modulus (G') compared to the loss modulus (G'') at each tested frequency. Additionally, the gels turned out to be completely developed as assessed by the independence of G' over angular frequency. Moreover, CHP407-5-10CD showed slightly higher G' at high frequencies, indicating that in this condition the sample became more rigid than upon application of deformation at lower frequencies. Probably, this supramolecular hydrogel had the capacity to adapt to different frequencies to which deformation was applied. Instead, comparing the storage moduli achieved in these tests for formulations differing in polyurethane content, it was observed that hydrogels containing a greater amount of polyurethane (5% w/v) had a G' of an order of magnitude higher than the hydrogels with a lower synthetic material content (1%w/v) (at 37 °C and 100 rad/s, 26000 Pa *vs* 5800 Pa for CHP407-5-10CD and CHP407-1-10CD, respectively). Hence, by increasing polyurethane content in the supramolecular hydrogels, improved mechanical properties can be obtained. Supramolecular hydrogels based on CHP407/SHF68 blends had the same behaviour as the systems based on a single polyurethane, with a higher storage modulus with increasing amount of synthetic material. More in detail, at 37 °C and 100 rad/s the storage modulus of the sample BLEND-0.8-0.2-10CD was 4200 Pa while that of the gel BLEND-4-1-10CD was 21000 Pa. Comparing formulations of supramolecular hydrogels with the same synthetic polymer content but composed of different polyurethanes (Figure 68 and Figure 69), BLEND-based supramolecular hydrogels at 1% w/v concentration of synthetic materials had a storage modulus comparable to that of the sample SHP407-1-10CD (about 4100 Pa). Differently, CHP407-1-10CD was the system giving the highest storage modulus of about 5800 Pa. For what concerns hydrogels at 5% w/v synthetic material concentration, CHP407- and BLEND-supramolecular hydrogels had a very similar storage modulus of about 23000 Pa, while SHP407-5-10CD supramolecular hydrogels had a storage modulus of 14700 Pa.

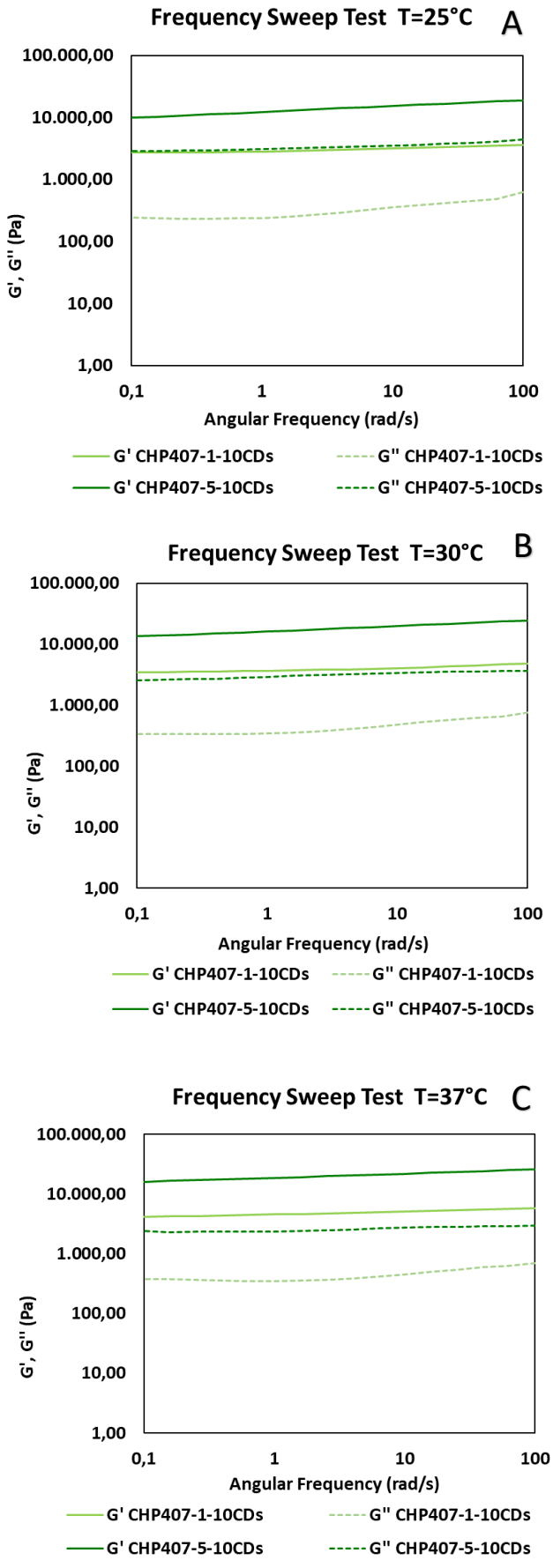

Figure 66 Trend of storage (G') and loss (G'') moduli as a function of angular frequency for supramolecular hydrogels based on CHP407 and αCDs, measured at A)25°C, B) 30°C and C) 37°C

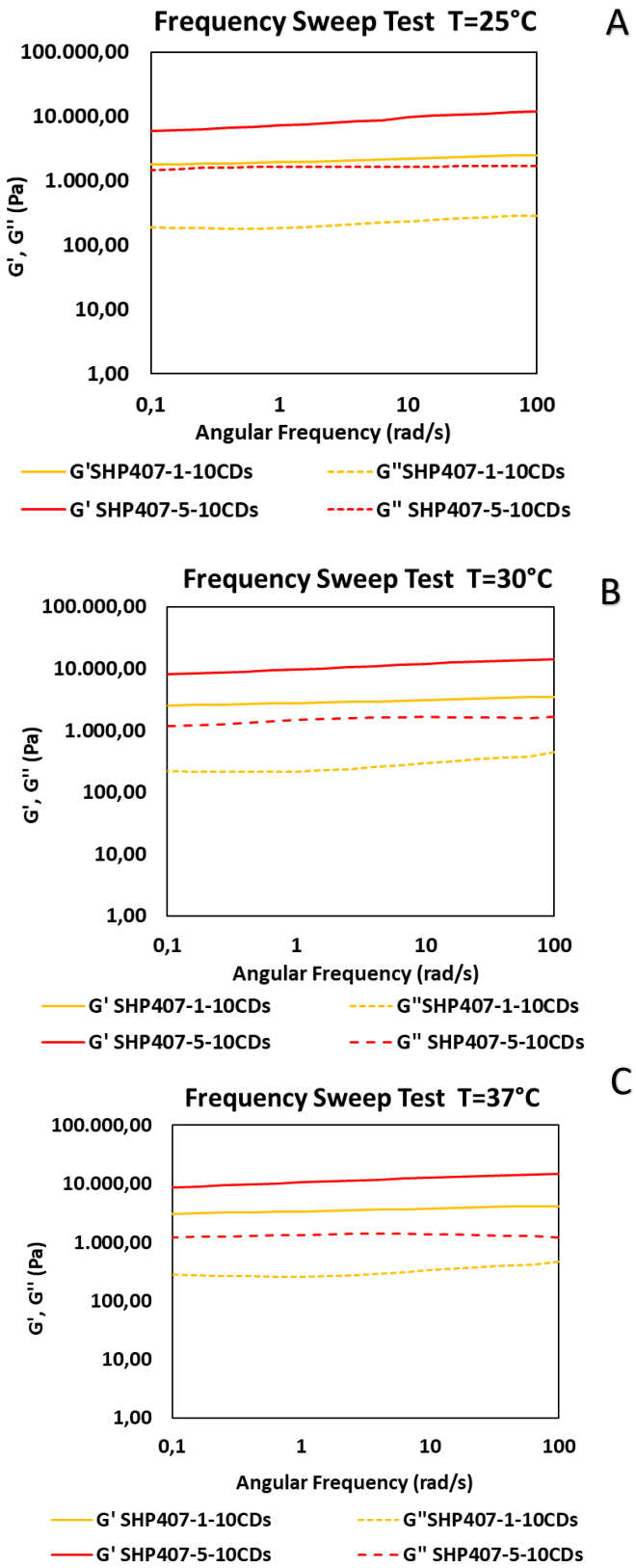

Figure 67 Trend of storage (G') and loss (G'') moduli as a function of angular frequency for supramolecular hydrogels based on SHP407 and αCDs, measured at A)25°C, B) 30°C and C) 37°C

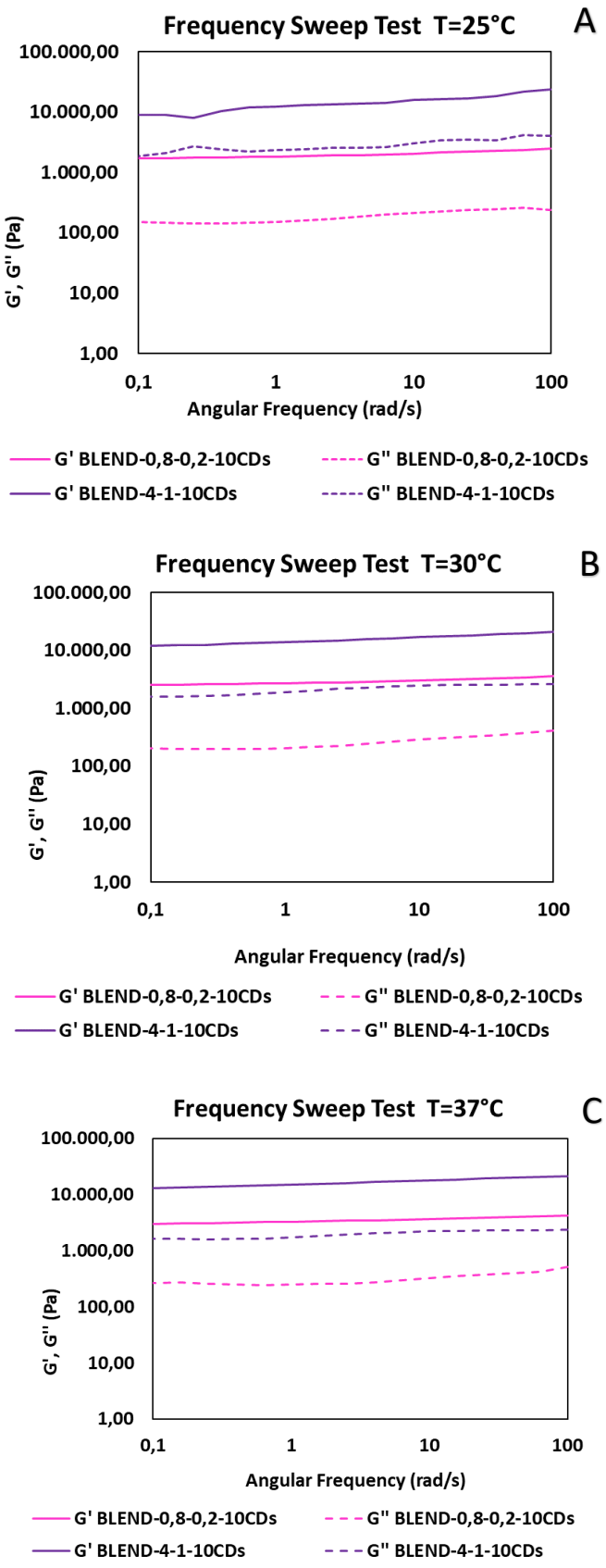

Figure 68 Trend of storage (G') and loss (G'') moduli as a function of angular frequency for supramolecular hydrogels based on BLEND and αCDs, measured at A)25°C, B) 30°C and C) 37°C

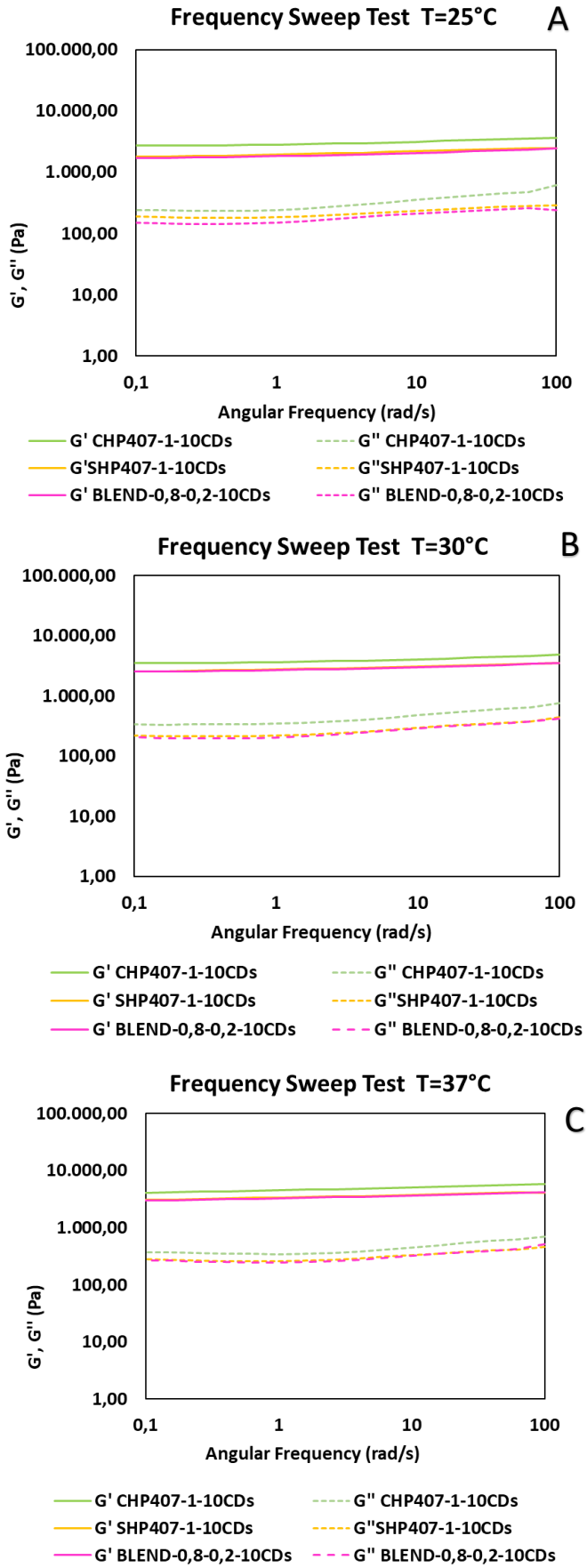

Figure 69 Trend of storage (G') and loss (G'') moduli as a function of angular frequency for supramolecular hydrogels with 1%w/v and 10%w/v concentration of synthetic polymer and αCD, respectively, measured at A)25°C, B) 30°C and C) 37°C

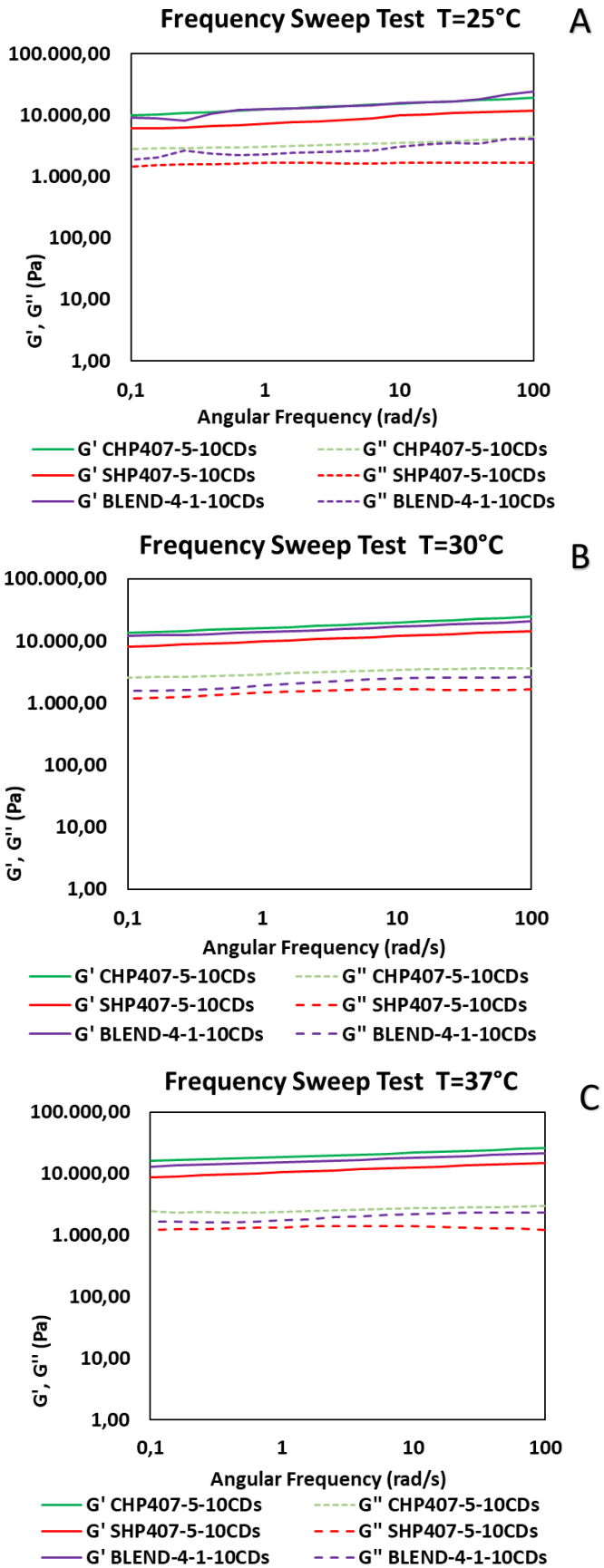

Figure 70 Trend of storage (G') and loss (G'') moduli as a function of angular frequency for supramolecular hydrogels with 5%w/v and 10%w/v concentration of synthetic polymer and αCD, respectively, measured at A)25°C, B) 30°C and C) 37°C

5.7.1.2 Strain Sweep Test

The same supramolecular hydrogel formulations were also characterized by strain sweep test. Using this test, it was possible to define the extension of the linear viscoelastic region (LVE) of the material. In addition, using the same sample already tested, the strain sweep test was repeated after 15 minutes of re-equilibration at 37 °C, so as to assess whether the material had self-healing capabilities.

The results obtained for the characterized samples c are reported in Figure 71. The sample CHP407-1-10CD had a storage modulus of about 5000 Pa and a linear region ranging approximately from 0% to 0.1% of strain. Instead, the supramolecular hydrogel with 5% w/v CHP407 content had a storage modulus in the order of 15000 Pa and the linear viscoelastic region between 0% and 0.2% of strain. Hence, also this test highlighted that with increasing the amount of the synthetic material in the supramolecular hydrogel, better mechanical properties can be achieved. Regarding the capacity of self-healing, both hydrogels recovered almost completely their initial mechanical properties after 15 minutes re-equilibration at 37° C (92% and 87% of the initial G' were recovered by CHP407-1-10CD and CHP407-5-10CD, respectively).

For what concerns SHP407-based supramolecular hydrogels (Figure 72), the sample SHP407-1-10CD had a storage modulus of 4100 Pa and an LVE region extending to approximately 0.7% strain, while the composition SHP407-5-10CD exhibited a storage modulus of approx. 10000 Pa and the viscoelastic linear region extended up to 0.2% of strain. Regarding the self-healing capacity, in the first case (1%w/v of SHP407) 86% of storage modulus was recovered while, in the second case (5%w/v of SHP407), a recovery of 91% of initial G' was observed.

Supramolecular hydrogels based on CHP407/SHF68 blends showed a similar behaviour to the compositions based on CHP407 as such (Figure 73). The formulation BELND-0.8-0.2-10CD (1%w/v synthetic material) showed storage modulus of 3700 Pa, LVE region extended up to 0,2% and a recovery of the 92% of the initial G' upon breakage. Instead, for the formulation BELND-4-1-10CD (5%w/v polyurethane), the storage modulus was of about 15000 Pa, the LVE region extended up to 0,3% strain and mechanical properties were recovered up to 87%.

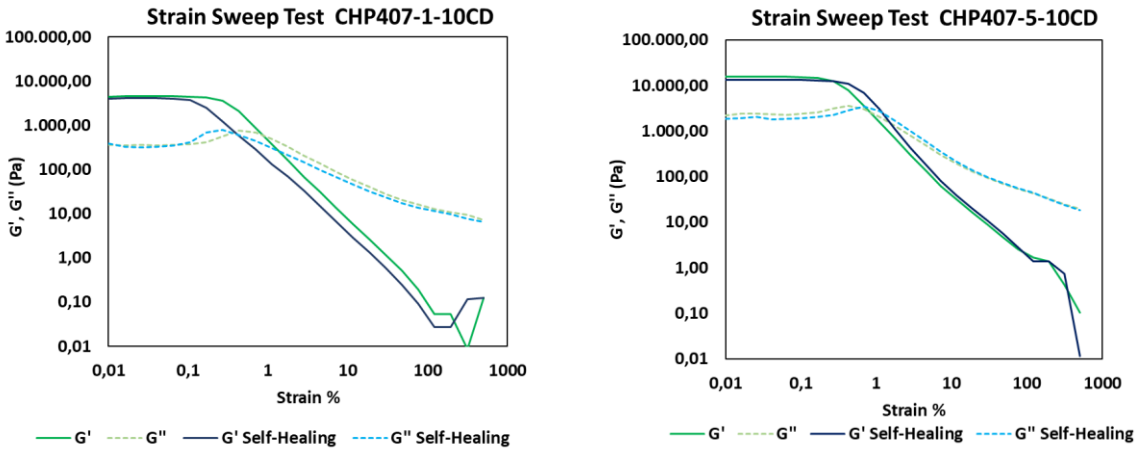

Figure 71 G' and G'' trends as a function of applied strain (measured before and after self-healing for 15 min) for supramolecular hydrogels based on CHP407 (1 and 5% w/v) and αCDs at 10% w/v concentration.

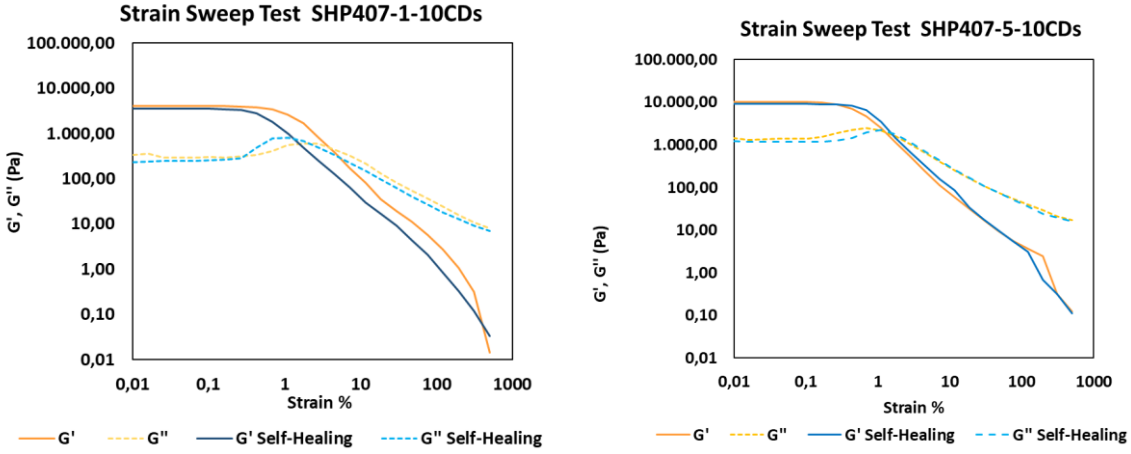

Figure 72 G' and G'' trends as a function of applied strain (measured before and after self-healing for 15 min) for supramolecular hydrogels based on SHP407 (1 and 5% w/v) and αCDs at 10% w/v concentration

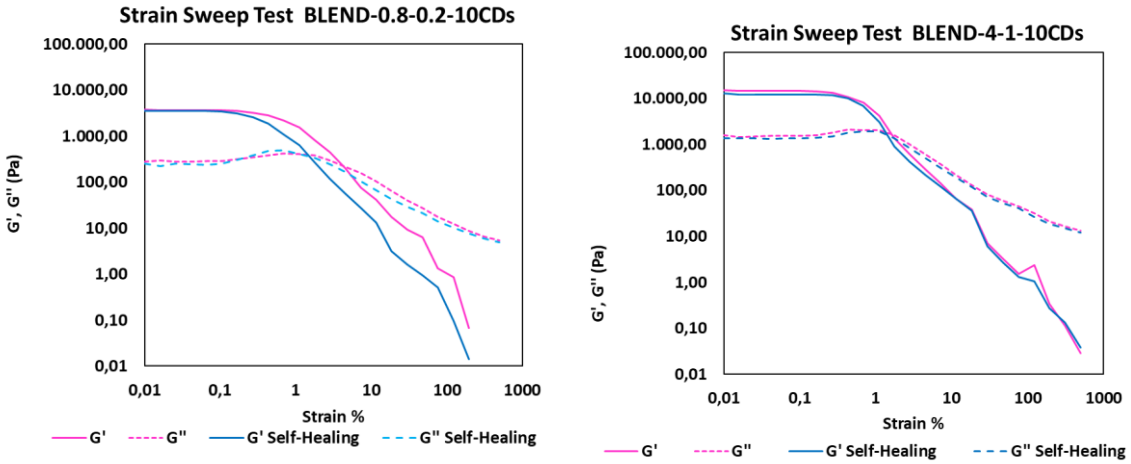

Figure 73 G' and G'' trends as a function of applied strain (measured before and after self-healing for 15 min) for supramolecular hydrogels based on BLEND (1 and 5% w/v) and αCDs at 10% w/v concentration

5.7.1.3 Strain Test

Further confirmation of the ability to self-heal was obtained through strain test. This capacity of supramolecular hydrogels could be very useful in view of their application because it allows the system to restore its original mechanical characteristics even after a deformation that led to complete breakage. In fact, considering biomedical applications, the designed systems could be easily applied through injection with no loss of their original mechanical properties.

All tested formulations (CHP407-1-10CDs, CHP407-5-10CDs, SHP407-1-10CDs, SHP407-5-10CDs, BLEND-0.8-0.2-10CDs and BLEND-4-1-10CDs) showed strong self-healing capabilities (Figure 74, Figure 75 and Figure 76). In fact, in a few seconds after the breakage of the hydrogel (where G'' is higher than G'), the sample restored almost completely its initial storage modulus (bringing back G' higher than G''), resuming the original mechanical performances. Table 15 reports the percentage of self-healing obtained by comparing the calculated G' value within the first and the last interval tested during the analysis.

Table 15 Percentage of self-healing of the characterized supramolecular formulations.

	1%w/v of polyurethane	**5%w/v of polyurethane**
CHP407	89%	92%
SHP407	72%	70%
CHP407/SHF68 (blend)	94%	98%

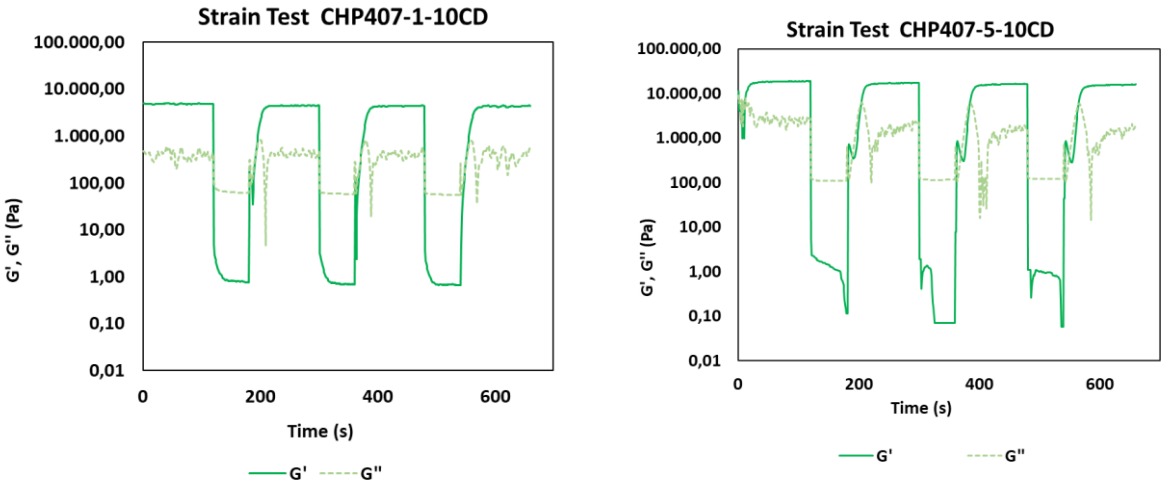

Figure 74 G' and G'' trends as a function of time for gels based on CHP407 and αCDs. Samples were tested at 37 °C by applying a cyclic deformation (0.1% strain for 2 minutes followed by a 100% strain for 1 min) for three times and a final strain of 0.1%.

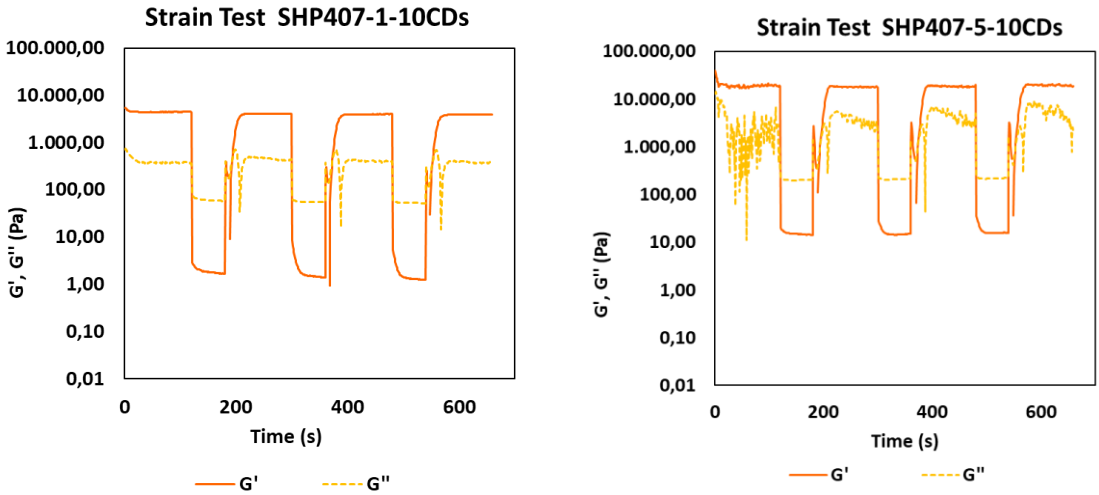

Figure 75 G' and G'' trends as a function of time for gels based on SHP407 and αCDs. Samples were tested at 37 °C by applying a cyclic deformation (0.1% strain for 2 minutes followed by a 100% strain for 1 min) for three times and a final strain of 0.1%.

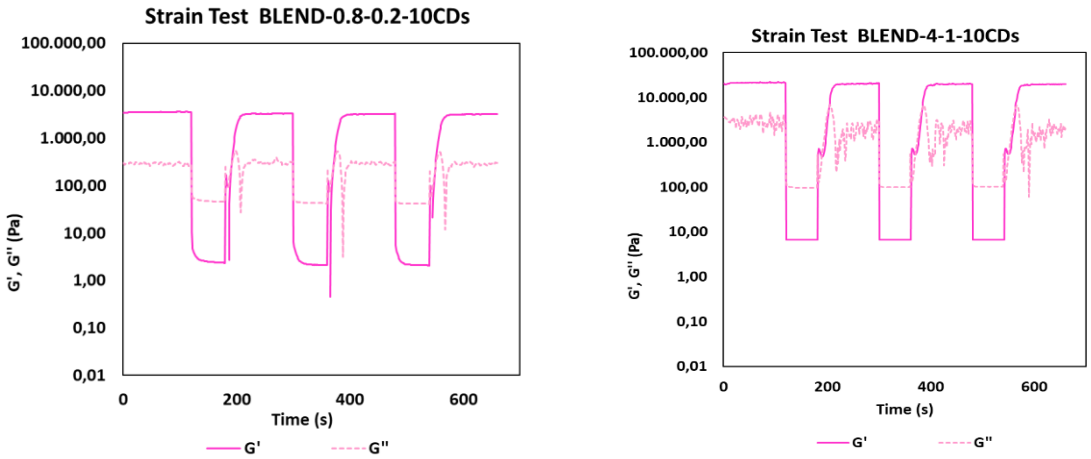

Figure 76 G' and G'' trends as a function of time for gels based on BLEND and αCDs. Samples were tested at 37 °C by applying a cyclic deformation (0.1% strain for 2 minutes followed by a 100% strain for 1 min) for three times and a final strain of 0.1%.

5.8 Cytotoxicity evaluation

In view of a potential application in the biomedical field, the designed supramolecular hydrogels were also characterized in terms of biocompatibility through indirect contact tests (Figure 77 A, Figure 77 B, Figure 77 C). All formulations were cytocompatible with NIH-3T3 cells and in all cases cell viability was comparable to control samples (100% cell viability). These results suggested the possible applicability of these supramolecular systems in the biomedical field as promising systems for drug release.

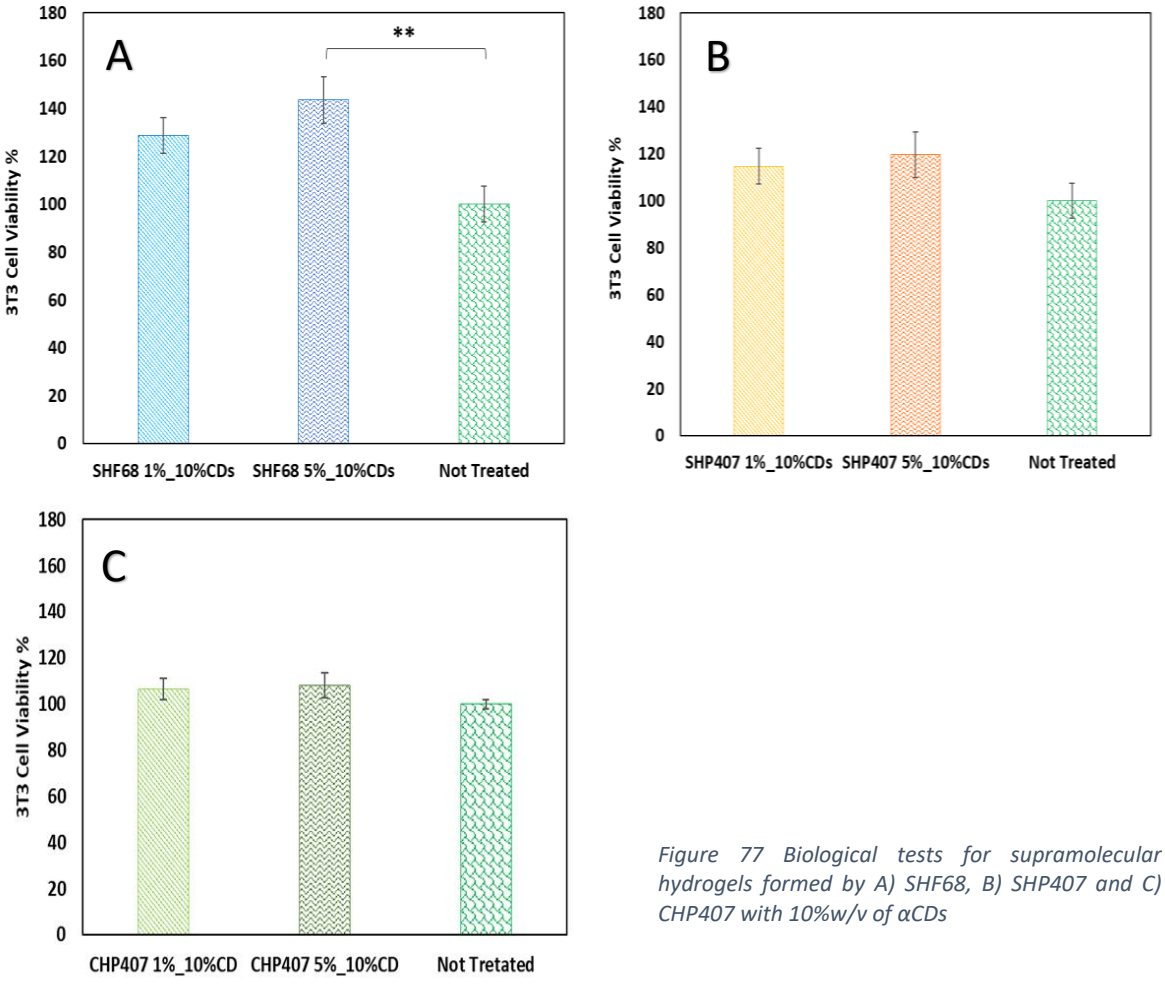

Figure 77 Biological tests for supramolecular hydrogels formed by A) SHF68, B) SHP407 and C) CHP407 with 10%w/v of αCDs

5.9 Encapsulation of curcumin into Supramolecular Hydrogels: release and quantification results

The previous results indicated that all the selected hydrogels were characterized by a thixotropic and self-healing behaviour with good mechanical properties, thus opening the possibility to be easily injected or processed in different manners (e.g., 3D printing) to fabricate specific devices for drug delivery. Moreover, the presence of α-cyclodextrins could help the solubilization and avoid the degradation of the encapsulated drugs, whereas the purpose of the hydrogel itself is to transport the molecule locally and release it in a controlled manner in a time interval compatible with application requirements and in a concentration within the therapeutic window.

The drug selected for the encapsulation and release tests was Curcumin, a highly hydrophobic molecule, difficult to solubilize in aqueous solutions (solubility lower than 0.002 mg/mL [33]) and characterized by high susceptibility to degradation in solvents containing chlorides, phosphates or in basic environments [32]. Curcumin is an antioxidant and anticancer drug which does not require high concentration to be effective (100 µmol/L induced necrosis and 50 µmol/L induced apoptosis of cancer cells [51]). For this reason, curcumin has a lot of possibilities of applications in the biomedical field, but it turns out of difficult use because of its hydrophobicity. In this regard, α-cyclodextrins can be used to increase the solubility of the molecule in an aqueous environment and to preserve it from degradation even inside the hydrogel. Therefore, increasing the solubility of the drug also implied an enhanced encapsulation into the supramolecular hydrogel and an increased delivery rate of molecules.

As regards the release of curcumin from the developed supramolecular hydrogels, PBS was used as eluate in contact with the systems. At each time points, curcumin-loaded hydrogel systems were expected to release in the PBS eluate not only the drug but also cyclodextrins and polyurethanes. For this reason, several calibration curves were obtained at different concentrations of α-cyclodextrins in the solutions to assess potential effects of αCD on curcumin absorbance spectrum. The calibration curve in the absence of cyclodextrins was obtained by dissolving curcumin in ethanol (1 mg/mL) and then diluting the obtained solution with PBS in order to obtain standards differing in curcumin concentration. For

what concern the other calibration curves, they were obtained from a solution of cyclodextrins (10%w/v) and curcumin (50 µg/mL) prepared in PBS and then diluted with the required cyclodextrin solutions in order to obtain the correct concentrations. The obtained calibration curves (Figure 78) did not show significant differences in terms of slope, thus evidencing that the presence of cyclodextrins does not affect curcumin absorbance spectrum. Hence, the calibration curve based on standards containing only curcumin was used to quantify the amount of drug released from the gels. This decision was further supported by the results of hydrogel dissolution tests. Indeed, assuming a consistent release of hydrogel components into the elutes, the concentration of α-cyclodextrins should never exceed a value around 2% w/v, thus suggesting a negligible

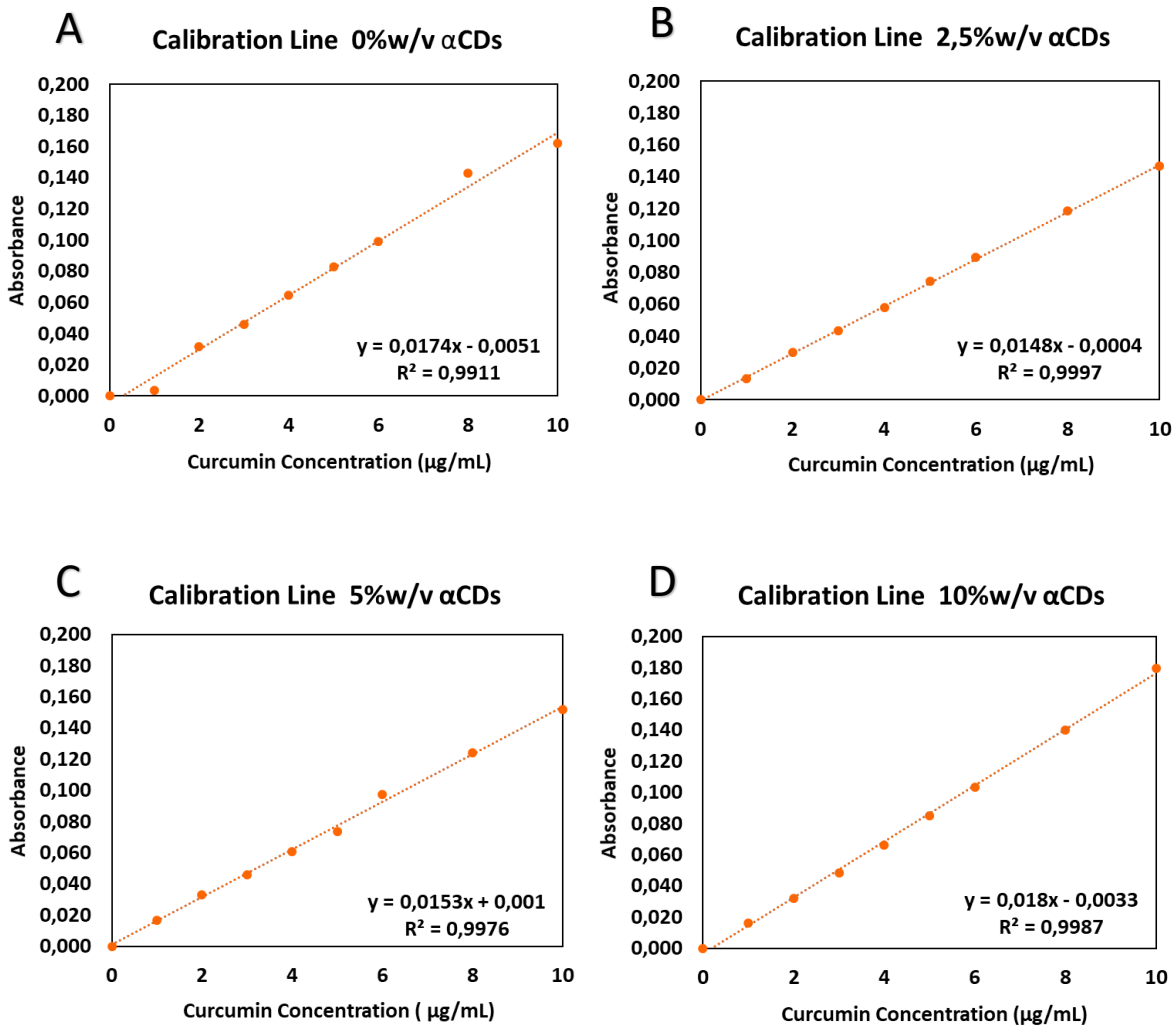

Figure 78 Calibration curves obtained from standards containing curcumin (from 0 µg/mL to 10 µg/mL) and αCDs at different concentrations: A) 0%w/v αCDs B) 2,5%w/v αCDs C) 5%w/v αCDs and D) 10%w/v αCDs

effect of these cyclic molecules in the quantification of curcumin.

The protocol for curcumin encapsulation within the supramolecular hydrogels was optimized so as to (i) be able to encapsulate an amount of drug that could induce necrosis for cancer cells, (ii) avoid the degradation of the drug, and (iii) permit the sol-gel transition of the hydrogel systems.

Initially, to completely avoid contact between curcumin and phosphate ions [52], supramolecular hydrogels were produced using bi-distilled water as solvent for each component (polyurethane and α-cyclodextrins with curcumin). However, in this case, supramolecular hydrogels containing polyurethanes at 1%w/v or 3%w/v concentration (CHP407, SHP407 and the blend formed by 80:20w/w CHP407/SHF68) and α-cyclodextrins at 10%w/v did not reached the sol-gel transition up to 72 hours observation. This may have been caused by two factors: (i) the use of bi-distilled water as solvent of each component hindered the onset of the ionic interactions that could be fundamental for the achievement of the transition to gel state, and (ii) residual free cyclodextrins molecules (i.e., those not involved in interactions with curcumin) were not sufficient to form enough poly(pseudo)rotaxanes to allow the transition. For this reason, half of the α-cyclodextrins required to obtain the here developed supramolecular hydrogels was used to solubilize curcumin in bi-distilled water, while all the rest was dissolved in PBS and then added to poly(urethane) solution. In this way, the solution prepared in PBS had both free α-cyclodextrins available for the formation of poly(pseudo)rotaxanes with the polyurethane chains and ions which could help the sol-gel transition of the hydrogel. On the other hand, curcumin solubilization in bi-distilled water in the presence of α-cyclodextrins allowed to both increase its solubility and protect it from degradation. By analysing curcumin solutions prepared in pure bi-distilled water and in bi-distilled water added with α-cyclodextrins (14% w/v) through UV-visible spectroscopy (Figure 79) differences in the absorption spectra were observed, with a slight shift of the characteristic curcumin peak (430 nm) in samples containing also cyclodextrins. Additionally, in the presence of α-cyclodextrins the convoluted peak at 350 nm was significantly less pronounced compared to the signal registered from the sample containing curcumin dissolved in bi-distilled water. This peak around 350 nm could be attributed to the formation of vanillin, a degradation product of

curcumin [32]. This proves the capability of α-cyclodextrins to protect curcumin from degradation.

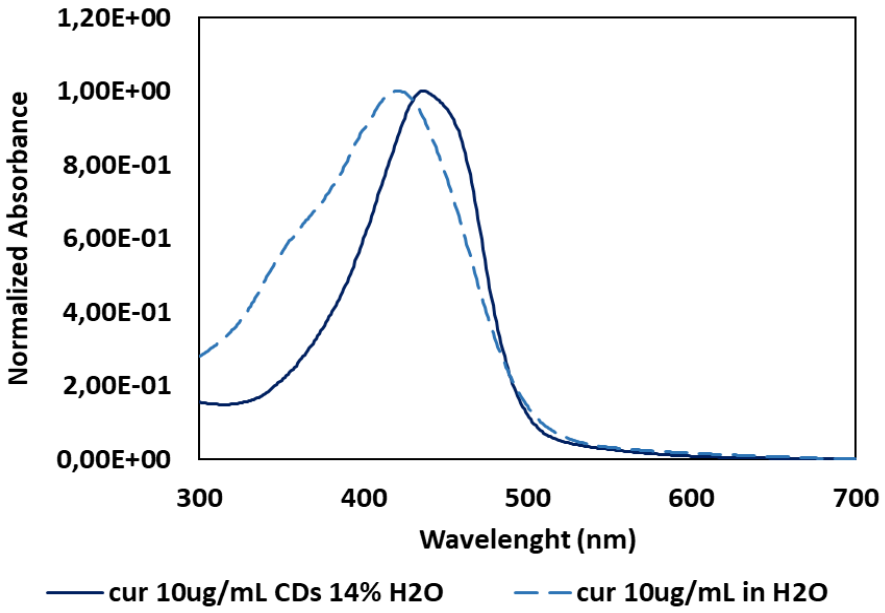

Figure 78 UV-visible spectra of curcumin dissolved in bi-distilled water (dotted line) and bi-distilled water with CDs (continues line)

To further investigate this aspect, the same analyses were conducted on curcumin solutions prepared in pure PBS and in with cyclodextrins (Figure 79). The spectrum of the sample containing curcumin dissolved in pure PBS a shoulder at 350 nm was observed, which was more pronounced compared to what observed by solubilizing curcumin in bi-distilled water. Hence, a higher amount of vanillin forms when the drug is solubilized in PBS. On the other hand, the spectrum of curcumin dissolved in PBS with cyclodextrins did not have any shoulder at 350 nm; however, a shoulder appeared at higher wavelengths (520 nm) which could be attributed to another product of degradation. For this reason, curcumin molecules were dissolved in bi-distilled water in the presence of α-cyclodextrins before addition to the supramolecular formulation.

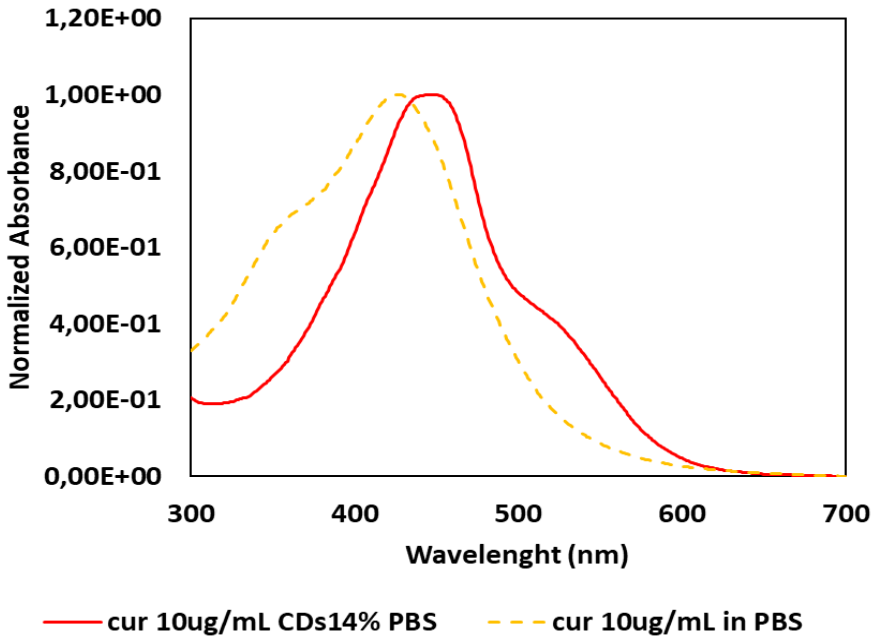

Figure 79 UV-visible spectra of curcumin dissolved in PBS (dotted line) and PBS with CDs (continuous line)

By increasing the concentration of α-cyclodextrins dissolved in bi-distilled water, the concentration of soluble curcumin also increased. For this reason, a solution containing the maximum concentration for α-cyclodextrins (i.e., 14% w/v) was used to solubilize curcumin, in order to be able to encapsulate the maximum amount of drug into the hydrogels (80 µg/mL). Complete solubilization of curcumin in the solution of bi-distilled water and α-cyclodextrins was obtained by stirring and using the sonicator, which allowed to obtain a clear solution with no aggregates (Figure 80).

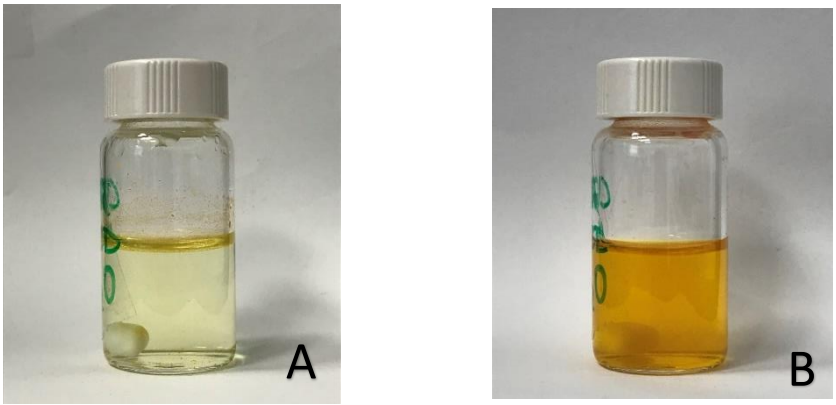

Figure 80 Solution of α-cyclodextrins (14%w/v) and curcumin (230 µg/mL) in bi-distilled water A) before and B) after stirring and sonication.

The supramolecular hydrogels characterized in terms of curcumin release profile contained the synthetic polymer at 1%w/v or 3%w/v concentration, α-cyclodextrins at 10%w/v

concentration and they theoretically loaded with curcumin at 80 μg/mL concentration. These compositions were chosen because they contained a low amount of synthetic material and a high concentration of curcumin, excellent to cause cell apoptosis.

Figures 81 reports the release curves of curcumin from the produced supramolecular hydrogels. The release pattern turned out to be very similar for all formulations tested. CHP407- and SHP407-based supramolecular hydrogels initially released a significantly higher quantity of curcumin from the systems with 1%w/v synthetic material concentration. On the other hand, after thirty hours incubation in PBS, hydrogels with a 3%w/v polyurethane concentration had an increased release that turns out to be higher compared to the other investigated formulations. This crossover behaviour did not occur in formulations based on CHP407/SHF68 blends: in this case, supramolecular hydrogels with a total 1%w/v concentration of synthetic material release a higher amount of curcumin compared to those with a 3%w/v polyurethane concentration at each time point analysed.

At longer time intervals (i.e., 78 hours and 96 hours), the standard deviations calculated for the quintuplicate of samples increased for all formulations. This behaviour could be correlated to the progressive instability of the supramolecular hydrogels in aqueous environments. In particular for the blend formulations, the observed high variability could be ascribed to presence of SHF68 as constituent.

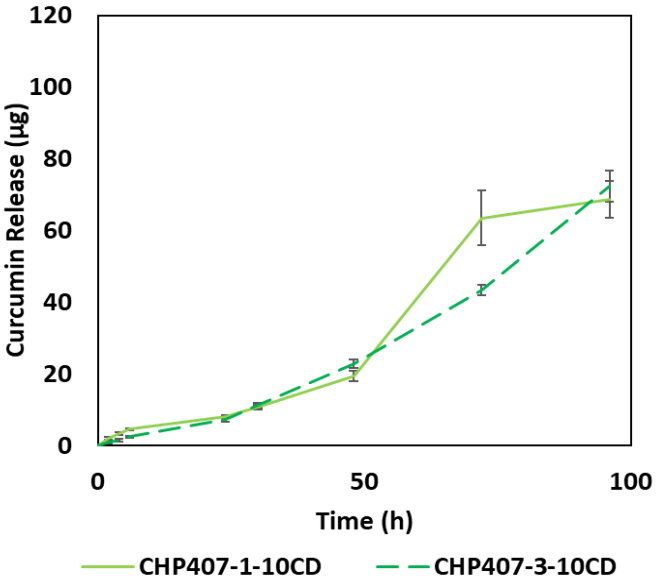

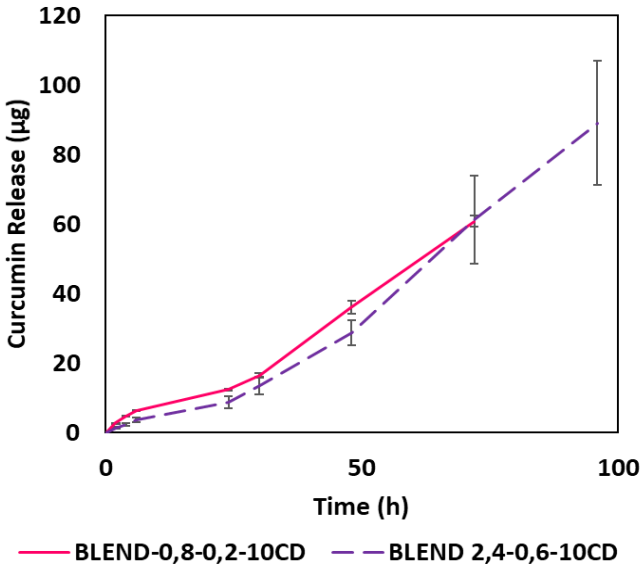

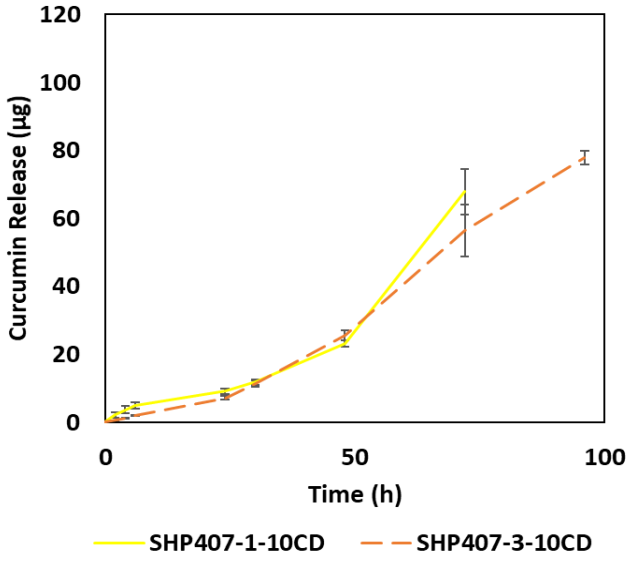

Figure 81 Release profile of curcumin from different supramolecular hydrogels

Irrespective of the composition of the supramolecular hydrogels, no burst release was observed. Hence, all the supramolecular hydrogels designed in this work of thesis could be excellent carriers for highly hydrophobic drugs such as curcumin. Additionally, they proved to be able to release the molecules in a controlled and progressive way that led to complete dissolution of hydrogels within a week. In addition, the optimized protocol for curcumin solubilization and encapsulation allowed to load supramolecular hydrogels with a high amount of drug, thus opening the way to a wide range of potential applications. Finally, thanks to the presence of α-cyclodextrins, the solubilization and release of curcumin were enhanced and molecules were not degraded.

6. Conclusions and Future Development

Nowadays, many medical treatments are associated to the prescription of medicines for oral use that do not arrive directly to the treated area and, for this reason, the administered quantity is elevate compared to the necessary, because it must be ensured that the region is reached. Drug delivery systems have aroused much interest in recent years and different typologies have been developed. Following this path of interest, in this thesis work a library of bioartificial supramolecular hydrogels formed by different custom-made polyurethanes in combination with α-cyclodextrins was developed. These systems, composed of a minimum amount of synthetic material, were found to be cytocompatible, thixotropic, with great mechanical properties, economic to produce and, for all these characteristics, they were used as carrier for drug release.

In this work, five different polyurethanes were synthesized using the same optimized protocol and they were coded considering the chemical components. NHP407 and NHF68 were both composed of N-Boc serinol as chain extender, 1,6-Hexamethylene diisocyanate as diisocyanate but they have been differentiated from the used macrodiol, P407 and F68, respectively. The deprotection process was conducted on NHP407 and NHF68, in order to obtain two polyurethanes with free amino groups exposed by serinol groups, the SHP407 and SHF68, respectively. This treatment had opened the possibility to further functionalize these polymers through specific chemical treatments (e.g. carbodiimide chemistry). Instead, CHP407 was composed of the P407 as macrodiol, 1,6-Hexamethylene diisocyanate as diisocyanate and 1,4-cyclohexane dimethanol as chain extender. To evaluate that the synthesis has been conducted with success, every polyurethane has been analysed through Attenuated total reflectance – Fourier Transformed Infra-red spectroscopy. The molecular weights of each polyurethane were measured using Size Exclusion Chromatography: with this analysis it was possible to confirm that SHF68 and SHP407 were not degraded. Precisely for the calculation of the number of free amino groups exposed by these last two polyurethanes, Ninhydrin assay was performed and it was obtained that SHP407 exposed $0{,}07 * 10^{18}$ units of NH_2/gram and SHF68 exposed $1{,}6 * 10^{18}$ units of NH_2/gram. Dynamic Light scattering characterisation was used to evaluate the stability of micelles and their aggregates formed by solution of CHP407, SHP407 and SHF68 at 1% w/v: only SHF68 had shown instability for the tested temperature (25°C and 37°C). Therefore, for the formation of supramolecular hydrogels, CHP407, SHP407 and SHF68 have been chosen as synthetic

material, used in concentrations between 1%w/v and 5%w/v with 10%w/v of α-cyclodextrins. CHP407- and SHP407-based supramolecular hydrogels had shown fast gelation kinetics, good mechanical properties (about between 5000 and 10000 Pa storage modulus), thixotropic and self-healing characteristics (about 90% of storage modulus recovery after complete rupture), evaluated with rheological characterization. On the contrary, the SHF68-based supramolecular hydrogels have shown slow gelation kinetics and scant stability in aqueous environment, compared to the great stability shown by the other hydrogels. However, all tested formulations were found to be cytocompatible with 100% of cell viability. To combine the excellent mechanical properties of the CHP407 with the good biological properties of free amino groups and the easy dissolution of the SHF68, a new platform of supramolecular hydrogel was designed using a combination of CHP407 and SHF68 as synthetic materials (80:20 %w/w of CHP407/SHF68, with an overall of polyurethane concentration of 1%w/v, 3%w/v and 5%w/v) and 10%w/v of α-cyclodextrins. Assessing the stability and swelling of supramolecular hydrogels obtained with the use of SHP407 and CHP407 alone and in combination with SHF68, it was observed that all the designed systems had shown a remarkable weight loss associated with a slight de-swelling process during the first three days of incubation: this behaviour was therefore the result of a substantial mass exchange towards the external environment and, at the same time, a preservation of the original shape. Precisely for this trend, these designed supramolecular hydrogels were used for the encapsulation and the release of drugs. To this purpose, Curcumin was chosen as loaded drug for its anti-inflammatory and anticancer properties. Maintaining the drug preserved from degradation, 80 μg/mL of curcumin were encapsulated in supramolecular hydrogels and the release kinetics were investigated. All designed systems had released the drug up to three days, avoiding burst release behaviour and also showing a promising release rate for future clinical treatments (for example, prostate cancer therapy). In addition, in this thesis work, porous poly (ε-caprolactone) (PCL) scaffolds have been produced through an easy and conventional procedure (porogen leaching). Supramolecular hydrogels containing inside a model molecule (Fluorescein isothiocyanate–dextran, FD4, 4000 Da) were encapsulated into the porous structure of scaffolds in order to evaluate the release kinetic of FD4 from the entire hybrid system. The easy integration of the supramolecular hydrogel inside a previously formed 3D structure

and the resulting controlled release profiles from the whole system enforced the possibility to obtain promising matrices to support tissues to be regenerated (as bone tissue).

In the future, the in vivo application of these supramolecular hydrogels could be tested and the integration with other matrices could be optimised (e.g., utilising rapid prototyping techniques to specifically trace the defect of a tissue to be regenerated) to obtain smart and multi-functional devices for clinical treatments.

Bibliography

[1] A. S. Hoffman, “Hydrogels for biomedical applications ☆,” *Adv. Drug Deliv. Rev.*, vol. 64, pp. 18–23, 2012.

[2] J. Li and D. J. Mooney, “Designing hydrogels for controlled drug delivery,” vol. 1, no. 12, pp. 1–38, 2018.

[3] N. Sultana and T. H. Khan, “Water Absorption and Diffusion Characteristics of Nanohydroxyapatite (nHA) and Poly (hydroxybutyrate-co-hydroxyvalerate-) Based Composite Tissue Engineering Scaffolds and Nonporous Thin Films,” vol. 2013, 2013.

[4] M. Boffito *et al.*, “Novel polyurethane-based thermosensitive hydrogels as drug release and tissue engineering platforms: Design and in vitro characterization,” *Polym. Int.*, vol. 65, no. 7, pp. 756–769, 2016.

[5] B. B. V Slaughter, S. S. Khurshid, O. Z. Fisher, A. Khademhosseini, and N. A. Peppas, “Hydrogels in Regenerative Medicine,” pp. 3307–3329, 2009.

[6] W. Seong and X. Jun, “Advances in hydrogel delivery systems for tissue regeneration,” *Mater. Sci. Eng. C*, vol. 45, pp. 690–697, 2014.

[7] J. Zhu, “Biomaterials Bioactive modi fi cation of poly (ethylene glycol) hydrogels for tissue engineering,” *Biomaterials*, vol. 31, no. 17, pp. 4639–4656, 2010.

[8] H. Shin, S. Jo, and A. G. Mikos, “Biomimetic materials for tissue engineering,” vol. 24, pp. 4353–4364, 2003.

[9] J. L. Hill-west, S. M. Chowdhuryt, J. Marvin, and A. Jeffrey, “Inhibition of thrombosis and intimal thickening by in situ photopolymerization of thin hydrogel barriers,” vol. 91, no. June, 1994.

[10] L. E. Bromberg and E. S. Ron, “Temperature-responsive gels and thermogelling polymer matrices for protein and peptide delivery 1,” vol. 31, pp. 197–221, 1998.

[11] Y. Qiu and K. Park, “Environment-sensitive hydrogels for drug delivery,” vol. 53, pp. 321–339, 2001.

[12] G. Wanka, H. Hoffmann, and W. Ulbricht, “Phase Diagrams and Aggregation Behavior of Triblock Copolymers in Aqueous Solutions,” pp. 4145–4159, 1994.

[13] W. Park, Y. J. P. D, W. Park, D. Ph, H. Park, and D. Lee, “Thermo-sensitive injectable hydrogel based on the physical mixing of hyaluronic acid and Pluronic F-127 for sustained NSAID delivery Thermo-sensitive injectable hydrogel based on the physical mixing of hyaluronic acid and Pluronic F-127 for sustained NSAI,” *Carbohydr. Polym.*, vol. 156, no. January 2018, pp. 403–408, 2016.

[14] A. V Kabanov, E. V Batrakova, and V. Yu, “Pluronic block copolymers as novel polymer therapeutics for drug and gene delivery,” vol. 82, pp. 189–212, 2002.

[15] R. Nagarajan, “Solubilization of hydrocarbons and resulting aggregate shape transitions in aqueous solutions of Pluronic ® (PEO – PPO – PEO) block copolymers,” vol. 16, pp. 55–72, 1999.

[16] L. Zhao *et al.*, “Colloids and Surfaces B : Biointerfaces Curcumin loaded mixed micelles composed of Pluronic P123 and F68 : Preparation , optimization and in vitro characterization,” *Colloids Surfaces B Biointerfaces*, vol. 97, pp. 101–108, 2012.

[17] M. K. Calabretta, A. Kumar, A. M. Mcdermott, and C. Cai, “Antibacterial Activities of Poly (amidoamine) Dendrimers Terminated with Amino and Poly (ethylene glycol) Groups,” pp. 1807–1811, 2007.

[18] M. Huang, Y. Wang, Y. Luo, and K. Polyurethanes, “Biodegradable and bioactive porous polyurethanes scaffolds for bone tissue engineering,” no. February, pp. 36–40, 2009.

[19] V. Chiono *et al.*, “Poly (ester urethane) Guides for Peripheral Nerve Regeneration,” pp. 245–256, 2011.

[20] C. Pontremoli *et al.*, “Hybrid injectable platforms for the in situ delivery of therapeutic ions from mesoporous glasses,” vol. 340, no. January, pp. 103–113, 2018.

[21] Villiers, “Sur la fermentation de la fécule par l’action du ferment butyrique.,” vol. C. R. Acad, pp. 536–538, 1891.

[22] Schardinger, “Uber die Zulässigkeit des Warmhaltens von zum Gebußbestimmten Nahrungsmittel mittelst Wärme speichernder Apparate,” *Thermophore.Wien. Klin. Wochenschr*, pp. 468–474.

[23] Schardinger, “Über Thermophile Bakterien aus verschiedenen Speisen und Milch, sowie über einige Umsetzungsprodukte derselben in kohlenhydrathaltigen Nährlösungen, darunter krystallisierte Polysaccharide (Dextrine) aus Stärke,” vol. . Z. Unter, pp. 865–880, 1903.

[24] Schardinger, “Bildung kristallisierter Polysaccharide (Dextrine) ausStärkekleister durch Microben,” *Zentralbl. Bakteriol. Parasitenk.*, vol. Abt. II 29, pp. 188–197, 1911.

[25] S. V Kurkov and T. Loftsson, “Cyclodextrins,” vol. 453, pp. 167–180, 2013.

[26] C. News, “Introduction and General Overview of Cyclodextrin Chemistry,” vol. 2665, no. 97, 1998.

[27] M. E. Davis and M. E. Brewster, “CYCLODEXTRIN-BASED PHARMACEUTICS : PAST , PRESENT AND FUTURE,” vol. 3, no. December, 2004.

[28] M. Munteanu, S. Choi, and H. Ritter, “Cyclodextrin Methacrylate via Microwave-Assisted Click Reaction,” pp. 9619–9623, 2008.

[29] G. Wenz, B.-H. Han, and A. Müller, “Cyclodextrin Rotaxanes and Polyrotaxanes,” *Chem. Rev.*, vol. 106, no. 3, pp. 782–817, 2006.

[30] L. E. I. Liu and Q. Guo, “The Driving Forces in the Inclusion Complexation of Cyclodextrins,” pp. 1–14, 2002.

[31] R. K. Maheshwari, A. K. Singh, J. Gaddipati, and R. C. Srimal, “Multiple biological activities of curcumin : A short review,” *Life Sci.*, vol. 78, no. 18, pp. 2081–2087,

2006.

[32] B. Analysis, “Stability of curcumin in buffer solutions and characterization of its degradation products,” vol. 15, pp. 1867–1876, 1997.

[33] N. M. Patro, A. Sultana, K. Terao, and D. Nakata, “Comparison and correlation of in vitro , in vivo and in silico evaluations of alpha , beta and gamma cyclodextrin complexes of curcumin,” pp. 471–483, 2014.

[34] M. Mohan, M. Jaggi, and S. C. Chauhan, “Colloids and Surfaces B : Biointerfaces □ - Cyclodextrin-curcumin self-assembly enhances curcumin delivery in prostate cancer cells,” *Colloids Surfaces B Biointerfaces*, vol. 79, no. 1, pp. 113–125, 2010.

[35] A. Harada, J. Li, and M. Kamachi, “Preparation and Properties of Inclusion Complexes of Poly(ethylene glycol) with α-Cyclodextrin,” *Macromolecules*, vol. 26, no. 21, pp. 5698–5703, 1993.

[36] A. Manuscript, “Polymer Chemistry,” 2018.

[37] J. Li, X. Ni, and K. W. Leong, “Injectable drug-delivery systems based on supramolecular hydrogels formed by poly (ethylene oxide) s and □ - cyclodextrin,” 2002.

[38] K. Nidhi, S. Indrajeet, M. Khushboo, K. Gauri, and D. J. Sen, “Microstructural Imaging of Early Gel Layer Formation in HPMC Matrices,” *J. Pharm. Sci.*, vol. 95, no. 10, pp. 2145–2157, 2006.

[39] J. Li, “polymer – cyclodextrin inclusion complexes for drug delivery,” vol. 2, no. July, pp. 112–118, 2010.

[40] J. Li, X. Li, Z. Zhou, X. Ni, and K. W. Leong, “Formation of Supramolecular Hydrogels Induced by Inclusion Complexation between Pluronics and α-Cyclodextrin,” pp. 7236–7237, 2001.

[41] C. Pradal, K. S. Jack, L. Grøndahl, and J. J. Cooper-White., “Gelation kinetics and viscoelastic properties of pluronic and α-cyclodextrin-based pseudopolyrotaxane hydrogels,” *Biomacromolecules*, vol. 14, no. 10, pp. 3780–3792, 2013.

[42] S. M. N. Simões *et al.*, “Syringeable Pluronic-α-cyclodextrin supramolecular gels for sustained delivery of vancomycin,” *Eur. J. Pharm. Biopharm.*, vol. 80, no. 1, pp. 103–112, 2012.

[43] I. Yamaguchi, Y. Takenaka, K. Osakada, and T. Yamamoto, “Preparation and Characterization of,” pp. 2051–2054, 1999.

[44] E. A. Hasan, T. Cosgrove, and A. N. Round, “Nanoscale Thin Film Ordering Produced by Channel Formation in the Inclusion Complex of R -Cyclodextrin with a Polyurethane Composed of Polyethylene Oxide and Hexamethylene,” pp. 1393–1400, 2008.

[45] D. Ferri, “Reometria di polimeri in regime oscillatorio,” pp. 3–17, 2006.

[46] Alessandro Torchio, “Stimuli sensitive polyurethane-based hydrogels encapsulating mesoporous silica nanoparticles for drug release,” 2016.

[47] G. C. Alessandro Torchio1,3,#, Monica Boffito1,#,*, Andrea Gallina1, Mario Lavella1, Claudio Cassino2, “Supramolecular hydrogels based on custom-made poly(ether urethane)s and cyclodextrins as potential systems for drug release: design and characterization.”

[48] Q. L. and J. D. Jing Chen, Fangyingkai Wang, “Antibacterial polymeric nanostructures for biomedical applications,” *Chem. Commun.*, 2014.

[49] M. L. Heilig, “United States Patent Office,” *ACM SIGGRAPH Comput. Graph.*, vol. 28, no. 2, pp. 131–134, 1994.

[50] R. Challa, A. Ahuja, J. Ali, and R. K. Khar, “Cyclodextrins in drug delivery: An updated review,” *AAPS PharmSciTech*, vol. 6, no. 2, pp. 329–357, 2005.

[51] C. Syng-ai and A. L. Kumari, “Effect of curcumin on normal and tumor cells : Role of glutathione and bcl-2,” vol. 3, no. September, pp. 1101–1109, 2004.

[52] S. Mondal, S. Ghosh, and S. P. Moulik, “Journal of Photochemistry & Photobiology , B : Biology Stability of curcumin in different solvent and solution media : UV – visible and steady-state fl uorescence spectral study,” *JPB*, vol. 158, pp. 212–218, 2016.